

Summer 1976

ASYMMETRIC CATALYTIC HOMOGENEOUS HYDROGENATION BY A MACROCYCLIC COBALT COMPLEX

RICHARD WILLIAM WALDRON

Follow this and additional works at: <https://scholars.unh.edu/dissertation>

Recommended Citation

WALDRON, RICHARD WILLIAM, "ASYMMETRIC CATALYTIC HOMOGENEOUS HYDROGENATION BY A MACROCYCLIC COBALT COMPLEX" (1976). *Doctoral Dissertations*. 1135.
<https://scholars.unh.edu/dissertation/1135>

This Dissertation is brought to you for free and open access by the Student Scholarship at University of New Hampshire Scholars' Repository. It has been accepted for inclusion in Doctoral Dissertations by an authorized administrator of University of New Hampshire Scholars' Repository. For more information, please contact nicole.hentz@unh.edu.

INFORMATION TO USERS

This material was produced from a microfilm copy of the original document. While the most advanced technological means to photograph and reproduce this document have been used, the quality is heavily dependent upon the quality of the original submitted.

The following explanation of techniques is provided to help you understand markings or patterns which may appear on this reproduction.

- 1. The sign or "target" for pages apparently lacking from the document photographed is "Missing Page(s)". If it was possible to obtain the missing page(s) or section, they are spliced into the film along with adjacent pages. This may have necessitated cutting thru an image and duplicating adjacent pages to insure you complete continuity.**
- 2. When an image on the film is obliterated with a large round black mark, it is an indication that the photographer suspected that the copy may have moved during exposure and thus cause a blurred image. You will find a good image of the page in the adjacent frame.**
- 3. When a map, drawing or chart, etc., was part of the material being photographed the photographer followed a definite method in "sectioning" the material. It is customary to begin photoing at the upper left hand corner of a large sheet and to continue photoing from left to right in equal sections with a small overlap. If necessary, sectioning is continued again — beginning below the first row and continuing on until complete.**
- 4. The majority of users indicate that the textual content is of greatest value, however, a somewhat higher quality reproduction could be made from "photographs" if essential to the understanding of the dissertation. Silver prints of "photographs" may be ordered at additional charge by writing the Order Department, giving the catalog number, title, author and specific pages you wish reproduced.**
- 5. PLEASE NOTE: Some pages may have indistinct print. Filmed as received.**

University Microfilms International

300 North Zeeb Road
Ann Arbor, Michigan 48106 USA
St. John's Road, Tyler's Green
High Wycombe, Bucks, England HP10 8HR

77-3465

WALDRON, Richard William, 1946-
ASYMMETRIC CATALYTIC HOMOGENEOUS
HYDROGENATION BY A MACROCYCLIC COBALT
COMPLEX.

University of New Hampshire, Ph.D., 1976
Chemistry, inorganic

Xerox University Microfilms , Ann Arbor, Michigan 48106

ASYMMETRIC CATALYTIC HOMOGENEOUS HYDROGENATION
BY A MACROCYCLIC COBALT COMPLEX

by

RICHARD W. WALDRON
A.B., Bowdoin College, 1970

A THESIS

Submitted to the University of New Hampshire
In Partial Fulfillment of
The Requirements for the Degree of
Doctor of Philosophy
Graduate School
Department of Chemistry
August, 1976

This thesis has been examined and approved.

James H. Weber

James H. Weber, Thesis Director
Associate Professor of Chemistry

Helmut M. Haendler

Helmut M. Haendler
Professor of Chemistry

Alexander R. Amell

Alexander R. Amell
Professor of Chemistry

Charles W. Owens

Charles W. Owens
Associate Professor of Chemistry

Paul L. Bishop

Paul L. Bishop
Associate Professor of
Civil Engineering

Aug. 9, 1976

Date

ACKNOWLEDGEMENTS

The author would like to acknowledge the guidance and direction of Professor James H. Weber in the area of research and in the preparation of the thesis.

A University of New Hampshire Assistantship and two Graduate School Summer Fellowships are gratefully acknowledged.

The author would like to thank the Chemistry Faculty, in particular Professors Albert F. Daggett, Helmut M. Haendler, and Charles W. Owens for encouragement and help in completing the work for the degree. In addition, the author wishes to thank the many graduate students who have been helpful.

Last, but not least, the author would especially like to thank his wife, Jean, for her help, encouragement, and support. Without her assistance during this period, this thesis would not have been possible.

TABLE OF CONTENTS

LIST OF FIGURES.....	vii
LIST OF TABLES.....	ix
ABSTRACT.....	xi
INTRODUCTION	
Historical Background.....	1
History of Transition Metal Homogeneous Catalytic Hydrogenation.....	1
Factors Affecting Homogeneous Catalysis.....	4
Asymmetric Catalytic Reduction.....	8
Asymmetric Polymer Bound Catalysts.....	16
Cobalt in Homogeneous Catalysis.....	17
Hydroformylation with $\text{Co}_2(\text{CO})_8$ and Similar Catalysts.....	18
Hydrogenation with $\text{HCo}(\text{CN})_5^{3-}$ and Similar Catalysts.....	24
Cobaloxime and Related Compounds.....	35
The Nature of the Research.....	52
EXPERIMENTAL.....	54
Materials.....	54
Analyses.....	54
Gas Liquid Phase Chromatography.....	54
Ultraviolet-Visible Spectra.....	55
Proton Magnetic Resonance Spectra.....	55
Optical Rotations.....	55
Preparation of Authentic Samples.....	56
Preparation of Methyl Mandelate.....	58

Preparation of Propionitrile.....	58
Catalyst Preparation.....	59
Ligand Preparation.....	59
Preparation of $\text{Co}^{\text{II}}(\text{DMG})_2 \cdot 2\text{H}_2\text{O}$	59
Preparation of $\text{Co}^{\text{II}}(\text{BDML},3\text{pn})^+$	60
Preparation of $\text{Co}^{\text{III}}(\text{BDML},3\text{pn})\text{Br}_2$	60
Reduction Procedures.....	60
Method 1.....	61
Method 2.....	61
Method 3.....	61
Typical $\text{Co}^{\text{II}}(\text{DMG})_2 \cdot 2\text{H}_2\text{O}$ Reduction.....	62
Typical $\text{Co}^{\text{II}}(\text{BDML},3\text{pn})^+$ Reduction.....	62
Substrates Reduced by $\text{Co}^{\text{II}}(\text{DMG})_2 \cdot 2\text{H}_2\text{O}$	62
Substrates Reduced by $\text{Co}^{\text{II}}(\text{BDML},3\text{pn})^+$	64
Reaction Conditions Investigated.....	69
Factorial Experiments.....	72
Six Factor Screening Factorial.....	72
First Two Factor Factorial.....	74
Three Factor Factorial.....	74
Second Two Factor Factorial.....	74
Reactions Leading Directly to the Mechanism.....	80
Racemization of Benzoin.....	80
Addition of CH_3I to the Reduction Mixture.....	80
Formation and Reactions of $\text{Co}^{\text{I}}(\text{BDML},3\text{pn})$	81
Formation and Reactions of $\text{HCo}^{\text{III}}(\text{BDML},3\text{pn})^+$	82
Deuterium Experiments.....	82
STATISTICAL ANALYSIS OF DATA.....	84
Experimental Design.....	85
Mathematical Operations.....	87
Tests of Significance.....	94

Fractional Factorials.....	96
Cuthbert Daniel Half Normal Plot.....	100
RESULTS AND DISCUSSION.....	104
Ligand Synthesis.....	104
Catalyst Synthesis.....	106
Co(DMG) ₂ Reductions.....	107
Co ^{II} (BDML,3pn) ⁺ Reductions.....	109
Factorial Experiments.....	111
Six Factor Screening Experiment.....	112
First Two Factor Experiment.....	123
Three Factor Experiment.....	126
Second Two Factor Experiment.....	129
Factorial Conclusions.....	130
Mechanism of the Reduction.....	132
BIBLIOGRAPHY.....	145

LIST OF FIGURES

Figure 1.	Classification of Homogeneous Hydrogenation Catalytic Cycles.....	6
Figure 2.	A Qualitative Molecular Orbital Diagram for an $M(CO)_6$ or $[M(CN)_6]^{n-}$ Compound.....	10
Figure 3.	Asymmetry Inducing Phosphines.....	13
Figure 4.	Hydroformylation of an Olefin.....	20
Figure 5.	Mechanism of Reduction of a Polyaromatic Hydrocarbon.....	25
Figure 6.	Activated Olefin Hydrogenation by $HCo(CN)_5^{3-}$	27
Figure 7.	$Co(CN)_5^{3-}$ Catalyzed Butadiene Hydrogenation Mechanism.....	28
Figure 8.	$Co(CN)_5^{3-}$ Reaction with α -Amino Acids in the Presence of Butadiene.....	33
Figure 9.	Ohgo's Reaction Mechanism for the Reduction of Sodium Atropate.....	34
Figure 10.	The Structure of Cobaloxime Type Catalysts....	37
Figure 11.	Quinine and Related Polyfunctional Bases.....	41
Figure 12.	Ohgo $Co(DMG)_2$ Reduction Mechanism.....	47
Figure 13.	$Co(\alpha\text{-cqd})$ Catalyzed Carbenoid Reaction.....	51
Figure 14.	First Two Factor Experiment.....	77
Figure 15.	Second Two Factor Experiment.....	79
Figure 16.	Experimental Plan for a 2^2 Factorial.....	86
Figure 17.	2^2 Factorial Design and Results.....	90
Figure 18.	Cuthbert Daniel Half-Normal Plot of Screening Factorial.....	103

Figure 19.	Relationship Between Energy Required for Formation of R and S Isomers, and the Number of Molecules Possessing that Energy...	115
Figure 20.	Small Factorial Using Data from Screening Factorial.....	118
Figure 21.	Results of First Two Factor Experiment.....	124
Figure 22.	Design and Results of Three Factor Experiment.....	127
Figure 23.	Co(BDM1,3pn) Reduction Mechanism.....	133
Figure 24.	Relationship Between Quinine and Benzoin at the Point that the Stereochemistry of the Product is Determined.....	139

LIST OF TABLES

Table 1.	Common Transition Metal Catalysts and Their Electronic Properties.....	9
Table 2.	Typical Hydroformylation Catalysts, Reactants and Products.....	23
Table 3.	Effect of CN^-/Co Ratio on Butadiene Reductions by $\text{HCo}(\text{CN})_5^{3-}$	29
Table 4.	Effect of Solvent on Butadiene Reductions by $\text{HCo}(\text{CN})_5^{3-}$	30
Table 5.	Typical Substrates and Their Reduction Products Catalyzed by $\text{HCo}(\text{CN})_5^{3-}$	32
Table 6.	Effect of Reaction Conditions on the Reduction of Sodium Atropate.....	36
Table 7.	Substrates Reduced Asymmetrically by Cobaloxime-Quinine Catalyst.....	42
Table 8.	Effect of Chiral Amine on Optical Yield and Configuration of the Predominant Isomer.....	44
Table 9.	Effect of Solvent on the Reduction of Benzil...	45
Table 10.	Effect of Temperature on the Reduction of Benzil.....	45
Table 11.	Conditions for Determining Optical Yield of Various Products.....	57
Table 12.	Substrates Reduced by $\text{Co}(\text{DMG})_2 \cdot 2\text{H}_2\text{O}$	63
Table 13.	Substrates Reduced by $\text{Co}(\text{BDMl}, 3\text{pn})^+$	65
Table 14.	IR Comparison of Unknown Product and Methyl Mandelate.....	66
Table 15.	NMR Comparison of Unknown Product and Methyl Mandelate.....	67
Table 16.	CHN Analyses of Unknown Product.....	68
Table 17.	Reaction Conditions Investigated.....	70

Table 18.	Effect of Solvent Upon the Reaction.....	71
Table 19.	Proposed Major Variables and Their Settings....	73
Table 20.	Design Matrix and Optical Yields Obtained for Screening Factorial Experiment.....	75
Table 21.	Center Points of Fractional Factorial.....	76
Table 22.	Results of Three Factor Factorial Experiment...	78
Table 23.	General Design Matrix for 2^2 Factorial.....	88
Table 24.	Analysis of Variance for Screening Factorial Experiment.....	98
Table 25.	Analyses of HBDM1,3pn Ligand.....	105
Table 26.	Optical Yields Predicted and Obtained for the Screening Factorial Experiment.....	121
Table 27.	Predicted Optical Yields as a Function of Reaction Conditions.....	122
Table 28.	Best Reaction Conditions.....	131
Table 29.	Deuterium Experiments and Results.....	142

ABSTRACT

ASYMMETRIC CATALYTIC HOMOGENEOUS HYDROGENATION BY A MACROCYCLIC COBALT COMPLEX

by

RICHARD W. WALDRON

The asymmetric catalytic homogeneous hydrogenation by 2,3,9,10-tetramethyl-1,4,8,11-tetraazaundeca-1,3,8,10-tetraen-11-ol-1-olato cobalt(II) cation was investigated, where BD_M1,3pn represents the tetradentate anion.

A variety of carbon-oxygen double bonds were reduced by this catalyst, and by bis(dimethylglyoximate)cobalt(II). Substrates reduced fastest when the weak base benzylamine was added to the reaction mixture. The products were identified by ir, nmr, and glpc.

The effect of varying experimental parameters was studied with the help of the technique of factorial experiments. The use of statistics allowed the most information for the least experimentation, and removed any personal bias from the results. It also allowed the effects of one variable on others to be examined and quantified.

The mechanism of the reduction takes place in six steps. The activation of hydrogen involves the formation of a cobalt-hydride, which then ionizes to form the cobalt(I) complex and a proton. This proton bonds to quinine in preparation for the fourth step, which determines the stereochemistry of the product. The protonated quinine blocks one face of the substrate and donates its proton as the cobalt(I) complex attacks the opposite face of the substrate. Electrophilic attack by another proton then cleaves the carbon-cobalt bond to form the reduced product. Finally, the cobalt(III) complex combines with a cobalt(I) complex to form the starting cobalt(II) complex.

The mechanism of the $\text{Co}(\text{BDML}, 3\text{pn})^+$ reduction was compared to that of the $\text{Co}(\text{DMG})_2$ system. The DMG system contains four nitrogen donor atoms in a plane similar to the system studied. Preliminary experiments were run with the $\text{Co}(\text{DMG})_2$ system. The effects due to the components of the reduction mixture were discussed.

INTRODUCTION

Catalysis (ka·tal' i·sis) 1. Dissolution, destruction, ruin (rare), 1660. 2. Chem. Berzelius' name for the effect produced in facilitating a chemical reaction, by the presence of substance, which itself undergoes no permanent change. Also called contact action, 1836.¹

Historical Background

Although some pioneering chemists in the 18th Century used catalysis without realizing it, catalysis remained generally unknown and undefined until 1836 when Berzelius² recognized the importance of it. He introduced the term "catalysis" to describe the action of a chemical reaction by substances he called "catalysts". He cautiously described their action as an example of electrochemical affinity that caused changes in the movement of molecules or influenced the polarity of atoms.

The development of physical chemistry in the late nineteenth century set the groundwork for further advancement of the definition by Ostwald.³ He stated several characteristics which defined their properties. (a) They could not contribute energy to a reaction. (b) They could not change the equilibrium point of reversible reactions. (c) They accelerated, but did not initiate reactions. (d) Small amounts of catalysts could transform large quantities

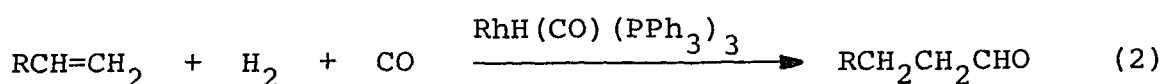
of the reacting substances by entering into the reaction again and again. (e) At the end of each cycle, the catalyst is regenerated into its original form.

It is known that in the course of a reaction, the catalyst usually lowers the energy of activation.⁴ This may be accomplished by providing an alternate reaction pathway where the catalyst interacts directly with the substrates. In the last thirty years, catalysis has become an important area of research. Only recently have the parallels between catalysts and enzymes been explored. Because life as we know it today could not exist without enzymes, scientific study of this area is most important.

There are several possible ways to classify catalysts. Two of these ways are (a) by the type of reaction they perform, or (b) by their physical state in relation to the rest of the system. The most basic classification is based on the second method, and results in homogeneous and heterogeneous catalysis. A homogeneous catalyst is a catalyst that is in the same phase as the substances it catalyzes. It may be dissolved in a suitable solvent; or no solvent may be present, as in the gas phase. In the gas phase, Br_2 catalyzes the chlorination of NO by Cl_2 .⁵



Hydroformylation of an olefin is an example of homogeneous catalysis in the solvent phase.⁶



A heterogeneous catalyst, on the other hand, is in a different phase than the substance it catalyzes. Heterogeneous catalysis is widely used in industry for this reason. This makes it easy to separate the catalyst from the reaction mixture by filtration, and allows the catalyst to be reused. Continuous processes require a heterogeneous catalyst. The oxidation of unburned hydrocarbons by platinum or palladium on a ceramic support in "catalytic converters" in newer model automobiles is an example of a continuous catalytic process.

History of Transition Metal Homogeneous

Catalytic Hydrogenation

The first example of homogeneous catalytic hydrogenation by a transition metal complex was published in 1938 when Calvin reduced quinone to hydroxyquinone using a cuprous acetate-quinoline system.⁷ In the 1950's, investigators found that the hydrogenation of olefins was a side reaction of the "oxo" process of hydroformylating olefins.⁸ Then, in 1954, Flynn and Hulbuet discovered the hydrogenation of ethylene by $[\text{Pt}(\text{C}_2\text{H}_4)\text{Cl}_2]_2$.⁹ These results opened up a new research area.

Homogeneous catalysis has become an important area of research for several reasons. When compared to heterogeneous catalysis, it enjoys several advantages in the ease of investigation.¹⁰ (a) Dissolving the catalyst in solution

allows reproducible experimental conditions. (b) Physical measurements, such as spectra, give direct insight as to the nature of the catalyst. (c) It is possible to tailor a catalyst to introduce efficiency and selectivity. Mildness of conditions, ease of catalyst regeneration and convenience may be added to this list. There are several excellent reviews on homogeneous catalysis and factors that affect it.¹¹⁻²⁴

Factors Affecting Homogeneous Catalysis

Three basic steps are usually necessary in the reduction of organic molecules by transition metal catalysts.

(1) The catalyst activates H_2 , usually forming M-H bonds.

(2) The catalyst activates the substrate, usually by coordination.

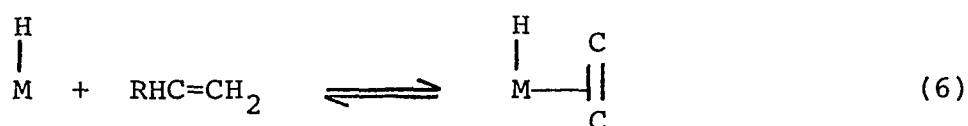
(3) The catalyst transfers hydrogen to the coordinated substrate.

Hydrogen activation takes place when coordinatively unsaturated complexes add H_2 . There are three possible ways for this to take place; n is the oxidation number of the metal.



The stability of the hydride is of great importance. It must be stable enough to form at a reasonable rate, but not so stable as to retard the transfer of hydrogen to the substrate. Figure 1 shows hydrogen activation in typical catalytic reactions.

Coordination of the substrate to the metal atom of the catalyst is accepted as necessary for hydrogenation to proceed.²⁴ Several π -olefin hydride complexes have been isolated and are thought to be intermediates in the hydrogenation of olefins.²⁵ Again, the nature of the transition metal and the ligands will affect the stability of the metal-substrate bond, and thus affect the rate of reduction.



Hydride transfer is the third basic step in the reduction.



Studies done on metal-alkyl systems give evidence of a four center mechanism.²⁶ This restricts the hydride and the substrate to cis sites on the metal complex. The metal complex thus formed can react by one of four possible hydrogen transfer reactions shown below. Note the similarity between

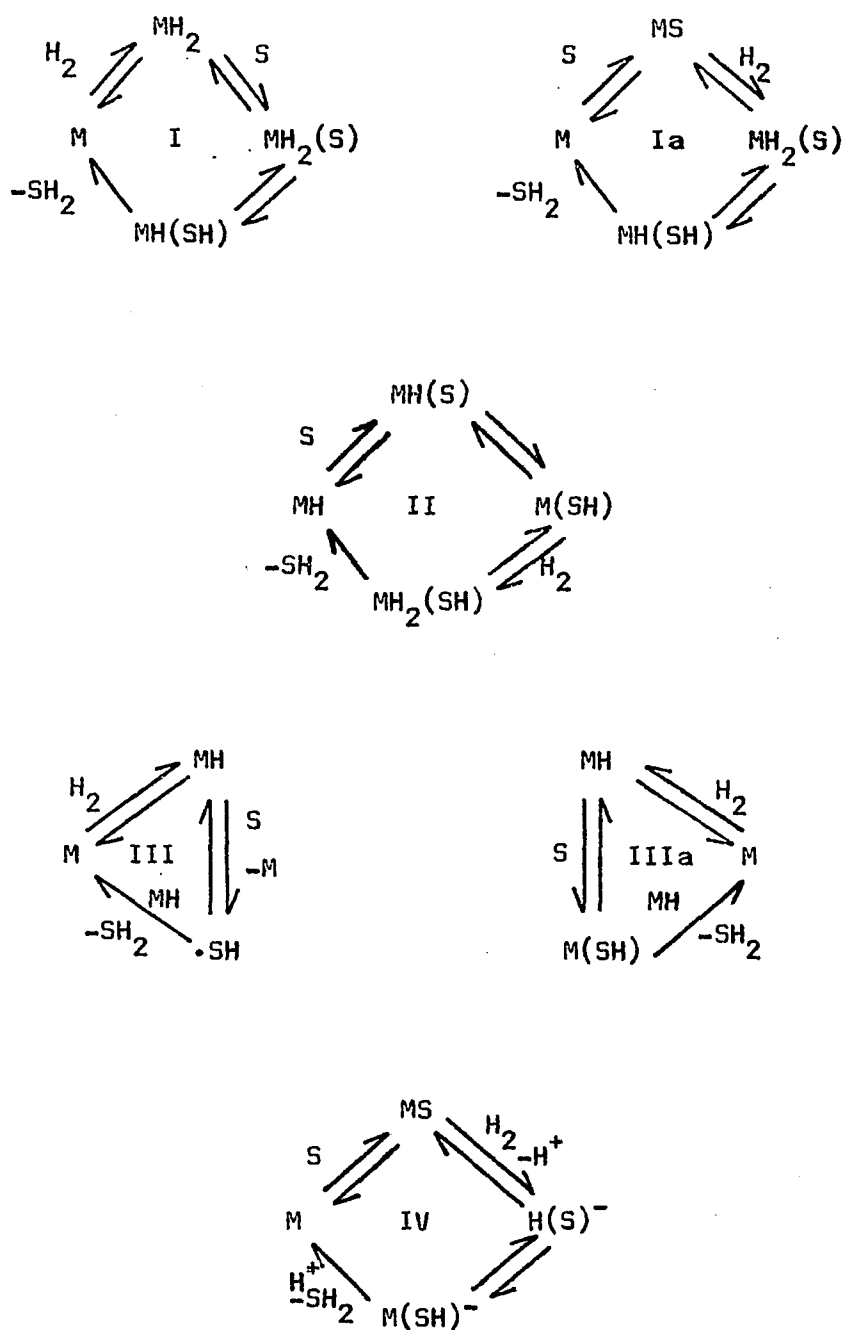
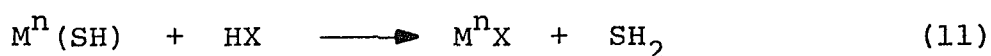
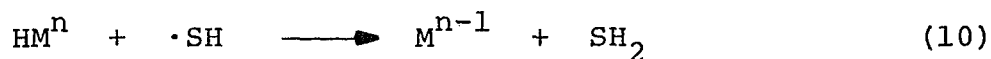
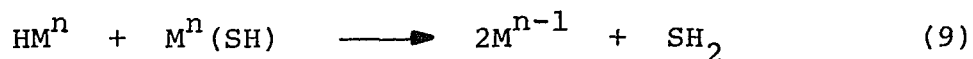
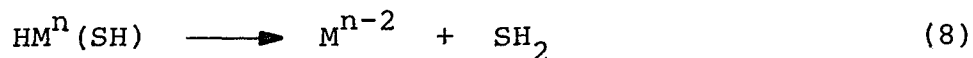


Figure 1. Classification of Homogeneous Hydrogenation Catalytic Cycles. Types I-III involve the homolytic cleavage of molecular hydrogen; Type IV involves heterolytic cleavage. M or MH = active catalyst species; S = substrate.

the final step and the initial activation of the H_2 . Figure 1 shows the steps in the four general mechanisms of substrate reduction.²⁷ SH is the half reduced substrate.



Many metals act as homogeneous catalysts, but the majority of them have d^6 to d^{10} electron configurations.²⁸ The electronic configuration determines the number of coordination sites occupied, and so plays an important role in the activity of the catalyst. If the catalyst is to activate hydrogen, it must somehow bring the hydrogen molecule into the coordination sphere. Thus the catalyst must have a vacant coordination site, or it must generate one by the dissociation of a labile ligand. Heat or irradiation is often necessary to remove the labile ligand. For example, upon heating, $RhCl(PPh_3)_3$ loses a PPh_3 ligand and is then able to activate hydrogen.²⁹

Tolman's 16 and 18 Electron Rule has two postulates.¹⁷

(1) Diamagnetic organometallic complexes of transition metals may exist in a significant concentration at moderate temperatures only if the metal's valence shell contains 16 or 18 electrons.

(2) Organometallic reactions, including catalytic ones, proceed by elementary steps involving only intermediates with 16 or 18 metal valence electrons.

Following these rules, $\text{Co}^{\text{III}}(\text{CN})_6^{3-}$ would have 6 metal and 12 ligand donated electrons, for a total of 18. If an electron were added to this very stable complex, the 19 electron complex would become very unstable and a CN^- ion would dissociate to form $\text{Co}^{\text{II}}(\text{CN})_5^{3-}$ with 17 electrons. This is also unstable and would react with H_2 to form $\text{HCo}^{\text{III}}(\text{CN})_5^{3-}$ with 18 electrons. Table 1 lists some common transition metal catalysts and their electronic properties.

If one constructs an MO diagram for octahedral $[\text{Co}^{\text{III}}(\text{CN})_6]^{3-}$, Figure 2, one can observe the instability when an electron is added to the complex.³⁰ The added electron occupies the strongly antibonding orbital e_g^* . This results in the destabilization of the coordination number 6, in favor of a 17 electron system of coordination number 5, with 5 electrons in the t_{2g} orbitals. When the $[\text{Co}^{\text{II}}(\text{CN})_5]^{3-}$ activates H_2 , the H atom incorporated in the complex brings one electron with it, giving filled t_{2g} orbitals and a stable 18 electron system. These results tend to confirm the 16 or 18 Electron Rule.

Asymmetric Catalytic Reduction

Asymmetric hydrogenations create asymmetric carbon atoms by addition of hydrogen across multiple bonds.¹³ The classification of heterogeneous and homogeneous catalysis

TABLE 1

Common Transition Metal Catalysts and Their Electronic Properties

Metal	Catalyst	Electronic Configuration	# of Valence Electrons	Coordination Number	Reaction
Ru (II)	$\text{RuCl}(\text{PPh}_3)_4$	d^6	16	5	Hydroformylation
Co (III)	$\text{HCo}(\text{CN})_5^{3-}$	d^6	18	6	Hydrogenation
Co (II)	$[\text{PyCo}(\text{DMG})_2]_2$	d^7	18	6	Hydrogenation
Co (I)	$\text{HCo}(\text{CO})_4$	d^8	18	5	Hydroformylation
Fe (0)	$\text{Fe}(\text{CO})_5$	d^8	18	5	Hydrogenation
Rh (I)	$\text{RhCl}(\text{CO})(\text{PPh}_3)_2$	d^8	16	4	Hydroformylation

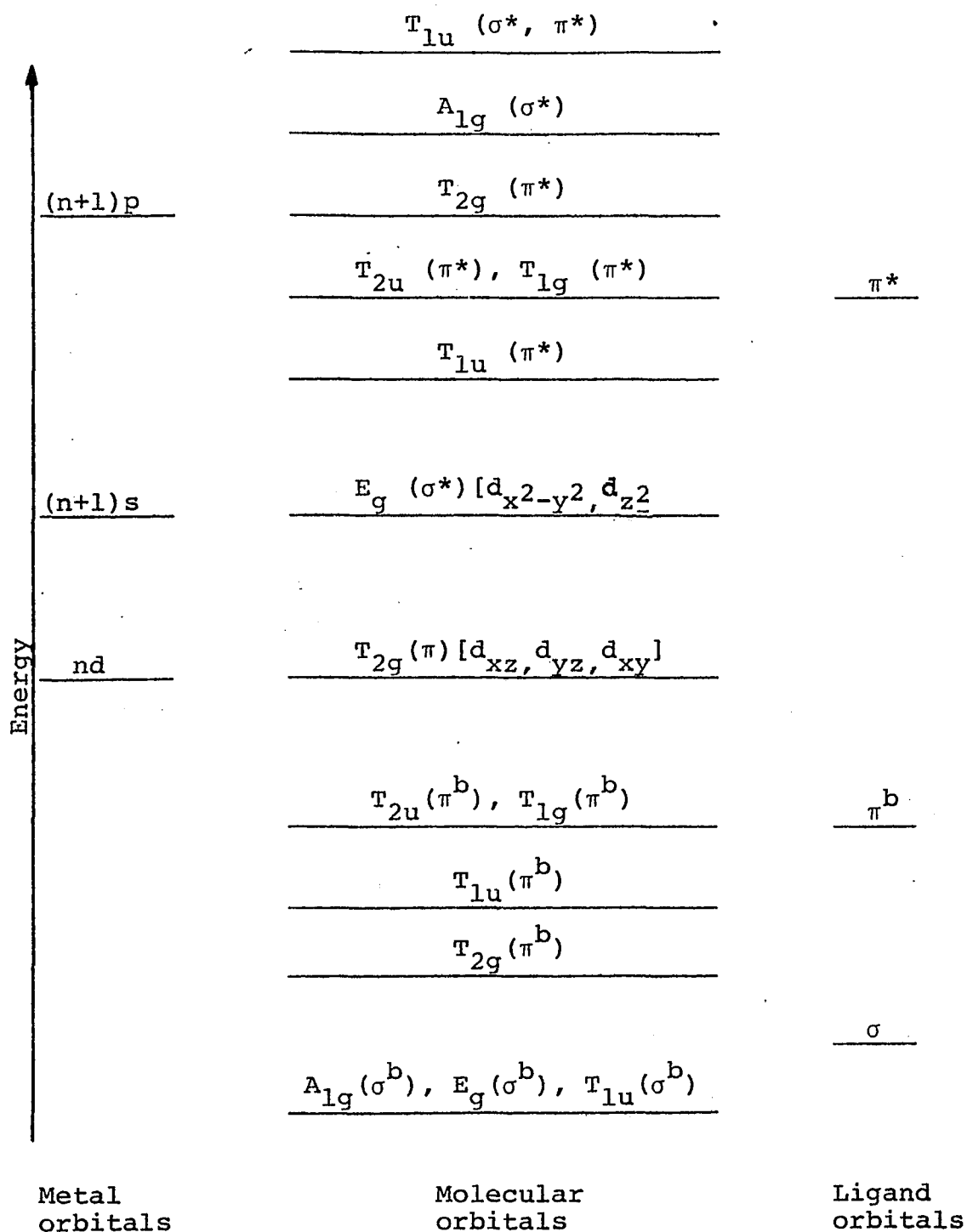


Figure 2. A Qualitative Molecular Orbital Diagram for an $M(CO)_6$ or $[M(CN)_6]^{n-}$ Compound.

may be extended to asymmetric catalytic hydrogenation. Most work has been done with homogeneous catalysts because heterogeneous catalysts are plagued by poor optical yields, non-reproducible conditions, and consequently, wide variations in optical purity. These problems are primarily due to the method of preparation of the catalysts.

Palladium deposited on silk has produced optically active phenylalanine, but optical purity was dependent on the origin of the silk and its chemical pretreatment.³¹ Modified Raney nickel has also been used for asymmetric hydrogenations, again with poor results.³² Research on heterogeneous systems has largely been abandoned in favor of homogeneous systems.

Most asymmetric homogeneous catalysis has been done using rhodium as the central metal. Cobalt and ruthenium have been used to a much lesser extent. Two approaches to the problem of forming a chiral homogeneous catalyst are illustrated by the following discussion. Knowles^{33,38} and Horner³⁴ have concentrated on asymmetric phosphorus atoms in their quest for high optical yields. At the same time, Morrison³⁵ and Kagan^{36,37} have synthesized ligands that have chiral alkyl groups on the phosphorus atom.

The chief disadvantage of the chiral phosphorus atom is that it involves a classical resolution step with a fractional crystallization. The chiral alkyl moiety approach starts with a resolved chiral alkyl group, but reaction conditions often cause the formation of hard to remove by-

products, or involve difficult multistep syntheses. Thus both have their disadvantages.

In 1968, Knowles and Sabacky³³ used RhL_3Cl_3 to reduce α -phenylacrylic acid. The ligand L was R-(-)-methylphenyl-n-propyl phosphine, a phosphine chiral at the phosphorus atom. About the same time Horner³⁴ published work using $[\text{Rh}(1,3\text{-hexadiene})_2\text{Cl}_2]_2$ and the S-(+)-form of the above phosphine. In these early experiments optical yields ranged up to 21%. Figure 3 shows the structures of various asymmetry inducing phosphine ligands.

In 1971, Morrison³⁵ synthesized neomenthyldiphenyl phosphine, NMDPP, which is chiral on carbon, not phosphorus. Using this phosphine with a rhodium catalyst he obtained a 61% optical yield in the synthesis of S-(+)-phenylbutanoic acid. It was noted that α,β -unsaturated carboxylates yielded greater optical purity than simple olefins. This was attributed to substrate coordination to the metal by both the olefinic double bond and the carboxylate anion.

About this time Dang and Kagan³⁶ reported a 72% optical yield with a novel diphosphine ligand, coined DIOP. Prepared from R-(+)-tartaric acid, this new ligand made use of a readily available common starting material which had been previously resolved. The high stereoselectivity of this system is thought to be the result of the rigidity of the ligand and the presence of a trans ring junction. Again, a rhodium catalyst was used.

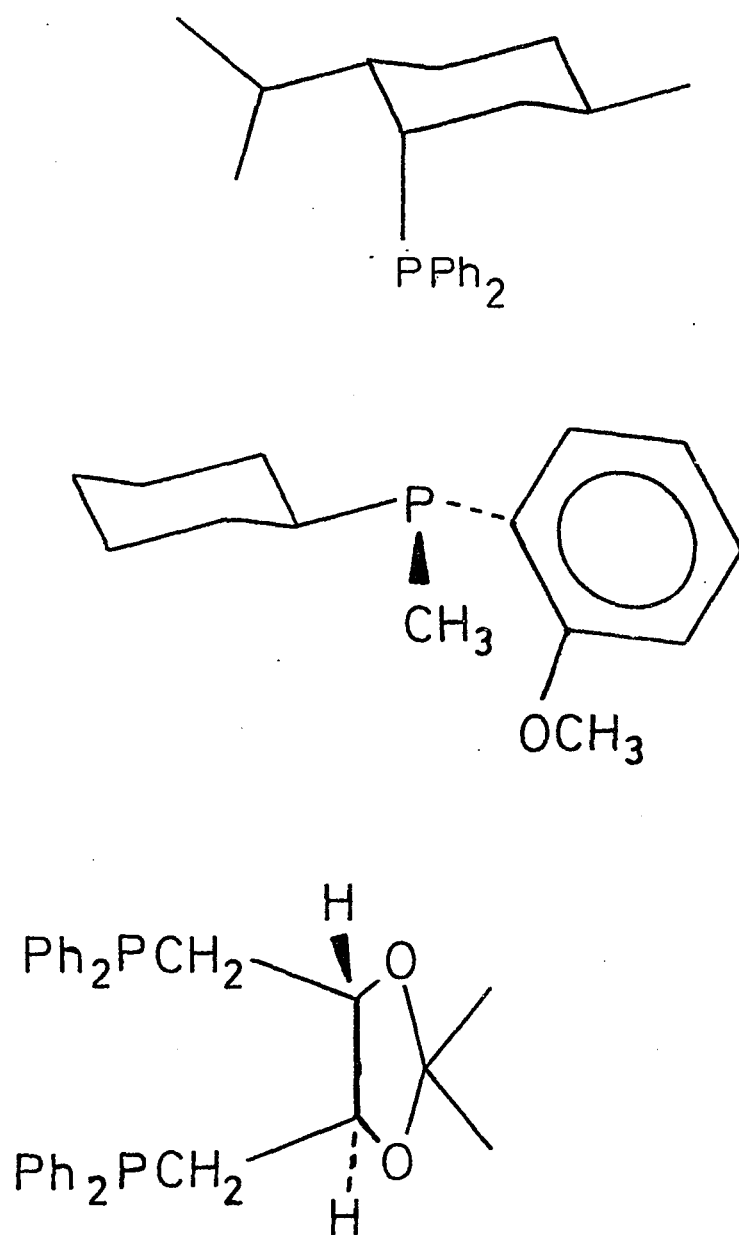


Figure 3. Asymmetry Inducing Phosphines. (A) Neomenthyl-diphenylphosphine, NMDPP; (B) O-Anisylcyclohexylmethylphosphine, ACMP; (C) (-)-2,3-O-isopropylidene-2,3-dihydroxy-1,4-bis(diphenylphosphino)butane, (-)-DIOP; (D) 1,2-bis(o-anisylphenylphosphino)ethane.

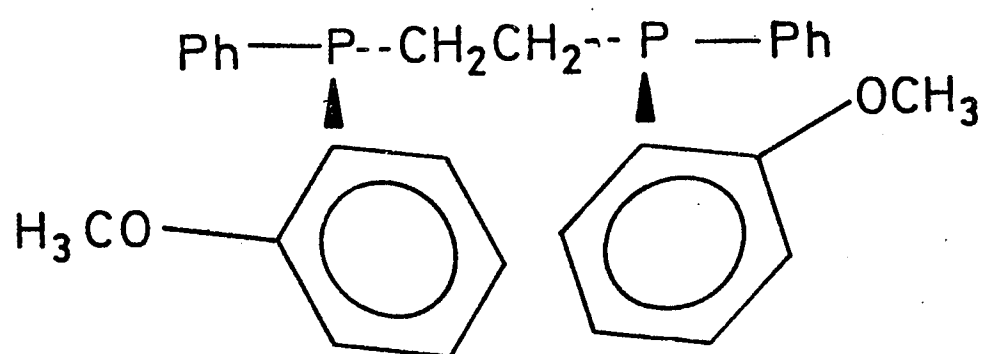
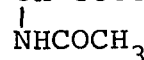


Figure 3. (continued)

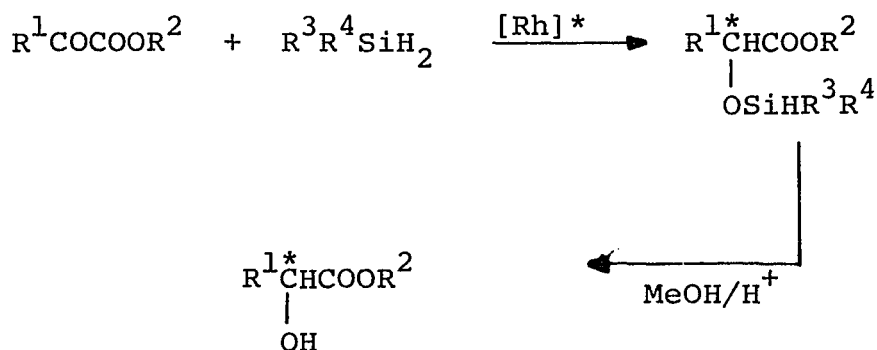
The next step in ligand design was the addition of methoxy groups to the aryl groups on the phosphine. Substrates could now hydrogen bond to the ligand system, and optical yields were improved to 90%.³⁷ The phosphine ACMP, in this category, is illustrated in Figure 3.

Recently Knowles and coworkers improved upon the ACMP ligand by forming the biphosphine illustrated in Figure 3.³⁸ When substrates of the type $R-CH=CCOOH$ are reduced by



$[\text{Rh}(1,5\text{-cyclooctadiene})(\text{biphosphine})]\text{BF}_4^-$, a 96% optical yield has been reported. This high optical yield has been attributed to the presence of a rigid 5-member ring formed by the rhodium and the biphosphine, and to the $\text{O}-\text{CH}_3$ group available for hydrogen bonding from the amide.

Ketones^{39,40}, α -ketoesters⁴¹, and silylenol ethers⁴² have been asymmetrically hydrogenated by rhodium catalysts. Optical yields range from about 2% to 85%. The best optical yields were obtained by first hydrosilylating the carbonyl group in the presence of the chiral catalyst, and then cleaving the silicon-oxygen bond in acidic methanol.



The optical yield obtained was dependent upon the hydrosilane and the chiral phosphine.

Asymmetric Polymer Bound Catalysts

R. B. Merrifield used polymer supported catalysts for his peptide synthesis in 1963.⁴³ Since that time the advantages of this method have led to many interesting applications. A polymer bound catalyst may have the properties of both heterogeneous and homogeneous catalysts. It combines the selectivity and reproducibility of a homogeneous catalyst with the ease of separation of a heterogeneous catalyst. This lends it to industrial continuous flow processes, as opposed to batch processes typical of homogeneous catalysts.

Other properties include greater air stability and exclusion of certain substrates due to steric effects. Large molecules may be excluded from the reaction site due to relatively small solvent channels in the polymer.⁴⁴ As the size of the olefin increases, the rate of reduction decreases because reduction takes place inside the polymer beads and the large olefin cannot pass through the solvent channels formed by crosslinking in the polymer.

Polymer supported catalysts are being used for a variety of reactions. They may be used in the reduction of alkenes, ketones and aldehydes, hydroformylation of olefins, and a variety of other catalytic applications. Two separate catalysts may be attached to the same polymer, or two

different polymer bound catalysts may be mixed to perform sequential reactions.⁴⁵

The mixing of $\text{RuCl}_3 \cdot 3\text{H}_2\text{O}$ and poly-L-methylethyimine in an acetate buffer resulted in the first example of a chiral ruthenium catalyst.⁴⁶ The optical yield was dependent upon the standing time, pH and the ratio of monomer to metal. The maximum optical yield, 5.3%, was obtained at pH=5.5, 6 days standing time, and a monomer-metal ratio of 10:1.

Kagan has also used a Merrifield resin to insolubilize a rhodium derivative of DIOP.⁴⁷ Optical yields of 58% have been observed using this catalyst system.

Industry will be using insolubilized homogeneous catalysts more and more as their properties and advantages are studied. They are ideally suited for industry because of their ease in continuous flow applications, and their adaptability to multistep reactions.

Cobalt in Homogeneous Catalysis

The activation of organic functional groups by cobalt catalysts makes possible a wide variety of reactions involving unsaturated organic compounds. Examples of these reactions are isomerization, polymerization, oxidation, hydrogenation and hydroformylation. The most important reactions are hydrogenation and hydroformylation.

There are many cobalt catalysts available for these reactions, with most falling into four distinct groupings.

- (1) Cobalt salts in the proper solvents.
- (2) $\text{HCo}(\text{Co})_4$ and related complexes used in hydroformylation reactions.
- (3) $\text{HCo}(\text{CN})_5^{3-}$ and related complexes used in hydrogenations.
- (4) Cobaloxime, $\text{Co}(\text{DMG})_2$, and related complexes used in hydrogenations.

Some catalysts not classified above are $\text{HCo}(\text{C}_2\text{PCH}_2\text{CH}_2\text{-P}\phi_2)_2$ and $\text{HCo}(\text{PPh}_3)_3$. For terminal olefins $\text{Co}(\text{NO})(\text{PPh}_3)_3$ and NaBH_4 is a hydrogenation catalyst, while for internal olefins $\text{Co}(\text{NO})(\text{PPh}_3)_2\text{I}_2$ may be used.

Ziegler-type catalysts, $\text{Co}(\text{acac})_3$, $\text{Co}(\text{PPh}_3)_2\text{Cl}_2$ and $\text{Co}(\text{acac})_2$ combined with alkyl aluminum hydrides and aluminum alkyls have also functioned as hydrogenation catalysts. The rate of hydrogenation decreases with increasing substitution on the alkene: disubstituted > trisubstituted > tetrasubstituted.¹⁴ These catalysts are often considered modified versions of one of the distinct groups named above.

Industrially, $\text{HCo}(\text{CO})_4$ and $\text{HCo}(\text{CN})_5^{3-}$ are the most important.⁴⁸ They have been researched for many years and are thought to be understood. $\text{HCo}(\text{CN})_5^{3-}$ is closely related to $\text{Co}(\text{DMG})_2$, but will be treated separately. Since $\text{Co}_2(\text{CO})_8$ was patented by Roelen in 1943 as an effective hydroformylating agent, it has been used in a wide variety of reactions.^{11,12,14-16,18}

Hydroformylation with $\text{Co}_2(\text{CO})_8$ and Similar Catalysts.

A typical hydroformylation reaction converts an olefin to an

aldehyde. Under extreme conditions, the aldehyde formed may be reduced to an alcohol. Typical reaction conditions are 150°C and 200 atms of pressure. Figure 4 shows the hydroformylation of an olefin. The CO incorporated into the organic molecule comes from a coordinated carbon monoxide ligand.⁴⁹

The catalyst is generated in situ so that the cobalt may be added in a number of forms. Thus $\pi\text{-C}_4\text{H}_7\text{Co}(\text{CO})_2\text{PBU}_3$ would give $\text{HCo}(\text{CO})_3\text{PBU}_3$ as the active catalyst. A minimum partial pressure of CO is needed to regenerate the catalyst. Beyond this minimum pressure, an increase in CO partial pressure increases the rate of reaction, up to a maximum. This maximum is dependent on the temperature and the olefin substrate. In a complete cycle, one mole of H_2 and one mole of CO are used for each mole of substrate. For the range 100-160° and 50-250 atmospheres, the rate equation may be written:⁵⁰

$$\text{Rate} = k[\text{olefin}][\text{Co}][\text{P}_{\text{H}_2}][\text{P}_{\text{CO}}]^{-1} \quad (12)$$

When using synthesis gas with a 1:1 ratio of CO to H_2 , the rate is largely independent of the gas pressure because the two pressure effects work in opposite directions.

When reaction conditions are varied, the product distribution may also be affected. The production of n-isomers is favored by high partial pressure of CO, the presence of phosphines and relatively low temperatures.⁵¹ Formation of

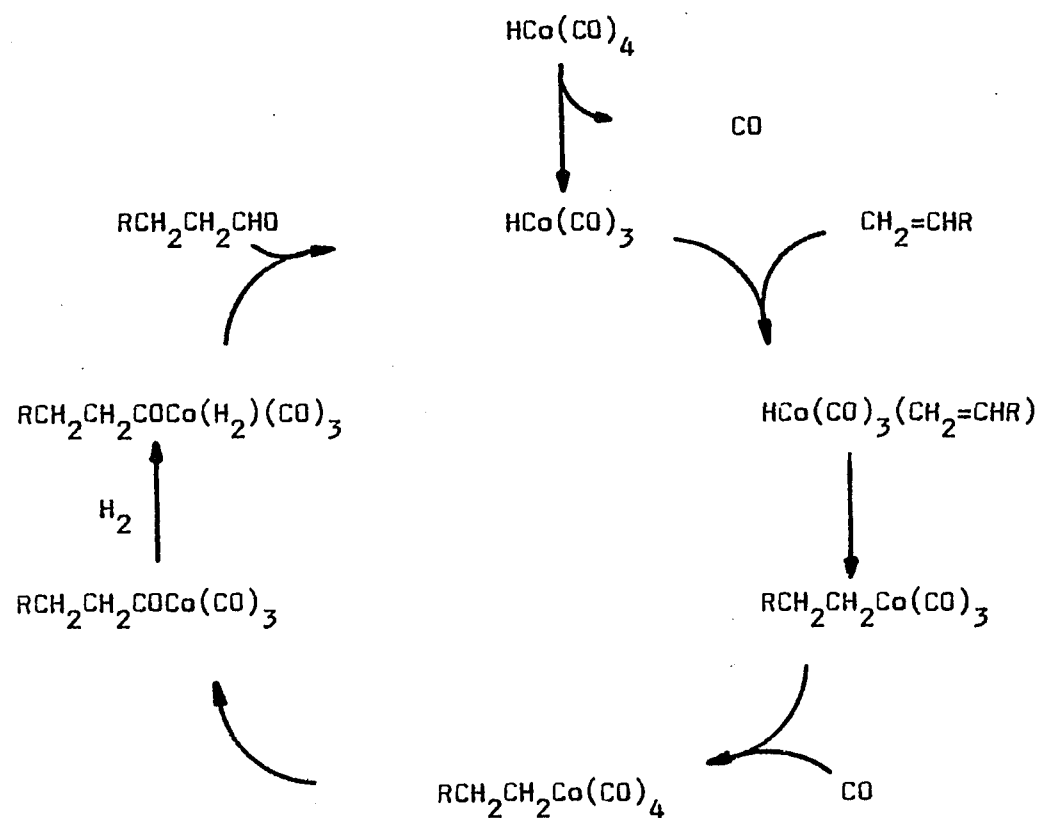


Figure 4. Hydroformylation of an Olefin.

aldehydes or saturated products, and the different isomers of each, depends on the catalyst precursors, location of the double bond in the substrate, and the organic functional groups on the olefin.⁵² Solvent effects are usually small and catalyst concentration has no effect on product distribution.⁵⁰ The rate of reaction decreases with increasing alkyl substitution on the olefin, decreasing in the order straight chain terminal olefins, straight chain internal olefins, branched chain olefins. The effect is largest when the branching is close to the double bond.⁵³

When olefins are hydroformylated in the presence of $\text{Co}_2(\text{CO})_8$ and the asymmetric ligand is (S)-N- α -methylbenzyl-salicylaldimine, low optical yields result.⁵⁴ When styrene is the olefin, 2-phenylpropanal is obtained in 0.3% optical yield. The drastic conditions required for the reduction may have caused racemization of the product. When ethyl orthoformate is added to the reaction mixture to form the diethyl-acetal derivative of the aldehyde, and thereby prevent racemization, the optical yield improved to 15.2% under identical conditions to the 0.3% yield above.

Asymmetric phosphines were ineffective for inducing asymmetry in the product when $\text{Co}_2(\text{CO})_8$ was the catalyst. However, when rhodium was the central metal instead of cobalt, optical yields ranged up to 27% when the chiral phosphine was DIOP. These results suggest that the olefin interacts directly with the chiral metal atom, and there is no hydro-

gen bonding to the chiral ligand system.

Alcohols may be the main product in hydroformylation reactions by the addition of phosphines. This also has the effect of increasing the straight chain products; probably due to steric effects. Ketones, acids, esters, and other organic compounds may be formed by this reaction. Table 2 lists some starting materials, catalysts and products of some hydroformylation reactions.^{50,55}

Cobalt carbonyl complexes also catalyze the hydrogenation of ketones⁵⁶, but early work has not developed into a useful general procedure. When tertiary phosphines are added separately to the reaction mixture, at 200°C and 200 atm pressure of H₂, reduction of the ketone to an alcohol was noted. The reduction did not take place if no phosphine was added, and if a 4:1 or higher ratio of phosphine to cobalt were used, the activity of the catalyst was inhibited. If a chiral phosphine, such as MePhPrP or MePhBuP was added, only insignificant optical activity was observed in the product. This was attributed to high temperature and/or lack of steric factors with the low coordination number of the catalyst.⁵⁶

CO₂(CO)₈ has been reported to reduce aromatic hydrocarbons under "oxo" conditions.⁵⁷ A new mechanism has been postulated to account for certain experimental results which cannot be explained by the conventional mechanism involving an organo-cobalt intermediate. This mechanism, illustrated

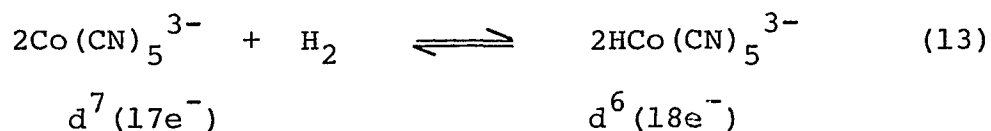
TABLE 2
Typical Hydroformylation Catalysts,
Reactants and Products

<u>Starting Materials</u>	<u>Proposed Catalyst</u>	<u>Products</u>
$\text{CH}_2=\text{CH}_2, \text{H}_2, \text{CO}$	$\text{RCo}(\text{CO})_3$	$(\text{C}_2\text{H}_5)_2\text{CO}$
$\begin{array}{c} \text{O} \\ \diagup \quad \diagdown \\ \text{H}_2\text{C} \text{---} \text{CHR}, \text{H}_2, \text{CO} \end{array}$	$\text{H Co}(\text{CO})_4$	$\text{CH}_3\text{C}(\text{O})\text{R}$
$\begin{array}{c} \text{R-HC} \text{---} \text{CH}_2, \text{CO} \\ \diagdown \quad \diagup \\ \text{O} \end{array}$	$\text{Co}_2(\text{CO})_8$	$\text{RCH}=\text{CHCOOH}$
$\text{RX}, \text{CO}, \text{R}'\text{OH}, \text{base}$	$\text{Co}(\text{CO})_4^-$	RCOOR'
$\text{RCH}=\text{CH}_2, \text{CO}, \text{CCl}_4$	$\text{Co}_2(\text{CO})_8$	$\begin{array}{c} \text{RCHCH}_2\text{CCl}_3 \\ \\ \text{COCl} \\ + \\ \text{RCH}_2\text{CH}_3 \\ \\ \text{Cl} \end{array}$
See References 11,15,18		

in Figure 5, is similar to the free radical mechanism which has been advanced for HCo(CN)_5^{3-} catalyzed hydrogenation of conjugated olefins.

Hydrogenation with HCo(CN)_5^{3-} and Similar Catalysts.

Pentacyanocobaltate(II), Co(CN)_5^{3-} , is also an important catalyst. It is used in hydrogenation of multiple bonds, usually carbon-carbon multiple bonds. Co(CN)_5^{3-} functions by activating H_2 in a reversible process as shown:

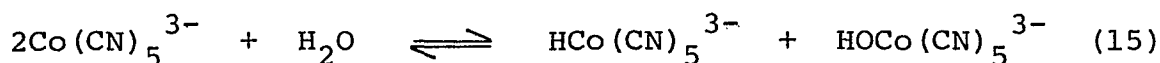


This is an oxidative-addition²⁰ of a hydrogen atom to the coordination sphere. Convention calls for the proton to have two electrons for an oxidation number of -1, even though it will leave as a proton without these electrons.

The rate law for hydrogen activation is of the form¹¹:

$$\frac{-d[\text{Co(CN)}_5^{3-}]}{dt} = k[\text{H}_2][\text{Co(CN)}_5^{3-}] \quad (14)$$

The cobalt hydride thus formed can then transfer hydrogen to various organic substrates.²⁰ Existence of the H-Co bond has been shown by NMR.⁵⁸ The hydride may also be generated by the oxidative addition of water to the starting Co(CN)_5^{3-} :



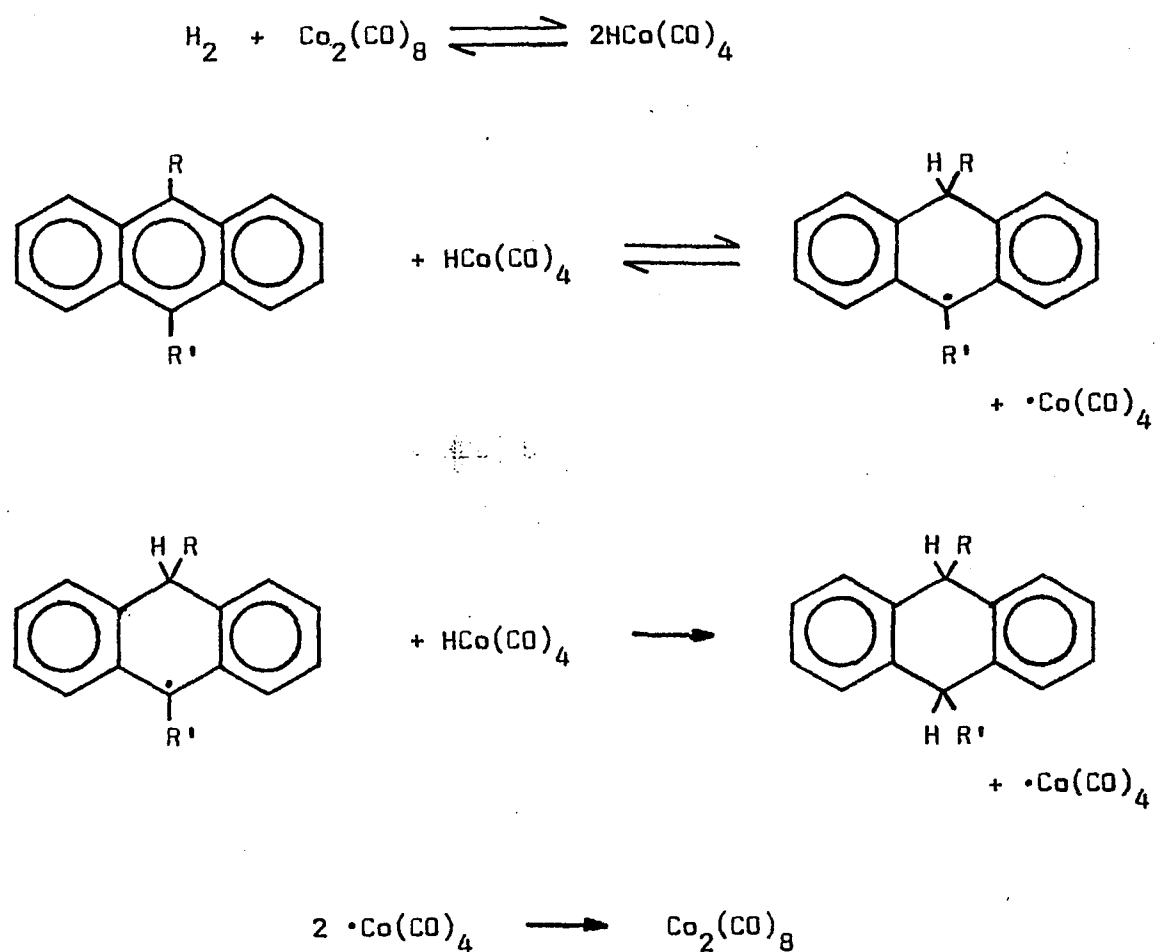


Figure 5. Mechanism of Reduction of a Polyaromatic Hydrocarbon.

The $\text{HCo}(\text{CN})_5^{3-}$ thus formed can react with H_2 to form H_2O and $\text{HCo}(\text{CN})_5^{3-}$. The hydrogenation of olefins and dienes is illustrated in Figures 6 and 7.

Olefins activated by electron releasing substituents, but not simple olefins, are hydrogenated by a free radical path, involving a free radical intermediate, as shown in Figure 6. The organocobalt complex is not directly involved in the catalytic cycle.²⁷ This is a type III cycle, illustrated in Figure 1.

A different mechanism, Figure 7, is responsible for the hydrogenation of conjugated dienes.⁵⁹ The $\text{HCo}(\text{CN})_5^{3-}$ first reacts with the diene to form the σ_1 -complex. This σ_1 -complex is then able to form a π -complex, or isomerize to a σ_2 -complex. The three possible intermediates, σ_1 , σ_2 and π , are able to add H by reacting with $\text{HCo}(\text{CN})_5^{3-}$ to form one of three possible products, 1-butene, trans-2-butene or cis-2-butene. A high degree of stereoselectivity is observed, and is dependent upon the cyanide/cobalt ratio, the solvent, and the $\text{HCo}(\text{CN})_5^{3-}$ concentration.^{27,59} This is type IIIa cycle, Figure 1.

In a series of experiments, Funabiki and Tarama studied the products as a function of the ratio of CN^-/Co (Table 3) and as a function of the solvent (Table 4).⁶⁰

These results show that an excess of CN^- ion favors the production of σ -complexes, as one would expect. Addition of alcohols favors the formation of the σ_2 -complex, but the

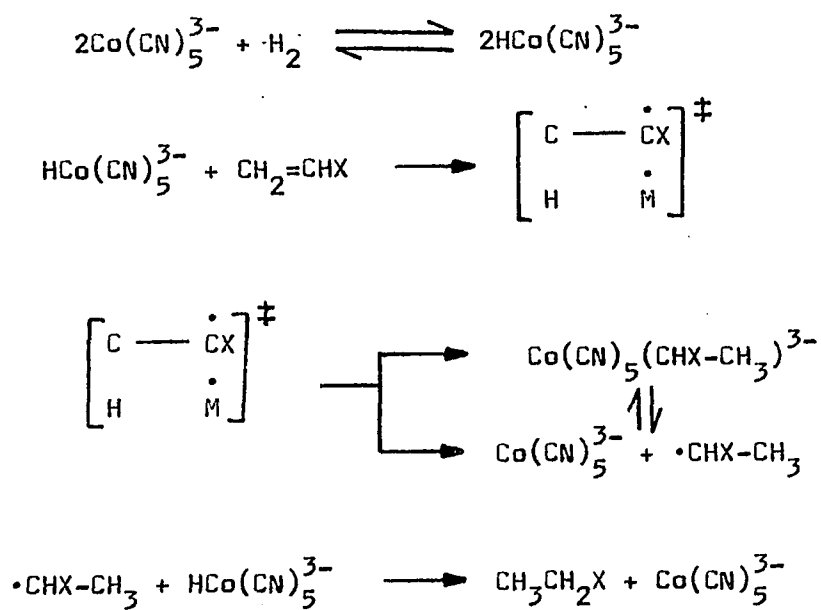


Figure 6. Activated Olefin Hydrogenation by $\text{HCo}(\text{CN})_5^{3-}$.

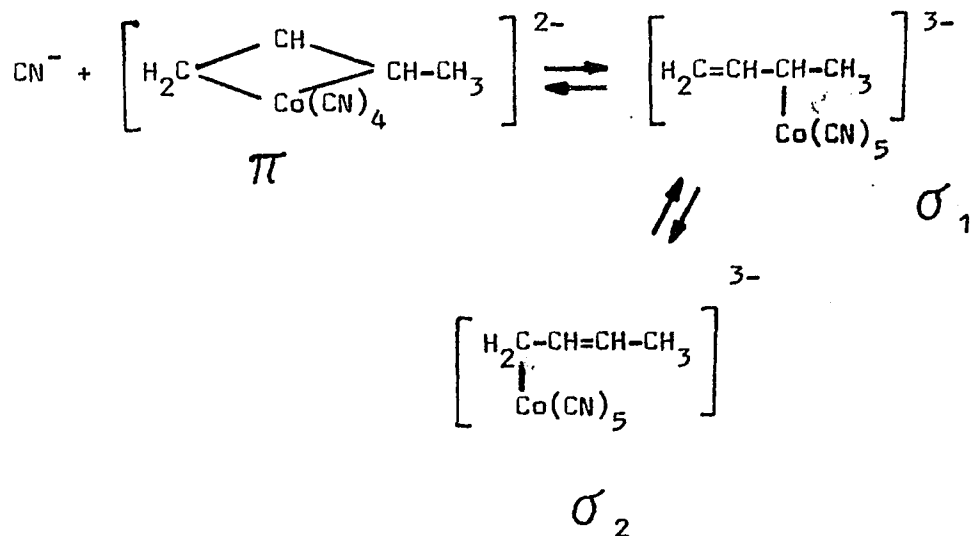
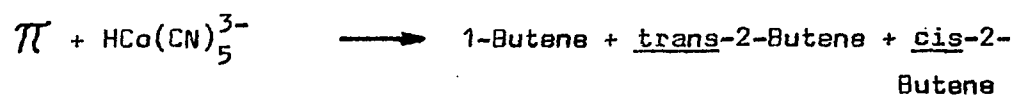
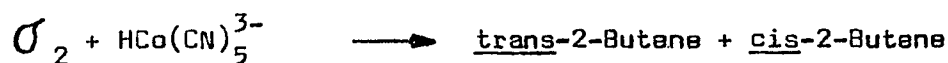
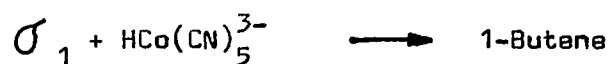
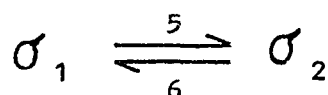
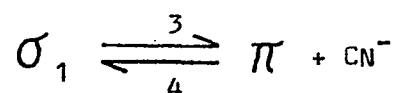
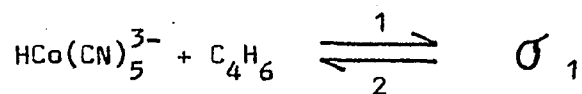
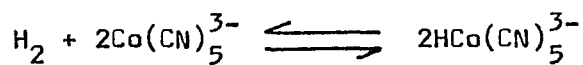


Figure 7. $\text{Co}(\text{CN})_5^{3-}$ Catalyzed Butadiene Hydrogenation Mechanism.

TABLE 3
Effect of CN^-/Co Ratio on Butadiene
Reductions by $\text{HCO}(\text{CN})_5^{3-}$

CN^-/CO Ratio	Butanes, mol %		
	1-	<u>trans</u> -2-	<u>cis</u> -2-
4.5	13	86	1
5.5	29	70	1
6.0	85	12	
8.5	80	19	1

TABLE 4
Effect of Solvent on Butadiene
Reductions by HCo(CN)_5^{3-}

Alcohol ml		H_2O ml	Butenes, mol %		
			1-	<u>trans</u> -2-	<u>cis</u> -2-
O		50	89%	5%	6%
MeOH	5	45	84	6	10
	10	40	80	6	14
	15	35	69	7	24
	20	30	56	5	39
EtOH	5	45	90	6	4
	10	40	88	6	6
	15	35	85	7	8
Ethylene Glycol	10	40	77	6	18
	15	35	71	7	22
	30	20	60	7	33
	40	10	45	6	49
			39	5	56

reason for this is not understood. trans-2-Butene is the preferred product of the π -complex intermediate. Because butene is not an activated olefin, the reduction stops at this point.

As shown in Table 5, $\text{HCo}(\text{CN})_5^{3-}$ reduces a wide variety of substrates. $\text{Co}(\text{dipy})(\text{CN})_3^-$ reacts in a similar manner, and appears to be somewhat more active.⁶¹

Suzuki and Kwan^{62,63} report that $\text{Co}(\text{CN})_5^{3-}$ reacts with α -amino acids in a 1:1 ratio to form complexes of the type $\text{K}_2[\text{Co}(\text{CN})_4\text{NH}_2\text{RCOO}]\cdot\text{nH}_2\text{O}$. When butadiene is added to the reaction mixture all three possible butenes are produced. The proposed mechanism of amino acid addition is illustrated in Figure 8. The α -amino acid complex is formed by adding $\text{CoCl}_2\cdot 6\text{H}_2\text{O}$, KCN and $\text{R-CH}(\text{NH}_2)\text{COOH}$ in the ratio 1:5:1.

This led Y. Ohgo⁶⁴ to theorize that chiral α -amino acids could be used in a hydrogenation, similar to Suzuki and Kwan's method, to produce an optically active product from an achiral olefin.

Using $\text{Co}(\text{CN})_5^{3-}$ and the chiral α -amino acid L-isoleucine, Ohgo hydrogenated sodium atropate.⁶⁴ After the reaction mixture was worked up, a 0.1% optical yield was reported. He therefore proposed a reaction scheme, Figure 9, which did not have an asymmetric cobalt hydride as the hydrogenating agent. These reaction schemes were not catalytic in that two moles of the chiral α -amino acid were required for each mole of substrate.

TABLE 5

Typical Substrates and Their ReductionProducts Catalyzed by $\text{HCo}(\text{CN})_5^{3-}$

<u>Substrate</u>	<u>Product</u>
Ph-CH=CHX	$\text{Ph-CH}_2\text{-CH}_2\text{X}$
R-CH=CH-COOH	$\text{RCH}_2\text{CH}_2\text{COOH}$
R-CH=CH-CHO	$\text{RCH}_2\text{CH}_2\text{CHO}$
PhC(O)C(O)Ph	PhC(O)CH(OH)Ph
$\text{RCH}_2\text{N}^+\text{O}_2^-$	RCH_2NH_2

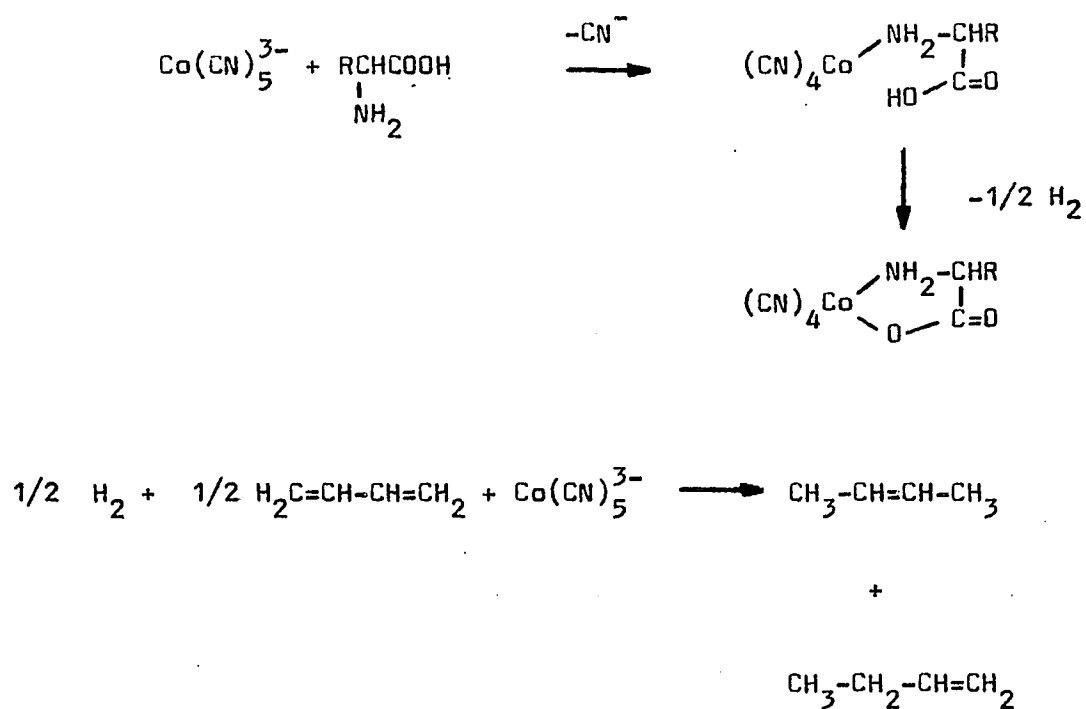


Figure 8. Co(CN)_5^{3-} Reaction with α -Amino Acids in the Presence of Butadiene.

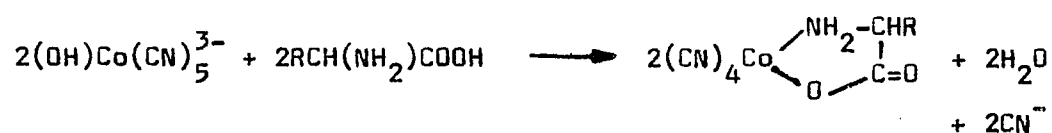
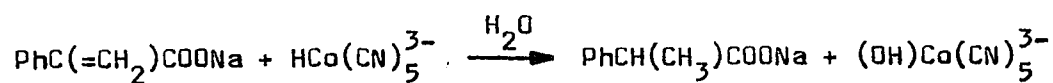
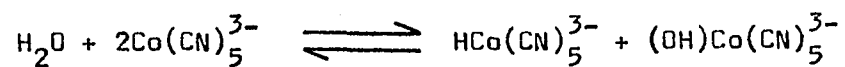


Figure 9. Ohgo's Reaction Mechanism for the Reduction of Sodium Atropate.

By using an optically active amine and H_2 in place of the optically active α -amino acid, Ohgo improved the optical yield to 7.1%.⁶⁵ The reaction was carried out over 1 atm of H_2 at room temperature. Table 6 lists the various reaction mixtures and the results.

The increase in optical yield brought about use of S-(+)-N,N'-dimethyl-1,2-propane-diamine, is attributed to steric effects, a rigid conformation of the catalyst, and the proximity of asymmetric groups to the reaction center. However, because of these steric effects, coordination of the substrate is hindered and a lower chemical yield is obtained. A catalyst with a bulky rigid structure and the ability to attract the substrate was needed if higher optical yields were to result.

Cobaloxime and Related Compounds. The low optical and chemical yields of the $Co(CN)_5^{3-}$ -amino acid systems caused Ohgo to seek a catalyst that could draw the substrate to the catalyst with a weakly attractive force.⁶⁶ Cobaloxime, with its planar ring of four nitrogen donors and rigid structure, was the system of choice and is illustrated in Figure 10.

Schrauzer and Windgassen^{67,68} report that the vitamin B_{12} model compound cobaloxime reacts with hydrogen to form a cobalt-hydride which then adds across a carbon-carbon double bond to form a cobalt-alkyl complex. If a highly reactive olefin, one with electron releasing substituents was used, the reaction stopped at this point. With less

TABLE 6
Effect of Reaction Conditions on the Reduction
of Sodium Atropate

Amine	Co	CN ⁻	Amine	Reaction Time	Yields	
					Chem.	Optical
Pn	1	4	3	3 days	99.5	1.0
Pn	1	2	3	2 days	94.5	1.1
diMePn	1	4	2	N.R.	50	7.1

N.R. = not reported

Pn = R(-)-1,2-propanediamine

diMePn = S-(+)-N,N'-dimethyl-1,2-propanediamine

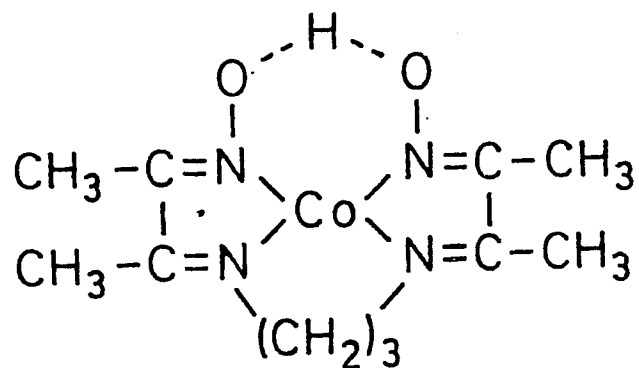
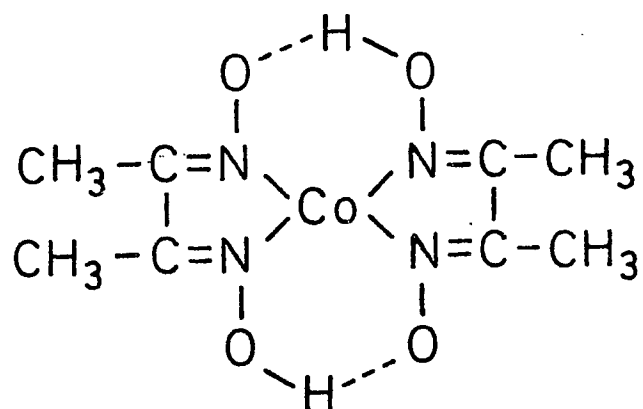


Figure 10. The Structure of Cobaloxime Type Catalysts.
 (A) $\text{Co}(\text{DMG})_2$; (B) $\text{Co}(\text{BDML}, 3\text{pn})$.

reactive olefins, hydrogenation would continue and substituted ethanes would form. Unreacted cobaloxime(I) appeared to catalyze the decomposition of the cobalt-alkyl intermediate. The reason highly reactive olefins stop at the alkyl-cobalt stage is probably due to the higher stability of this complex. The intermediate must be stable enough to form, yet not so stable as to tie up the catalyst and prevent further reaction. Only less reactive olefins meet these demands.

Cobaloxime(I) acts as a strong nucleophile in its reactions with carbon-carbon double bonds. This is due to the filled d_{z^2} orbital with its high charge density and directional characteristics.⁶⁹ Axial coordination of a strong electron donor increases the electron density in the d_{z^2} orbital and therefore increases its nucleophilicity.

Hydridocobaloxime, $\text{H-Co(DMG)}_2\text{B}$, where B is the axial base, $\text{n-Bu}_3\text{P}$, is a weak acid with a $\text{pK}_a = 10.5$.⁷⁰ It may be formed by careful acidification of an alkaline solution of cobaloxime(I), and was thought to add across double bonds to form alkyl-cobalt complexes.⁶⁸ However, in carefully dried aprotic media, the hydride did not undergo typical reactions of the cobaloxime(I). This indicated that the earlier interpretation was incorrect and that the proton screened the d_{z^2} orbital. In protic media, where the proton may dissociate, the cobalt hydride undergoes the typical reactions of cobaloxime. A strong π -backbonding ligand such as $\text{n-Bu}_3\text{P}$ is necessary if the hydride is to be isolated. If

a σ -bonding nitrogen base is the axial ligand, the hydride is short lived and difficult to isolate. In the absence of an axial base, H_2 and cobaloxime(II) are the products.⁷¹

Solutions of cobaloxime(II) activate hydrogen and are powerful hydrogenation catalysts.⁷²⁻⁷⁴ In the absence of a reducible substrate, the catalyst attacks the ligand ring system to form tetramethylpyrazine.⁷³

Simandi and coworkers investigated the activation of molecular hydrogen by cobaloxime(II)⁷³, and proposed the following mechanism, where B=axial base, Co(L)=cobaloxime:



In the absence of a reducible substrate, a $>C=NOH$ group on the ligand is reduced to $>CH-NHOH$. The coordination of pyridine in the axial position brought about a 200-300 fold increase in the reactivity towards H_2 . This was attributed to delocalization of the d_{z^2} unpaired electron of the cobaloxime(II), which increased its free radical properties and allowed homolytic splitting of the H_2 .

Ohgo and coworkers selected cobaloxime(II) as their catalyst because of its expected similarity to $Co(CN)_5^{3-}$. Its ability to catalyze activated multiply bonded carbon, nitrogen and oxygen was tested⁷⁵ and found satisfactory. With the addition of quinine, a polyfunctional asymmetric base, to the catalyst solution, asymmetric hydrogenation in high yields was finally realized.⁶⁶ Quinine and similar

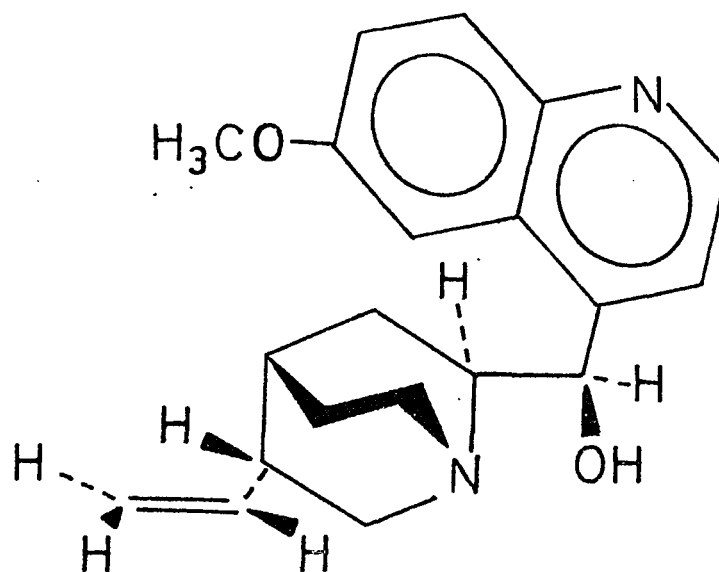
bases are illustrated in Figure 11.

Ohgo first thought that the quinine would hydrogen bond to the oxygen on the planar ring formed by the dimethylglyoxime ligands.⁷⁶ He theorized that the hydrogen bond would cause the ring to twist, and the asymmetry of the quinine would be transferred to the product. The direction of the twist would be determined by the absolute configuration of the optically active amine, at C₈ and C₉.

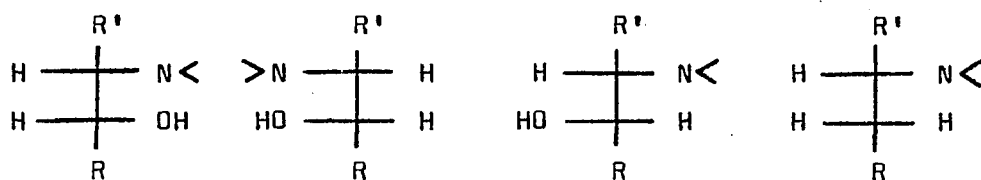
A model for the quinine-cobaloxime system was synthesized, and its structure determined.⁷⁶ The axial base, D-(-)-erythro-1,2-diphenyl-2-hydroxyethyl amine, contains the same function group, N-C-C-OH, that Ohgo postulated would twist the planar ring. However, no hydrogen bonding between the OH and the ring was observed, and the ring was undisturbed. The hydroxyl group pointed away from the ring system, and did not affect it.

The cobaloxime-quinine catalyst reduced a number of C=O and C=C substrates with varying degrees of success. Table 7 shows the results of these early experiments. The high optical yields of I and II suggest that some attractive forces between the carbonyl group of each, and the catalyst play a major role.⁷⁷

The nature of the chiral amine is very important.⁷⁸ A series of chiral amines was used to induce asymmetry into the reduction product. The configuration of the predominant product is determined by the vicinal carbons attacking amino



Quinine



I

II

III

IV

Quinine

Quinidine

ψ Ephedrine

Brucine

Cinchonidine

Ephedrine

Projections of Asymmetric Centers

Figure 11. Quinine and Related Polyfunctional Bases.

TABLE 7

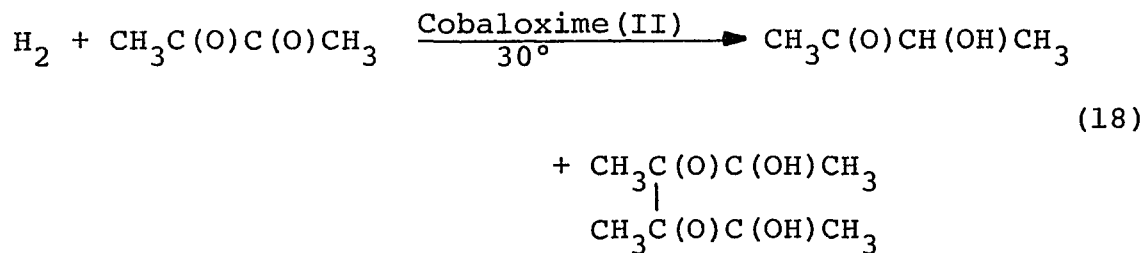
Substrates Reduced Asymmetrically by Cobaloxime-Quinine Catalyst

Substrate	Substrate/ Cobalt	Chemical Yield	Optical Yield	Configuration
PhC(O)C(O)Ph I	10	98	61.5	S
PhC(=CH ₂)C(O)Ph II	10	95	49.2	S
PhC(=CH ₂)COOCH ₃ III	9	80	7	S
CH ₃ OCNHC(=CH ₂)COOCH ₃ IV	8.4	62	19	S
PhCH ₂ ONHC(=CH ₂)COOCH ₃ V	8	60	7	S

acid hydroxyl groups, C_8 and C_9 , respectively. With brucine and S-(-)- α -methylbenzyl amine, which do not have the hydroxyl groups, there is little or no induced asymmetry. Thus the hydroxyl group plays an important role in the transfer of asymmetry. This is shown in Table 8.

Solvent and temperature also play an important part in asymmetric reactions.^{66,78} As the solvent becomes less polar, the optical yield increases. The results in a series of similar reactions are shown in Table 9. Temperature affects both the rate and the optical yield as shown in Table 10.

Reductive dimerization takes place with certain esters and diacetyl.⁷⁹ Diacetyl is reduced to acetone and a dimer, as shown below.



Lowering the temperature of the reaction, and lowering the substrate/cobalt ratio lowers the yield of the optically active dimer.

Ohgo has postulated a reaction mechanism to explain some of the puzzling features of the reduction.^{80,81} He compares the reduction to enzymes, where the catalytic sites and the selectivity determining sites are separated. Addi-

TABLE 8

Effect of Chiral Amine on Optical Yield and
Configuration of the Predominant Isomer

<u>Amine</u>	<u>Configuration from Figure 5</u>	<u>Optical Yield</u>	<u>Configuration of Predominant Isomer</u>
Quinine	I	33.8	S
Quinidine	II	33.8	R
Cinchonidine	I	33.6	S
Ephedrine	I	16.7	S
ψ Ephedrine	III	7.8	S
Brucine	IV	1.3	R
(-)- α -methyl- benzylamine	IV	0	-

TABLE 9
Effect of Solvent on the Reduction of Benzil

Run	Solvent Ratio	Chemical Yield	Optical Yield
1	MeOH	98.5	8.7
2	MeOH/ ϕ H 1.4:1	99	23
3	MeOH/ ϕ H 1.07:1	85	28
4	MeOH/ ϕ H .43:1	96.5	42
5	ϕ H	98	61.5
6	THF/ ϕ H 0.6:1	97	50
7	THF	95.5	36

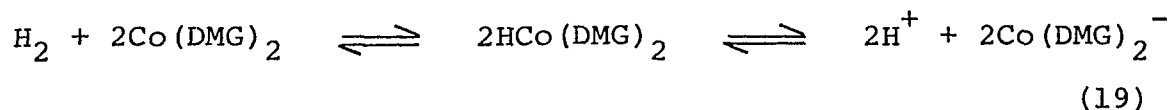
TABLE 10
Effect of Temperature on the Reduction of Benzil

Reaction Temperature	Chemical Yield	Optical Yield	Rate Constant
10°	95	71	$5.19 \times 10^{-3} \text{ min}^{-1}$
20°	95	66.7	$9.8 \times 10^{-3} \text{ min}^{-1}$
30°	99	61.5	$14 \times 10^{-3} \text{ min}^{-1}$

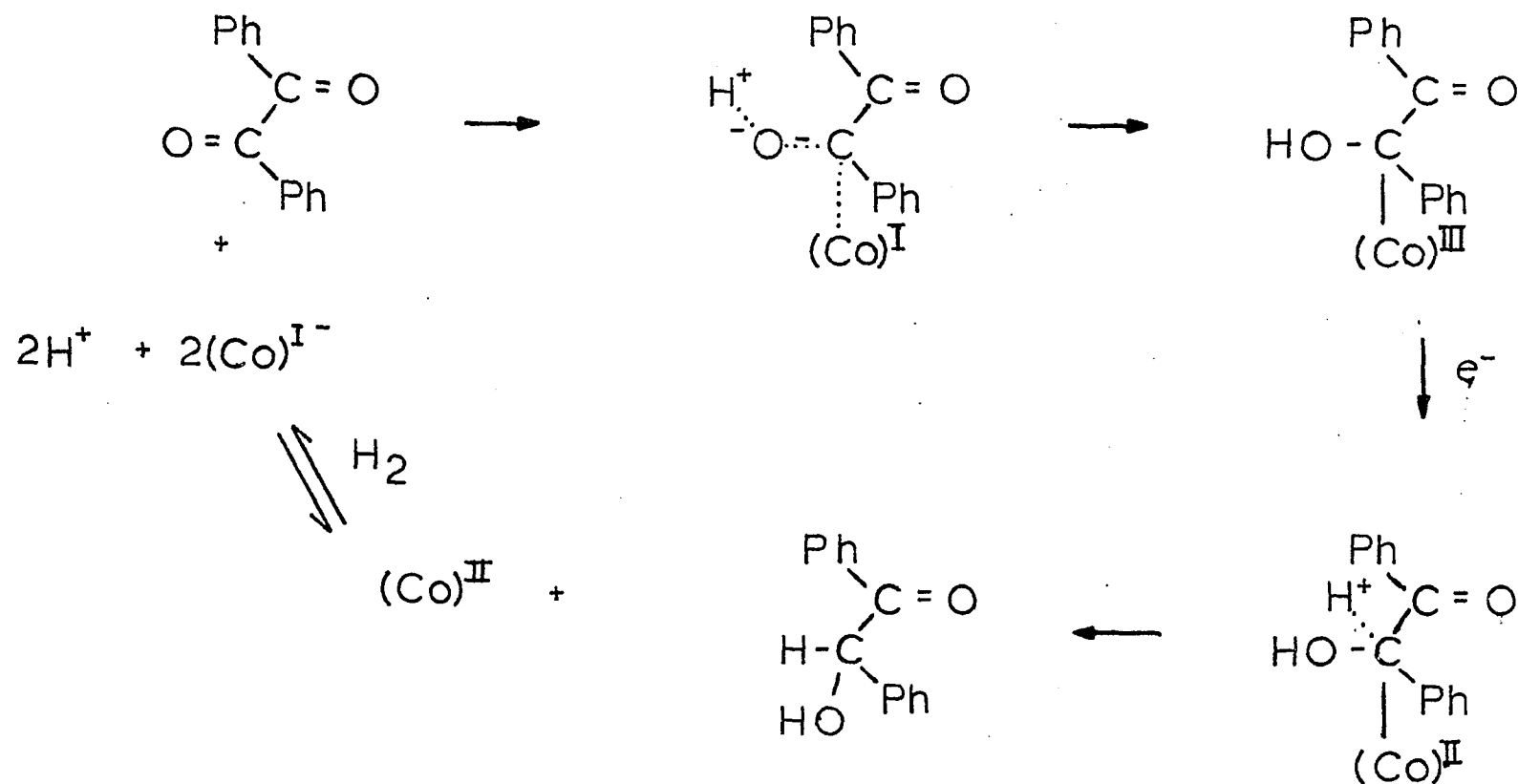
tion of an achiral base, such as benzylamine, speeds up the reduction, but does not lower the optical yield. As a rule, reaction rates increased with increasing electron donor ability of the achiral base.

This suggested that perhaps the quinine was not coordinated to the cobalt atom. Circular dichroism studies showed that $|\Delta E|$, the absolute value of the difference of the molar absorptivities for left and right circularly polarized light, increased with increasing mole ratio of quinidine/cobalt, yet was erased when an equimolar amount of benzylamine was added to the solution. Thus benzylamine selectively coordinates under these conditions.⁸⁰

If an achiral base stronger than benzylamine is used, then the optical yield is decreased. This suggests that the achiral base is in competition with the chiral amino alcohol or a possible cobalt hydride for protons to donate to the substrate. With no strong axial base, such as a phosphine, to stabilize the cobalt-hydride, the proton can ionize, and leave the cobaloxime(I) to react with the substrate.



The protons formed are free to protonate the chiral base in preparation for the first step of the reduction. Figure 12 shows the mechanism of the reduction as proposed by Ohgo.



(Co) = Cobaloxime, $\text{Co}(\text{DMG})_2$

Figure 12. Ohgo $\text{Co}(\text{DMG})_2$ Reduction Mechanism.

The cobaloxime(I) reacts with the substrate to produce an alkyl-cobaloxime(III) complex. As the cobalt-carbon bond forms, the protonated quinine donates its proton to the oxygen of the carbonyl. At this point in Ohgo's mechanism, the Co(III) intermediate is reduced to Co(II) by addition of an electron. The final step is backside attack by another protonated quinine to give the reduced substrate and cobaloxime(II).

If models of intermediates at A of Figure 12 are constructed, the one leading to the S-isomer has the least steric repulsion. The same is true for addition of the second proton to the substrate. Evidence of a backside attack was obtained by deuterogenation of R- α -methoxycarbonyl-ethyl(pyridine)bis(dimethylglyoximate)cobalt⁸⁰, whose structure had been determined by X-ray. After deuterogenation the product was S-(+)-propionic acid-2-d with S-configuration.

In support of Ohgo's mechanism, Schrauzer¹⁹ and Windgassen found that reductive cleavage is catalyzed by cobaloxime(I) which would exist in solution with the hydridocobaloxime. Also, introduction of an electronegative substituent in the α -position of an alkyl cobaloxime causes cleavage of the carbon-cobalt bond to occur more easily.¹⁹

Ricroch and Gaudemer⁸² have studied the reaction of α,β -unsaturated esters by H_2 or $NaBH_4$, in the presence of vitamin B_{12} or cobaloxime derivatives, in methanol. Three methods of reduction were studied, (a) vitamin B_{12} and

NaBH_4 ; (b) chloro(pyridine)cobaloxime(III) and NaBH_4 , and (c) pyridinecobaloxime(II)dimer and H_2 . All three methods worked equally well in the reduction of the esters, but certain esters formed stable addition products. Cobalt(II) complexes do not reduce the esters.

Some reductions are pH dependent. Reduction of methyl sorbate at pH=7 produces trans-methyl-2-hexeneoate, while at pH=9 methyl-3-hexeneoate is the product. In all cases, the reducing agent is either cobaloxime(I), vitamin $\text{B}_{12\text{s}}$ or one of the corresponding hydride forms. pH also affects the rate of reduction and the yield of the product. After 2 hr at pH=7, an 80% yield was obtained in the reduction of methyl formate, while at pH=9, only a 60% yield was obtained after 3 hr. This suggests that the cobalt hydride is the reducing agent, not the cobaloxime(I) anion. This hypothesis was confirmed by experiments performed in MeOD with NaBD_4 .

After a series of experiments in which MeOD and NaBH_4 , MeOH and NaBD_4 , or MeOD and NaBD_4 were used, it was found that one proton came from the reducing agent and one from the solvent. If NaBD_4 is used in place of NaBH_4 , the deuterium is β to the ester group. If MeOD is used in place of MeOH, a deuterium is α to the ester group.

After the cobalt hydride is formed, the first step is its addition to the conjugated double bond to form the alkyl complex. This alkyl complex is then attacked by either a hydride ion or cobaloxime(I), which causes heterolytic

rupture of the cobalt-carbon bond. The resulting carbanion then abstracts a proton from the alcohol solvent to form the final product.

Additional evidence for this mechanism was obtained by preparing a σ -alkyl cobalt complex from H_2 , cobaloxime(II) and ethyl- α -bromophenyl acetate. After 1/2 equivalent of H_2 was added, the alkyl complex was obtained in good yield. Addition of another 1/2 equivalent of H_2 resulted in ethyl phenylacetate as the final product. When the reaction is run in MeOD, the product obtained is mono-deuterated at C_2 , in accord with the formation of a carbanion intermediate.

A catalyst similar to $Co(DMG)_2$ is $Co(\alpha\text{-cqd})_2$ illustrated in Figure 13. Spectroscopic studies suggested two in-plane nitrogen and two oxygen atoms. The catalyst was used in a carbanoid reaction of a diazoacetate with styrene to form optically active cis- and trans-2-phenylcyclopropane carboxylates in above 80% optical yield.⁸² Only conjugated olefins with terminal methylene groups undergo the reaction. The use of the axial base pyridine results in decreased optical yield and slower rate of reaction. Highest optical yields are obtained at low temperature, and with bulky ester groups on the diazoacetate.

Cobalt complexes utilizing salicylaldehyde type ligands undergo reactions similar to those of cobaloxime complexes. H. Aoi and coworkers synthesized the complex lithium-N,N'-bis(salicylaldehyde)-1(R), 2(R)-1,2-trans-cyclohexanediiminatocobalt(I).⁷⁶ This complex exhibits a

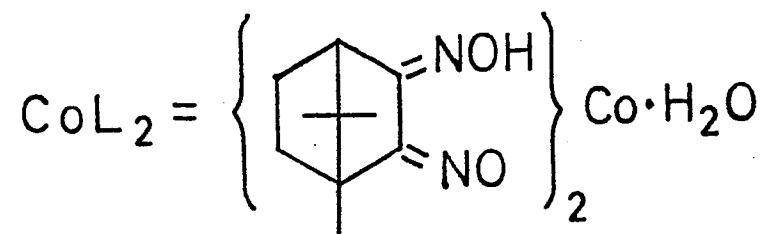
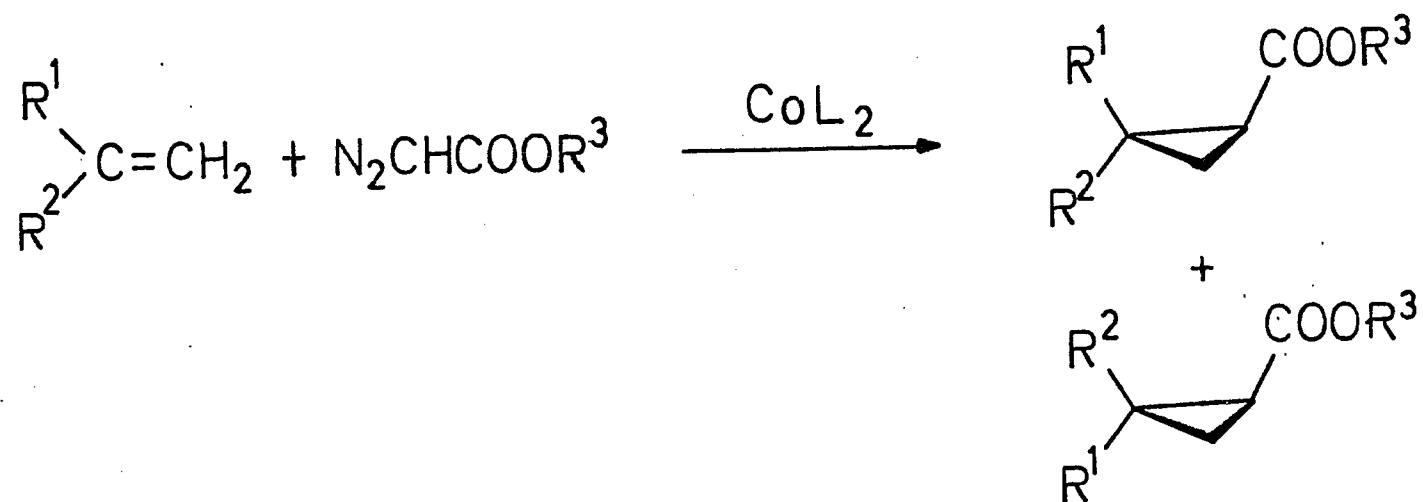


Figure 13. $Co(\alpha\text{-cqd})_2$ Catalyzed Carbenoid Reaction.

high degree of asymmetric selectivity in the resolution reaction of DL-propylene oxide. The optically active cobalt(I) complex acts as a nucleophile with the racemic propylene oxide mixture, but only the L-propylene oxide reacts to form acetone. The unreacted D-propylene oxide remains in the reaction mixture for later isolation from the acetone.

The Nature of the Research

Because of the complexities involved in catalysis research, historically it has been approached in an empirical manner. Often there are few parallels between typical metal reactions and the catalytic system itself. However, the field of cobalt-alkyl complexes has recently become an area of great interest, so it was hoped that a combination of empirical data and chemical intuition gleaned from similar compounds would lead directly to the mechanism of reduction.

One reason for the interest in cobalt-alkyl complexes is the fact that vitamin B₁₂ acts as a catalyst in the body. The central metal atom is cobalt, and one of the vitamin B₁₂ forms has a methyl group bound directly to the metal. This has spurred research in both cobalt-alkyl complexes and vitamin B₁₂ model compounds.

The model compounds studied were Co(DMG)₂ and Co(BDM1,3pn).⁺ These compounds differ in the ligand system around cobalt, but appear to react in similar ways. Because of the Ohgo research on the DMG system, the BDM1,3pn was chosen for a comparison, Figure 10.

α -Diketones and α -ketoesters were reduced by both catalysts to form α -hydroxyketones and α -hydroxyesters. In the presence of quinine, an excess of one enantiomer over the other is formed. Varying such factors as temperature, catalyst concentration, and quinine/cobalt ratio, for example, had a great effect upon the optical yield obtained for the reaction.

The complexity of the catalytic system forced a statistical approach to identify the factors that have the greatest effect on the reaction. Changing a single factor at a time can lead to erroneous results, or to long involved experiments. A factorial method of experimental design pointed out important variables. It also showed the direction to change variables to obtain the highest optical yield.

The future of asymmetric homogeneous catalysis lies in finding systems which reduce multiple bonds with 100% optical yield. These catalysts will find particular uses in organic synthesis and industrial processes. As more systems are investigated, catalyst tailoring will become a reality instead of a happy accident, and the factors which afford chemical and optical yields, as well as the mechanism, will be discovered. New catalysts will be designed and insolubilized for industrial applications. Perhaps the greatest impetus for continuing study will be the close relationship of catalysts to enzymes in the living world.

EXPERIMENTAL

Materials

Organic and inorganic compounds were used as purchased from VWR, Aldrich, Eastman or Fisher. Discolored liquids were distilled to remove the colored impurities. Solvents were dehydrated and distilled by published methods.⁸⁵

Analyses

Analyses for carbon, hydrogen and nitrogen were performed on an F&M Model 185 CHN Analyzer. Mrs. Deanna Cardin performed the analyses. Analysis for %OH in the reduced substrates were performed by an acylation method.⁸⁶

Gas Liquid Phase Chromatography

A Varian Aerograph Series 1860-1 gas chromatograph was used to identify products of some reductions. A flow-rate of 20 ml/min of N₂ was used with a 6' x 1/8" column packed with 10% QF-1 on Chromosorb W 80-100 mesh at 175°C to separate components of the reductions.

When used for quantative analysis, samples of known volume and concentration were injected into the instrument to generate a graph of instrument response vs. concentration for each compound being analyzed.

Ultraviolet-Visible Spectra

Spectra were run on a Cary 14 spectrophotometer. When samples from a reaction in progress were taken, the sample obtained from the reaction mixture was diluted to obtain an instrument readout of 0.8-1 absorbance units. When anaerobic conditions were necessary, the cell was fitted with a septum, filled with solvent, and flushed with N_2 through inlet and outlet needles. No means of controlling cell temperature was used.

Proton Magnetic Resonance Spectra

Proton magnetic resonance spectra were obtained using a JEOL JNM-MH 100 nuclear resonance spectrometer. Tetramethylsilane was used as an internal standard. D_2O was shaken with alcohol samples after the initial spectra were taken to remove the OH peak.

Optical Rotations

Optical rotations were taken on a Zeiss Photoelectric Precision Polarimeter 0.005° using 50 mm and 100 mm glass polarimeter cells. The Drude equation of the form shown in Equation 20 was used to convert rotations at 546 and 578 nm to a rotation at the sodium D-line, 589 nm.⁸⁷

$$\alpha_{589} = \frac{\frac{\alpha_{578}}{\alpha_{546} - \alpha_{578}}}{\frac{\alpha_{578}}{\alpha_{546} - \alpha_{578}} + 1.3727} \cdot \alpha_{546} \quad (20)$$

The specific rotation for the sample at the sodium D-line, α_D , was calculated from the rotation at 589 nm, α_{589} , the concentration of the sample in g/cc and the optical path length in decimeters, as shown in Equation 21.

$$\alpha_D = \frac{\alpha_{589}}{dm \text{ g/cc}} \quad (21)$$

The optical yield is the %S isomer-%R isomer and is calculated by Equation 22, where $[\alpha]_D$ is the specific rotation for the pure enantiomer, shown in Table 11.

$$\% \text{Optical Yield} = \%S - \%R = \frac{\alpha_D}{[\alpha]_D} \times 100 \quad (22)$$

Preparation of Authentic Samples

The volumes of nmr and ir spectra published by Sadtler⁸⁸ allowed identification of most products without the need of synthesizing authentic samples. However, glpc analysis of reaction yields and sample concentrations necessitated the use of known samples in known concentrations. Authentic samples of methyl mandelate and propionitrile were synthesized while all others were purchased.

TABLE 11
Conditions for Determining Optical Yield
of Various Products

<u>Product</u>	<u>Isolation</u> <u>Method</u>	<u>Solvent</u>	<u>Rotation of</u> <u>Pure Isomer</u>
$\text{CH}_3\text{C}(\text{O})\text{CH}(\text{OH})\text{CH}_3$	3	H_2O	$+105^\circ$
$\text{Ph}(\text{C}(\text{O})\text{CH}(\text{OH})\text{Ph})$	1 or 2	Acetone	$+118^\circ$
$\text{PhCH}(\text{OH})\text{COOCH}_3$	1 or 2	CS_2	$+252^\circ$
$\text{CH}_3\text{CH}(\text{OH})\text{COOCH}_3$	3	Neat	$+8.14^\circ$

Preparation of Methyl Mandelate. Mandelic acid (30.4 g, 0.20 mol), methanol (32.0 g, 1.0 mol) and 10 ml of concentrated H_2SO_4 were combined in a 500 ml round-bottom flask. After 4 hrs of reflux, the methanol was removed on the rotating evaporator and the residue was dissolved in 75 ml of CHCl_3 . The mixture was extracted with 30 ml volumes of H_2O , saturated NaHCO_3 and H_2O and then filtered through anhydrous Na_2SO_4 . The dry CHCl_3 was removed on a rotating evaporator and the product vacuum distilled, bp 108°C (1 torr); yield 27 g (82%).

Preparation of Propionitrile. Potassium cyanide, KCN, (39 g, 0.6 mol) was dissolved in 60 ml of H_2O in a 500 ml 3-neck flask fitted with condenser, addition funnel and magnetic stirrer. Ethyl iodide, $\text{CH}_3\text{CH}_2\text{I}$, (39 g, 20 ml, .25 mol) was dissolved in 200 ml of 95% EtOH and slowly added to the KCN solution. During the 1 hr necessary for the slow addition, the reaction mixture was held at 50°C .

When the ethyl iodide had been added, the mixture was slowly heated to 80°C and refluxed for 3 hrs, cooled to 0°C and the insoluble salts removed by filtration. The reaction mixture was then distilled until the distillate temperature at the top of the condenser reached 90°C . The distillate was dried (K_2CO_3) and redistilled. The liquid distilled at 77°C and was an azeotrope that consisted of 20% propionitrile, $\text{CH}_3\text{CH}_2\text{CN}$, and 80% ethanol as shown by glpc. No ethyl iodide was observed.

Catalyst Preparation. Two catalysts were investigated, $\text{Co}^{\text{II}}(\text{DMG})_2$ and $\text{Co}^{\text{II}}(\text{BDML},3\text{pn})^+$, Figure 10. Dimethylglyoxime (DMG) was used as purchased but HBDML,3pn was synthesized from 1,3-propanediamine and butanedionemonoxime.

Ligand Preparation. HBDML,3pn was prepared by the method of Schrauzer and coworkers¹⁰⁹ modified in the following way. The brownish oil formed from 0.6 mol of 2,3-butanediene-monoxime and 0.3 mol of 1,3-propanediamine was separated from the benzene reaction solvent, dissolved in 100 ml of dry acetone and allowed to stand in an ice bath until the pure ligand precipitated. The ligand was then filtered and washed with 20 ml of cold acetone, and dried in a vacuum dessicator. The acetone solutions were combined and any unprecipitated ligand was then used to form $\text{Co}^{\text{III}}(\text{BDML},3\text{pn})\text{Br}_2$.

Anal. Calcd for $\text{C}_{11}\text{H}_{20}\text{N}_4\text{O}_2$: C, 54.98; H, 8.39; N, 23.32. Found: C, 55.18; H, 8.44; N, 23.04.

Preparation of $\text{Co}^{\text{II}}(\text{DMG})_2 \cdot 2\text{H}_2\text{O}$. This catalyst was prepared by the method of Schrauzer.¹¹⁰ A measured amount of the isolated solid was added to the reaction mixture for each reduction. The dry solid remained active for several months if stored under N_2 . If stored in air, the catalyst became inactive over a period of several weeks.

The catalyst was also prepared in situ by addition of equimolar amounts of $\text{Co}(\text{OAc})_2 \cdot 4\text{H}_2\text{O}$, dimethylglyoxime and disodium dimethylglyoxime to the deoxygenated reaction solvent. If the reaction solvent was not deoxygenated by

bubbling N_2 through the solvent, the reduction would not start. No differences in activity between the two methods of preparation were noted.

Preparation of $Co^{II}(BDM1,3pn)^+$. $Co^{II}(BDM1,3pn)$ was prepared in situ for each reduction by addition of $CoCl_2 \cdot 6H_2O$ and $HBDM1,3pn$ to the reaction solvent. The addition of 20% excess ligand results in an increased optical yield. Because the catalyst is difficult to isolate it was not isolated in large quantities as was the neutral $Co(DMG)_2 \cdot 2H_2O$ catalyst.

Preparation of $Co^{III}(BDM1,3pn)Br_2$. Although the $Co^{III}(BDM1,3pn)Br_2$ was not an active catalyst, it could be reduced with $NaBH_4$ to the Co^{II} complex which is an active catalyst. Acetone was added to the acetone solutions from which the pure ligand was isolated to give a total volume of 400 ml, and this was combined with $CoBr_2 \cdot 6H_2O$ (60 g, 0.18 mol) dissolved in 100 ml of H_2O . Air was slowly bubbled through the resultant solution to form the $Co(BDM1,3pn)Br_2$, which precipitated from the solution. The product was filtered and washed with 20 ml of cold H_2O and 20 ml of cold acetone. The green crystals were soxhlet extracted with acetone to obtain pure crystals.

Reduction Procedures

All reductions were carried out in a similar manner. The chosen solvent was purged for 10-20 min with N_2 to remove dissolved O_2 which deactivated the catalyst. Next all liquid

and solid components of the reaction mixture were added while maintaining the N_2 atmosphere. Finally, the flask was flushed with H_2 , sealed, and warmed to $38^\circ C$ to activate the catalyst. The reaction mixture was then cooled to the desired temperature and allowed to run. The cooled reactions were run on an SK-2 Stir-Kool manufactured by Thermoelectrics Unlimited.

Method 1: For water insoluble substrates and products, the reaction mixture (usually 100 ml) was diluted with an equal volume of solvent, and then extracted twice with equal volumes (200 ml) of H_2O , 10% aqueous HCl , saturated aqueous $NaHCO_3$, and H_2O . The organic solvent was dried over anhydrous $MgSO_4$ and removed on a rotating evaporator.

Method 2: If the solvent was miscible with water, but the product insoluble in H_2O , the solvent was removed on a rotatory evaporator and replaced with $CHCl_3$. The above extraction process was then followed.

Method 3: If the product was water soluble, it was vacuum distilled from the reaction mixture. The distillate was then carefully distilled again to obtain a solvent-free product.

Once the product was obtained free of the solvent, chemical and optical yields were determined without any further attempt to purify the product. This prevents changes in optical yield during purification. Recrystallization of benzoin results in lowered optical activity in the

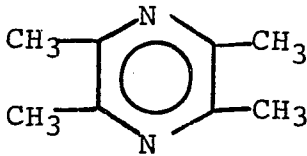
solid, and increased optical activity in the mother liquor.⁸⁰

Typical $\text{Co}^{\text{II}}(\text{DMG})_2 \cdot 2\text{H}_2\text{O}$ Reduction. $\text{Co}^{\text{II}}(\text{DMG})_2 \cdot 2\text{H}_2\text{O}$ (0.81 g, 0.0025 mol) previously prepared by the method of Schrauzer¹¹⁰, was combined with methylbenzoylformate (2.0 g, 1.7 ml, 0.012 mol) and quinine (1.90 g, 0.0050 mol) in 150 ml of deoxygenated benzene-methanol (9:1 v/v). The system was flushed with H_2 , warmed to 40°C to activate the catalyst, and then cooled to 25°C. After 48 hrs the flask was opened and 100 ml of benzene added. The mixture was then extracted by Method 1. The chemical yield as determined by glpc was 95%. The optical yield was 11.3%.

Typical $\text{Co}^{\text{II}}(\text{BDMl},3\text{pn})^+$ Reduction. Benzylamine (0.129 g, 0.131 ml, 0.0012 mol) was dissolved in 100 ml of deoxygenated benzene-methanol (9:1 v/v). $\text{CoCl}_2 \cdot 6\text{H}_2\text{O}$ (0.286 g, 0.0012 mol), HBDMl,3pn (0.288 g, 0.0012 mol), quinine (1.233 g, 0.0036 mol) and benzil (5.046 g, 0.024 mol) were added to the flask. The system was flushed with H_2 , warmed to 38°C and cooled to 30°C. After 12 hrs the flask was opened and the product isolated by Method 1. The chemical yield, as determined by the acylation method⁸⁶, was 99.8%. The optical yield was 35%.

Substrates Reduced by $\text{Co}^{\text{II}}(\text{DMG})_2 \cdot 2\text{H}_2\text{O}$. Table 12 shows the substrates reduced by $\text{Co}(\text{DMG})_2 \cdot 2\text{H}_2\text{O}$. The diketone reductions took place over a period of 3-6 hrs, while the other reductions required 24-72 hrs to go to completion. The diketones 2,3-butanedione and 1-phenyl-1,2-propanedione

TABLE 12
Substrates Reduced by $\text{Co}(\text{DMG})_2 \cdot 2\text{H}_2\text{O}$

Substrate	Substrate/Cobalt Ratio	Products	Yield	
			Chemical	Optical
$\text{PhC}(\text{O})\text{C}(\text{O})\text{Ph}$	10	$\text{PhC}(\text{O})\text{CH}(\text{OH})\text{Ph}$	99	1.0 ^a
$\text{PhC}(\text{O})\text{C}(\text{O})\text{CH}_3$	4	$\text{PhC}(\text{O})\text{CH}(\text{OH})\text{CH}_3$	60	b
		$\text{PhCH}(\text{OH})\text{C}(\text{O})\text{CH}_3$	40	b
$\text{CH}_3\text{C}(\text{O})\text{C}(\text{O})\text{CH}_3$	10	$\text{CH}_3\text{C}(\text{O})\text{CH}(\text{OH})\text{CH}_3$	80	8.0
$\text{CH}_3\text{C}(\text{O})\text{C}(\text{NOH})\text{CH}_3$	15		17	b
$\text{PhC}(\text{O})\text{C}(\text{O})\text{OCH}_3$	10	$\text{PhCH}(\text{OH})\text{COOCH}_3$	95	11.3

^aRecrystallization lowered optical yield.

^bOptical yield not figured.

formed unstable reduction products. 2-Hydroxy-3-ketone spontaneously racemizes⁸⁹ while 1-phenyl-1-hydroxy-2-propanone and 1-phenyl-2-hydroxy-1-propanone are in equilibrium at temperatures encountered in the isolation procedure.¹¹²

Substrates Reduced by $\text{Co}^{\text{II}}(\text{BDMl},3\text{pn})^+$. Table 13 lists the substrates reduced by $\text{Co}^{\text{II}}(\text{BDMl},3\text{pn})^+$. Again the diketones were reduced the fastest, followed by α -keto esters. Simple ketones and aldehydes were reduced slowly, if at all.

Methylbenzoylformate appeared to reduce smoothly to form methyl mandelate, but when several reductions were concentrated in CS_2 , a crystalline product precipitated from the solution. The unknown product had the following spectra and physical properties: mp 159-160°C; colorless platelets. An ir was compared to that of methyl mandelate. The close similarity suggests structures that are similar, but not exactly the same. Table 14 shows the spectra of each and their assignments. The bands have the same general shape and intensity, but some major bands are shifted as much as 50 cm^{-1} from the authentic sample of methyl mandelate.⁹⁰

Table 15 shows the nmr spectrum obtained, as compared to methyl mandelate. As can be seen by these assignments, the unknown does not have enough protons for two methyl esters required for a dimer. Also the protons on the aromatic ring integrate to form a trimer, as do the alcohol protons.

CHN analysis of the unknown is equally baffling. The % oxygen was found by difference in the analyzed samples. Table 16 shows the results of calculations for methyl

TABLE 13
Substrates Reduced by Co (BDML, 3pn)⁺

Substrate	Substrate/Cobalt Ratio	Products	Yield	
			Chemical	Optical
PhC(O)C(O)OCH ₃	6	PhCH(OH)COOCH ₃ a	93	48.2
PhC(O)C(O)Ph	20	PhC(O)CH(OH)Ph	99	79.2
PhCHO	35	PhCH ₂ OH	34	b
PhC(O)CF ₃	7	PhCH(OH)CF ₃	65	0
CH ₃ C(O)C(O)OH	11	CH ₃ CH(OH)C(O)OH	trace	b
C ₂ H ₅ O(O)CH(CH ₃)C(O)C(O)OC ₂ H ₅	5	c	≈70	b
CH ₃ C(O)C(O)OCH ₃	15	CH ₃ CH(OH)C(O)OCH ₃	97	48.1

^aUnknown racemic product in unknown yield.

^bOptical yield not calculated.

^cImpure starting material was reduced, exact nature of reduction product was not elucidated.

TABLE 14

IR Comparison of Unknown Product and Methyl Mandelate

<u>Methyl Mandelate</u>	<u>Unknown</u>	<u>Assignment</u>
3450 cm^{-1}	3500 cm^{-1} 3400	OH stretch
3030	3050	Ar-H stretch
2940	2960	C-H stretch
1750	1705	C=O stretch
1502	1500	Aromatic Skeletal vibrations
1460 1440	1450	Aromatic Skeletal vibrations
1190	1180	C-O stretch, esters
1073	1065	C-O stretch, alcohols
1030	1025	Aromatic in plane bending
736	715	Aromatic C-H bend
695	644	Aromatic C-H bend

TABLE 15
NMR Comparison of Unknown Product
and Methyl Mandelate

<u>Methyl Mandelate</u>	<u>Unknown</u>	<u>Assignment</u>
7.19 (5) ^a	7.07 (15)	Ar-H OH
5.06 (1)	5.38 (2)	Ø-C-COOR <u>H</u>
3.65 (3)	2.77 (3)	COOC- <u>H</u> ₃
3.52 (1)	6.77 (3)	Co- <u>H</u>

^aδ value (number of protons).

TABLE 16
CHN Analyses of Unknown Product

	Calculated		Found		
	Methyl Mandelate	Dimer	Crude Crystals	Recrystallized Crystals	Recrystallized and High Temperature Dried Crystals
%C	65.05	65.44	63.88	64.16	63.34
%H	6.07	5.49	5.29	5.46	4.96
%O ^a	28.88	29.06	30.87	30.38	31.70

^aBy difference.

mandelate and a possible dimer formed. Formation of a trimer would require even higher carbon and oxygen percentages, at the expense of hydrogen.

Diethyloxalpropionate was badly contaminated as purchased, but H_2 was taken up under typical reduction conditions. GLPC analysis of the starting material showed peaks at 28 and 88 mm from the injection point and the product showed peaks at 28, 57 and 74 mm. Individual compounds were not isolated, but the compound that eluted at 88 mm was completely reduced after 48 hrs.

Reaction Conditions Investigated

Numerous reaction conditions were investigated with varying degrees of success. Table 17 shows the reaction variables investigated for each catalyst. Early experiments with different solvents investigated the speed of reduction. Non-polar solvents did not dissolve the catalyst, so only mixed solvents, or moderately polar organic solvents, were investigated. Table 18 shows that only in dioxane was methyl benzoylformate reduced at a reasonable rate. An asymmetric reduction with the solvent dioxane resulted in a 4.4% optical yield. This corresponds to an optical yield of 8.8% under identical reaction conditions using benzene-methanol (9:1 v/v) as the solvent.

When dioxane was used as the solvent, the reaction solution turned deep blue as soon as H_2 was added. While

TABLE 17

Reaction Conditions Investigated

Co(DMG) ₂ ·2H ₂ O Catalyst	Co(BDML,3pn) ⁺ Catalyst
Temperature (5-40°C)	Temperature (-10-30°C)
Time (3-72 hrs)	Time (3-72 hrs)
Axial Bases ^a	Axial Bases ^a
Quinine/Cobalt Ratio (1-2)	Quinine/Cobalt Ratio (1-4)
Base/Cobalt Ratio (0-2)	Base/Cobalt Ratio (0-1)
	Ligand/Cobalt Ratio (1-1.2)
	Substrate/Cobalt Ratio (6-25)
	Catalyst Concentration (0.008 to 0.020M)
	Solvent ^b
^a Bu ₃ P, Ph ₃ P, Et ₃ N, PhCH ₂ NH ₂	^b See Table 18

TABLE 18
Effect of Solvent Upon the Reaction

Solvent	Reduction Rate	Time	Chemical Yield
Dioxane	Rapid	4 hrs	98%
CH ₃ Cl ₂ -MeOH (9:1 v/v)	NR ^a	--	--
Acetone	NR	--	--
Acetic Acid (Glacial)	Slow	15 days	60%
Benzene-MeOH (9:1 v/v)	Rapid	4 hrs	98%
Toluene-MeOH (9:1 v/v)	Rapid	4 hrs	98%
Toluene-2-propanol (9:1 v/v)	Moderate	24 hrs	98%
Toluene-2-methyl-2-propanol (9:1 v/v)	Slow	40 hrs	82%

^aNR = No Reaction

the solution remained blue, no reduction took place. After about 1 hr, the solution turned red-orange and reduction began. This suggests stabilization of the $\text{Co}^{\text{I}}(\text{BDM1,3pn})$ at the expense of reduction. Also, use of a water miscible solvent increased the complexity of the reaction work up by Method 2. The solvent had to be removed on a rotating evaporator before a water immiscible solvent could be added for the extraction procedure.

Toluene was investigated as a possible replacement for benzene. Benzene is a toxic substance that should be handled with care.^{91,92} The alkyl derivatives are less toxic, with the allowable concentration of toluene vapor 20 times higher than benzene. Early experiments indicated that the use of toluene in place of benzene caused a slight reduction in optical yield. When low temperature studies were performed, the higher freezing point of benzene negates this advantage.

Factorial Experiments

Four factorial experiments were performed, a six factor screening experiment, two two-factor experiments and one three-factor experiment. Taken together they give many clues to the mechanism of the reduction.

Six Factor Screening Factorial. Six factors, listed in Table 19, were studied. A total of 40 runs were made as outlined in "Statistical Analysis of Data". The reactions

TABLE 19

Proposed Major Variables and Their Settings

Variable	Letter Designation ^a	High	Settings Center	Low
Catalyst Concentration	A	0.012M	0.010	0.008
Quinine/Cobalt Ratio	B	3	2	1
Benzylamine/Cobalt Ratio	C	1	0.5	0
Substrate/Cobalt Ratio	D	20	15	10
Temperature	E	30°C	18.5°C	7°C
Reaction Time	F	12 hrs	9 hrs	6 hrs

^aOn Tables 22, 24.

were run as described previously. The eight reactions run at the center point were divided equally between the two types of apparatus to insure that any contribution by one would be cancelled by the other. Because only one warm and one cold reaction may be run each day, randomization was restricted to give this arrangement. Tables 20 and 21 show the results of the 40 runs.

First Two Factor Factorial. Because the screening factorial gave ambiguous results when catalyst concentration was involved with other factors, a small factorial was designed to investigate this factor further. Figure 14 shows the conditions under which this factorial was run. Because only 5 runs were needed to explore the experimental surface, each set of conditions was run twice to facilitate error analysis. Figure 14 shows the results of this factorial experiment.

Three Factor Factorial. In the screening factorial, catalyst concentration, substrate/cobalt ratio and time were important as three two-factor interaction and the three-factor interaction. Only the catalyst concentration was significant by itself. Table 22 lists the reaction conditions and the results obtained for each run. The last four runs are for error analysis and a test of the experimental surface.

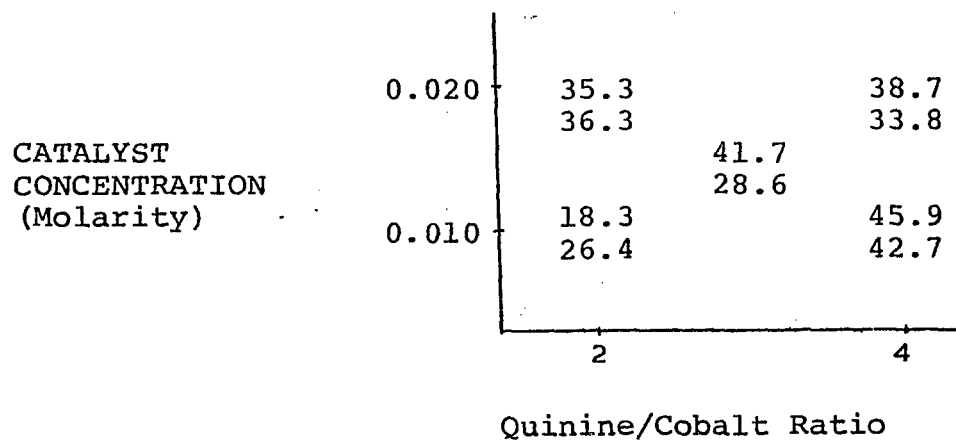
Second Two Factor Factorial. A final factorial to test the effects of the percent methanol in benzene and the ligand/cobalt ratio was performed. Figure 15 shows the

#	Main Effects						Two Factor Interactions										Confounded Three Factor Interactions										%EE					
	A	B	C	D	E	F	AB	AC	AD	AE	AF	BC	BD	BE	BF	CD	CE	CF	DE	DF	EF	DEF ABC	DEF ABD	DEF ABE	DEF ABF	DEF ACD		DEF ACE	DEF ACF	DEF ADE	DEF ADF	DEF AEF
1	+	+	+	+	+	+	+	+	+	+	+	+	+	+	+	+	+	+	+	+	+	+	+	+	+	+	+	+	+	+	+	35.0
2	-	-	+	+	+	+	+	-	-	-	-	-	-	-	-	+	+	+	+	+	+	+	+	+	+	-	-	-	-	-	-	10.2
3	-	+	-	+	+	+	-	+	-	-	-	-	+	+	+	-	-	-	+	+	+	+	-	-	-	+	+	+	-	-	-	26.6
4	+	-	-	+	+	+	-	-	+	+	+	+	-	-	-	-	-	-	+	+	+	+	-	-	-	-	-	-	+	+	+	10.8
5	-	+	+	-	+	+	-	-	+	-	-	+	-	+	+	-	+	+	-	-	+	-	+	-	-	+	-	+	+	-	-	44.1
6	+	-	+	-	+	+	-	+	-	+	+	-	+	-	-	-	+	+	-	-	+	-	+	-	-	-	+	+	-	-	+	26.0
7	+	+	-	-	+	+	+	-	-	+	+	-	-	+	+	+	-	-	-	-	+	-	+	+	+	+	-	-	-	-	+	43.8
8	-	-	-	-	+	+	+	+	-	-	+	+	-	-	-	+	-	-	-	-	+	-	+	+	+	-	+	+	+	+	-	6.4
9	-	+	+	+	-	+	-	-	-	+	-	+	+	-	+	+	-	+	-	+	-	-	-	+	-	-	+	-	+	-	+	59.7
10	+	-	+	+	-	+	-	+	+	-	+	-	-	+	-	+	-	+	-	+	-	-	-	+	-	+	-	+	-	+	-	14.0
11	+	+	-	+	-	+	+	-	+	-	+	-	+	-	+	-	+	-	-	+	-	-	+	-	+	-	+	-	-	+	-	54.5
12	-	-	-	+	-	+	+	-	+	-	+	-	+	-	+	-	+	-	-	+	-	-	+	-	+	+	-	+	+	-	+	16.1
13	+	+	+	-	-	+	+	+	-	-	+	+	-	-	+	-	-	+	+	-	-	+	-	-	+	-	-	+	+	-	-	53.1
14	-	-	+	-	-	+	+	-	+	+	-	-	+	+	-	-	-	+	+	-	-	+	-	-	+	+	+	-	-	+	+	10.2
15	-	+	-	-	-	+	-	+	+	+	-	-	-	-	+	+	+	-	+	-	-	+	+	+	-	-	+	-	+	+	+	23.7
16	+	-	-	-	-	+	-	-	-	-	+	+	+	+	-	+	+	-	+	-	-	+	+	+	-	+	+	-	+	-	-	46.4
17	-	+	+	+	+	-	-	-	-	-	+	+	+	+	-	+	+	-	+	-	-	-	-	-	+	-	-	+	-	+	+	42.5
18	+	-	+	+	+	-	-	+	+	+	-	-	-	-	+	+	+	-	+	-	-	-	-	-	+	+	+	-	+	-	-	16.0
19	+	+	-	+	+	-	+	-	+	+	-	-	+	+	-	-	-	+	+	-	-	-	+	+	-	-	-	+	+	-	-	45.7
20	-	-	-	+	+	-	+	+	-	-	+	+	-	-	+	-	-	+	+	-	-	-	+	+	-	+	+	-	-	+	+	9.7
21	+	+	+	-	+	-	+	+	-	+	-	+	-	+	-	-	+	-	-	+	-	+	-	+	-	-	+	-	-	+	-	40.5
22	-	-	-	+	+	-	+	-	+	-	+	-	+	-	+	-	+	-	+	-	+	-	+	-	+	-	+	+	+	-	+	9.7
23	-	+	-	-	+	-	-	+	+	-	+	-	+	-	+	-	+	-	+	-	+	-	+	-	+	-	+	-	+	-	+	27.2
24	+	-	-	-	+	-	-	-	+	-	+	+	-	+	+	-	+	-	+	-	+	-	+	-	+	+	-	+	-	+	-	9.3
25	+	+	+	+	-	-	+	+	+	-	-	+	+	-	-	+	-	-	-	+	+	+	-	-	-	+	-	-	-	-	+	48.5
26	-	-	+	+	-	-	+	-	-	+	+	-	-	+	+	+	-	-	-	+	+	+	-	-	-	+	+	+	+	+	-	14.5
27	-	+	-	+	-	-	-	+	-	+	+	-	+	-	-	-	+	+	-	+	+	-	+	+	+	-	-	+	+	-	-	59.1
28	+	-	-	+	-	-	-	+	-	-	+	-	+	-	+	+	-	+	+	-	+	+	-	+	+	-	+	+	-	-	+	9.9
29	-	+	+	-	-	-	-	+	+	+	+	-	-	-	-	-	-	+	+	+	-	+	+	+	+	+	+	-	-	-	-	53.9
30	+	-	+	-	-	-	-	+	-	-	-	-	+	+	+	-	-	-	+	+	+	-	+	+	+	-	-	-	+	+	+	12.9
31	+	+	-	-	-	-	+	-	-	-	-	-	-	-	-	+	+	+	+	+	+	-	-	-	-	+	+	+	+	+	+	33.5
32	-	-	-	-	-	-	+	+	+	+	+	+	+	+	+	+	+	+	+	+	+	-	-	-	-	-	-	-	-	-	-	7.2

TABLE 20. Design Matrix and Optical Yields Obtained for Screening Factorial Experiment.

TABLE 21
Center Points of Fractional Factorial

<u>Run #</u>	<u>Optical Yield</u>
1	20.4
2	16.7
3	26.7
4	22.4
5	20.9
6	26.2
7	19.9
8	22.3



Variables

	<u>High</u>	<u>Setting</u> <u>Center</u>	<u>Low</u>
Catalyst Concentration	0.020	0.015	0.010
Quinine/Cobalt Ratio	4	3	2

Constant Settings

Benzylamine/Cobalt Ratio = 1
 Substrate/Cobalt Ratio = 20
 Temperature = 30°C
 Reaction Time = 11 hrs

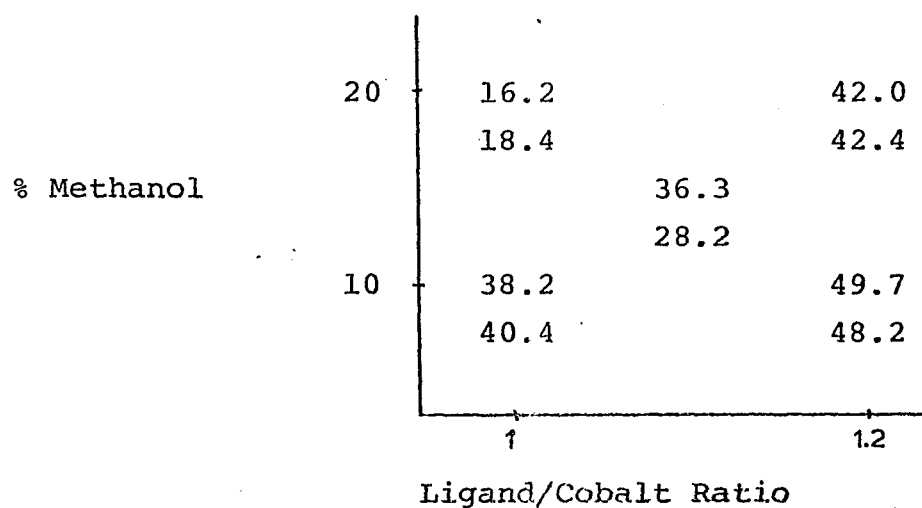
Figure 14. First Two Factor Experiment.

TABLE 22

Results of Three Factor Factorial Experiment

Reaction ^a Number	Catalyst Concentration	Substrate/Cobalt Ratio	Time (hrs)	Optical Yield
1	0.016	25	24	17.1
2	0.010	25	24	28.1
3	0.016	15	24	19.8
4	0.010	15	24	21.6
5	0.016	25	12	29.3
6	0.010	25	12	42.1
7	0.016	15	12	33.9
8	0.010	15	12	19.4
9	0.013	20	18	27.0
10	0.013	20	18	26.4
11	0.013	20	18	30.6
12	0.013	20	18	34.8

^aTemperature 30°C, Benzylamine/Cobalt = 1
Quinine/Cobalt = 3



<u>Variables</u>	<u>Settings</u>		
	<u>High</u>	<u>Center</u>	<u>Low</u>
% Methanol	20	15	10
Ligand/Cobalt Ratio	1.2	1.1	1.0

Constant Settings

Catalyst Concentration = 0.010M
 Quinine/Cobalt Ratio = 3
 Benzylamine/Cobalt Ratio = 1
 Substrate/Cobalt Ratio = 20
 Temperature = 30°C
 Time = 12 hrs

Figure 15. Second Two Factor Experiment.

results of this factorial, and lists reaction conditions. The factors from the screening factorial were set at levels predicted as best from the previous factorial experiments.

Reactions Leading Directly to the Mechanism

While the factorial experiments suggested possible steps in the mechanism, they did not specify exactly what the mechanism is. Individual experiments were performed for this.

Racemization of Benzoin. Optically active benzoin (5 gm) was placed in 100 ml of 9:1 benzene-methanol (v/v), and H_2 placed over the solution. Samples were withdrawn at 6 hr intervals and placed in a polarimeter to check optical rotation. No loss of optical rotation was noted. After 48 hrs and at 48 hr intervals, the following substances were added: benzylamine (0.129 g, 0.131 ml, 0.0012 mol); quinine (1.233 g, 0.0036 mol); $CoCl_2 \cdot 6H_2O$ (0.286 g, 0.0012 mol) and HBDM1,3pn (0.288 g, 0.0012 mol). The optical rotation remained constant until $CoCl_2 \cdot 6H_2O$ was added. At this point, there was slow loss in optical rotation until HBDM1,3pn was added. At this point the solution was deeply colored and rotations could not be accurately determined.

Addition of CH_3I to the Reduction Mixture. Two typical 0.01M catalyst concentration reactions were run in the usual manner except for the following. The first reduction was started and allowed to run until the reduction was

1/2 completed (1 hr). The methyl iodide (1 ml, 2.28 g, 0.016 mol) was added. Reduction quickly ceased. The second reduction was run in the same manner except no H_2 was added to start the reduction. Again methyl iodide was added after 1 hr.

Aliquots were withdrawn from the reaction mixtures and shaken with water 45 min after addition of the MeI. Visible spectra were then taken of each water solution. This was repeated every 45 min for 6 hr. The first reaction flask (with H_2) contained a constant concentration of $MeCo(BDML,3pn)^+$ in each determination, equal to 0.00927M. In the case of the second reaction mixture (without H_2) the concentration of $MeCo(BDML,3pn)^+$ increased steadily for 5 hrs before becoming constant at 0.00464M. After 24 hrs, the concentration in the reaction flask was 0.00465M.

Formation and Reactions of $Co^I(BDML,3pn)$. $Co^{III}-(BDML,3pn)Br_2$ was suspended in deoxygenated methanol. $NaBH_4$ in methanol (pH=13 by addition of NaOH) was slowly added until the solution just remained blue, indicating formation of the $Co^I(BDML,3pn)$. The complex decomposed after 1/2 to 2 hrs unless an axial base such as benzylamine or triphenylphosphine was added to stabilize the $Co^{(I)}$ oxidation state.

Addition of a substrate such as $CH_3C(O)C(O)CH_3$ or $\phi C(O)COOCH_3$ caused the blue $Co^{(I)}$ color to disappear, with a red solution, the color of $Co^{II}(BDML,3pn)^+$, to appear. Addition of $CH_2=CHCN$ caused no color change. Addition of weak acids of $pK_a > 4$ caused no color change, but if strong

acids, $pK_a < 3$, were added, the solution turned light yellow. Addition of a base such as NaOH in MeOH caused the solution to again turn deep blue. This blue-yellow to blue cycle could be repeated several times. Addition of CH_3I to the blue solution results in formation of orange solution of $CH_3Co^{III}(BDM1,3pn)^+$.

Formation and Reactions of $HCo^{III}(BDM1,3pn)^+$. $HCo^{III}-(BDM1,3pn)^+$ was prepared by addition of $HClO_4$ to a previously prepared solution of $Co^I(BDM1,3pn)$ stabilized by addition of excess benzylamine. When the solution changed color from blue to yellow, addition of $HClO_4$ was stopped. Addition of excess acid had no effect upon the $HCo(BDM1,3pn)$. Addition of $CH_3C(O)C(O)CH_3$, MeI and $CH_2=CHCN$ resulted in no color change. Addition of NaOH in MeOH results in solutions typical of $Co^I(BMD1,3pn)$ above.

Deuterium Experiments. (A) A typical reduction was run substituting MeOD for MeOH. Workup of the product by Method 1 showed (by nmr analysis) 55% deuterium incorporation in the product, $PhC(O)CD(OH)Ph$. (NOTE: Method 1 extraction was used, so possible D on the alcohol is replaced by H from water.)

(B) A typical reduction was run using MeOD and D_2 in place of MeOH and H_2 . NMR analysis of the product showed 40% deuterium incorporation on the hydroxyl carbon, $PhC(O)CD(OH)CH$.

(C) A typical reduction was run using MeOD and D_2 in place of MeOH and H_2 . No axial base was added. NMR analysis of the product showed 50% deuterium incorporation on the hydroxyl carbon, $PhC(O)CD(OH)Ph$.

(D) A typical reduction was run using MeOH and D_2 in place of H_2 . NMR analysis of the product showed 5% deuterium incorporation on the hydroxyl carbon, $PhC(O)CD(OH)Ph$.

STATISTICAL ANALYSIS OF DATA

A statistical approach to the study of these catalytic reductions was chosen for five reasons:

(1) The complexity of the system caused meaningless results when only one variable at a time was changed.

(2) The different variables must be examined without personal bias.

(3) Factorial experiments furnish the greatest amount of information for the least number of experiments performed.

(4) Significant effects may be separated from insignificant ones.

(5) The effect of one variable on other variables may be measured.

More complete discussions of factorial experiments may be found in References 93-96.

The use of a 2^n factorial design allows one to simultaneously investigate a number of different factors, termed independent variables. When there are n factors to be considered, 2^n experiments are necessary for all combinations of factors, with each factor set at a high and low value. When the required number of experiments are completed, all factors and their combinations may be ranked in the order of their effect on the response (or dependent) variable. An analysis of variance (ANOVA) will then tell the experimenter which factors and combinations have a significant effect on

the response variable.

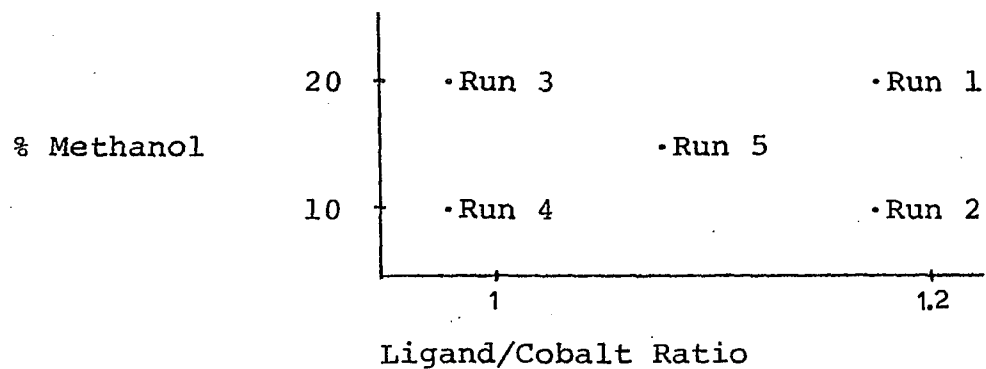
Experimental Design

The first step in setting up a 2^n factorial design is to list all factors that may have an effect on the response variable. Next, factor settings should be chosen in a manner that will adequately cover a range that is normally encountered by the experiment. If one normally uses reagents in 0.01M concentration, a concentration factor set at 0.10M would lie outside the normally encountered range, so results from the factorial experiment would not be applicable to the usual experimental conditions.

Once the factor settings are established, the high level is coded + and the low level -. ⁹⁷ The setting half way between the two may be coded 0. Figure 16 shows the experimental plan for a 2^n factorial with 2 factors in a typical experiment. $2^2 = 4$ Experiments must be run to obtain the peripheral points (Runs 1 to 4). A center point is also run to detect a maximum or minimum at the center of the experimental space (Run 5). 20% MeOH and 1.2:1 L/Co are coded +, and 10% MeOH and 1:1 L/Co -. Small factorials may also be represented graphically as shown.

In order to avoid any bias, the order in which the experiments are performed is randomized. ⁹⁸ With a repetitious operation, the order of events may be important for two reasons. A learning process may be involved that makes

Run	% Methanol (level)	Ligand/Cobalt Ratio (level)
1	20 (+)	1.2 (+)
2	10 (-)	1.2 (+)
3	20 (+)	1.0 (-)
4	10 (-)	1.0 (-)
5	15 (0)	1.1 (0)



Graphic Representation

Figure 16. Experimental Plan for a 2^2 Factorial.

later operations more efficient, or carelessness may have an opposite effect on later operations. The aging of reagents could also affect experimental results. Such systematic bias can be avoided by randomizing the order in which the experiments are performed. To randomize a set of experiments, either a random number generator (such as some modern calculators) or a random number table may be used. The experiments are then run in this random order.

Mathematical Operations

A design matrix is generated by listing the coded factors for each run, and the signs of the interactions of the coded factors. The interaction of X_1 and X_2 is X_1X_2 and is generated by multiplying the signs of X_1 and X_2 together. Table 23 shows a design matrix for a two factor factorial, with response variables R_{jk} with the runs they represent.⁹⁹ For n factors, there are n main effects, $n(n-1)/2$ two factor interactions, $n(n-1)(n-2)/6$ three factor interactions, and so on, to

$$\frac{n(n-1)(n-2)\dots(n-(n-1))}{(1)(2)(3)\dots(n)}$$

The statistical analysis of the results is straightforward.¹⁰⁰ A response matrix is generated by multiplying the response variable R_{jk} times each coded element of the design matrix for that particular set of experimental conditions. Each column is then summed to obtain the product summation for that particular variable. All general equations

TABLE 23

General Design Matrix for 2^2 Factorial

Run	Factors and Interactions			Response Variable	
	x_1	x_2	x_1x_2	R	
1	x_{11}	x_{21}	x_{31}	R_{11}	R_{12}
2	x_{12}	x_{22}	x_{32}	R_{21}	R_{22}
3	x_{13}	x_{23}	x_{33}	R_{31}	R_{32}
4	x_{14}	x_{24}	x_{34}	R_{41}	R_{42}
5	x_{15}	x_{25}	x_{35}	R_{51}	R_{52}

i = 2 variables and 1 interaction

j = 5 sets of conditions

k = 2 replications

refer to i factors and interactions, j number of sets of experimental conditions and k number of replications of the experimental design. X_i is the i th factor or interaction, Equation 1. PS is the Product Summation.

$$\text{Product Summation for } X_i = \sum_{j=1}^j \sum_{k=1}^k x_{ij} (R_{jk}) = \text{PS} \quad (23)$$

From Figure 17 Product Summation of $X_1 = -57.9$.

The product summation is the total effect that X_i exerts over all experiments performed.

The calculated effect for X_i is a measure of the average effect X_i has on the response variable. By squaring x_{ij} , all signs are removed and the result is that the denominator is the number of reactions run at the peripheral points, Equation 24.

$$\text{Calculated Effect for } X_i = \frac{2 \sum_{j=1}^j \sum_{k=1}^k x_{ij} (R_{jk})}{\sum_{k=1}^k \sum_{j=1}^j (x_{ij})^2} = \frac{2\text{PS}}{j \cdot k} \quad (24)$$

From Figure 17 Calculated Effect for $X_1 = -14.475$.

Note that the calculated effect for X_i is twice the product summation divided by the number of peripheral reactions.

To determine what factors and interactions are significant, an analysis of variance may be utilized. The sum of

Runs	X_1	X_2	X_1X_2	R_{j1}	R_{j2}
1	+	+	+	42.0	42.4
2	-	+	-	49.7	48.2
3	+	-	-	16.2	18.4
4	-	-	+	40.4	38.6
5	0	0	0	36.3	38.2

Source of Variation	Analysis of Variance		Sum of Squares	Degrees of Freedom	Variance	F	95% Significant
	Product Summation	Calculated Effect					
X_1	-57.9	-14.475	419.05	1	419.05	297.2	yes
X_2	68.7	17.175	589.96	1	589.96	418.4	yes
X_1X_2	30.9	7.725	119.35	1	119.35	84.6	yes
Lack of Fit			0.11	1	0.11	0.1	no
Error			7.05	5	1.41	1.0	no
Correction Term			<u>13719.62</u>	<u>1</u>			
TOTAL			14855.14	10			

$n_1 = 1; n_2 = 5; F = 6.61$

Figure 17. 2^2 Factorial Design and Results

squares for each factor and interaction (each X_i) may be calculated by squaring the product summation and dividing by the number of reactions run at the peripheral points, Equation 25.

$$\text{Sum of Squares for } X_i = \frac{\frac{1}{j} \frac{1}{k} (\sum_j \sum_k x_{ij} R_{jk})^2}{k \sum_{j=1}^k (x_{ij})^2} = \frac{(PS)^2}{j \cdot k} \quad (25)$$

From Figure 17 Sum of Squares for $X_1 = 419.05$.

Next, an error term, a lack of fit term and a correction term may be calculated. These terms, when added to the sums of squares for the X_i 's, equal a total sum of squares term that may be calculated separately. If the two totals do not agree, a calculation error is indicated.

The error sum of squares is the sum of squares of the deviation from an average¹⁰¹, and its calculation is dependent upon the experimental design. If each point in the experimental design is duplicated, the error sum of squares would be equal to the sum of the difference between duplicate measurements, squared, and then divided by two, Equation 26.

For Duplicates:

$$\text{Error Sum of Squares} = \frac{\sum_{j=1}^j (R_{j1} - R_{j2})^2}{2} \quad (26)$$

From Figure 17 Error Sum of Squares = 7.05.

If more than two replications are made, the formula assumes the form of Equation 27.

$$\text{Error Sum of Squares} = \sum_{j=1}^j \sum_{k=1}^k (R_{jk} - \bar{R}_j)^2 \quad (27)$$

where j is the number of sets of conditions replicated, k is the number of replications for each j and \bar{R}_j is the average response variable for the conditions specified for the j th setting.

If a large factorial design is undertaken, the number of experiments becomes prohibitive if duplicate experiments are run on each point. Error may be calculated by running, one point in the design $n + 1$ times, where n is the number of factors. The center point is usually the chosen point. This approach assumes that the error is approximately constant in the experimental space. If this form of error estimation is chosen, the equation for error sum of squares has the form of Equation 28.

$$\text{Error Sum of Squares} = \sum_{k=1}^k (R_{jk} - \bar{R}_j)^2 \quad (28)$$

where k is the number of replications of the point and \bar{R}_j is the average of response of the k points.

Because the center point response is not always the average of the peripheral point responses, a lack of fit

term must be calculated.¹⁰² This sum of squares term must be added to the other sums of squares because the center and peripheral point averages are not equal. If the lack of fit term is large, a curvature in the experimental response surface is indicated, and smaller ranges of the factors should be chosen, Equation 29.

$$\text{Sum of Squares Lack of Fit} = \frac{N_c N_p}{N_c + N_p} (\bar{R}_c - \bar{R}_p)^2 \quad (29)$$

From Figure 17 Lack of Fit = $\frac{(2)(8)}{10}(36.99-37.25) = 0.11$.
 where N_c = number of center experiments, \bar{R}_c = average center experiment, N_p = number of peripheral experiments, \bar{R}_p = average peripheral experiment.

A correction term¹⁰³ may be obtained by totaling the response variables, R_{jk} , squaring the total and dividing by the number of experiments performed, Equation 30.

$$\text{Correction Term Sum of Squares} = \frac{\sum_j \left(\sum_k R_{jk} \right)^2}{\sum_k \left(\sum_j x_{ij} \right)^2} \quad (30)$$

From Figure 17 Correction Term = 13719.62

This correction term allows one to check all sums of squares calculations. The total sum of squares should equal all sums of squares computed, and may be separately calculated, Equation 31.

$$\text{Total Sum of Squares} = \sum_{j=1}^j \sum_{k=1}^k (R_{jk})^2 \quad (31)$$

From Figure 17 Total = 14855.14.

Tests of Significance

The significance of each factor and interaction may now be calculated. This is done by assigning the degrees of freedom to each sum of square term. The degrees of freedom are the number of independent parameters required to describe each factor or interaction.¹⁰⁴ The total number of degrees of freedom equals the number of experiments performed and are allocated as follows; one to each factor and interaction, one to lack of fit, one to the correction term, and the remainder to error. The number allocated to the error term should be one less than the number of experiments used to determine the error if Equation 28 was used. If Equation 26 was used, then the number of pairs of duplicate runs is used. If reactions are run in triplicate, then twice the number of pairs of duplicate runs is used, and so on.

By dividing each sum of squares by its associated degrees of freedom, the variance, or mean square as it is also known, may be obtained. The error variance is obtained in the same manner, by dividing the error sum of squares by the degrees of freedom associated with the error. The variance for each X_i is then divided by the error variance to

generate the F statistic, a variance ratio, Equation 32.

$$F \text{ of Effect } X_i = \frac{\text{Variance of } x_i}{\text{Error Variance}} \quad (32)$$

Before any decision may be made about the significance of each F statistic, one must decide how much confidence is required for the results. If a risk of 1 chance in 10 of a wrong answer is allowable, then the 90% confidence level would be selected. Tables of values for different confidence limits are in statistics texts⁹³⁻⁹⁶ and reference books.¹⁰⁵

When the confidence limit is selected, the table corresponding to that limit is entered with the number of degrees of freedom in the error estimate, and the number of degrees of freedom in the variance of X_i . Because Equation 32 has the variance of X_i divided by the error variance, n_1 is the number of degrees of freedom associated with X_i and n_2 is the number associated with error. Because all effects X_i have one degree of freedom associated with them, and the error has 5 degrees of freedom, the F statistic for Figure 17 would correspond to $n_1 = 1$, $n_2 = 5$. At the 95% confidence limit, this would correspond to $F = 6.61$. Any F that exceeds 6.61 means that the effect X_i corresponding to the F is significant, and X_i cannot be neglected in further experimentation. In Figure 17, all three effects are significant, but lack of fit is not significant.

The other two and three factor factorials were worked in the same manner. All conclusions are presented in the

Results and Discussion.

Fractional Factorials

When a large number of factors are to be investigated, it is possible to run a fractional factorial.¹⁰⁶⁻¹⁰⁷ Six factors would mean that $2^6 = 64$ experiments would have to be run. Excluding replications of the peripheral points, and running $n + 1$ center points for error determination, a total of 71 experiments would be run. Unless experiments may be run quickly, the time required for a full factorial would be prohibitive. Another reason to run fractional factorials is that sometimes it is not practical to plan an entire experimental program at once. A smaller fractional factorial can be used as a guide for a larger experimental design.

Because all experiments are not run, complete information about some interactions will not be obtained. This is called confounding, and results in two interpretations for each combination of observations. The five factor interaction ABCDE has the same sign as the factor F in all runs, and is thus confounded with it. The same is true for all other factors and interactions. Thus ABC and DEF are identical. So are AB and CDEF, ACE and BDF, etc. An important assumption is that the higher order interactions reflect random error, and do not affect the lower order interactions. Thus, even though AB and CDEF are not separable, the contribution by CDEF is assumed to be negligible. If the interaction AB

is significant, it is due only to AB with no contribution by CDEF. Confounding must be kept to a minimum.

For a $1/2$ fractional factorial, this may be done most easily by choosing the highest order interaction as the defining contrast.¹⁰⁶ A defining contrast is any variable or interaction whose effect may not be measured. Effects may not be measured unless the sum of the column of signs for X_i is 0. Remembering that the interaction code is generated by multiplying the individually coded factors together, the design matrix is set up in such a way that the highest order interaction equals + (or -) in all cases. Table 20 shows the design matrix for a six factor $1/2$ fractional factorial. Note that if the signs of each of the six factors (main effects) are multiplied together, the result is always +. Thus the six factor interaction ABCDEF is always + and becomes the defining contrast. Each column in the design matrix must total 0, or the interaction may not be measured.

A response matrix may again be generated as before. The responses of the eight center points are listed in Table 21. Table 24 lists the results of all calculations. The calculations were done in the following manner. OY is the optical yield obtained for a particular run. From Equation 23:

$$\text{Product Summation of } x_i = \sum_{j=1}^{32} X_{ij}(\text{OY}) = \text{PS} \quad (33)$$

For main effect A, PS = 79.1.

Source of Variation	Product Summation	Calculated Effect	Sum of Squares	Degrees of Freedom	Mean Square (Variance)	Calculated F Statistic	95% Significant	Rank	Probability
A	79.1	4.944	195.53	1	195.53	17.95	Yes	24	75.8
B	462.1	28.879	6673.01	1	6673.01	614.36	Yes	31	98.4
C	60.9	3.086	115.90	1	115.90	10.64	Yes	18	56.5
D	24.9	1.556	19.38	1	19.38	1.78	No	5	14.5
E	-113.7	-7.106	403.99	1	403.99	39.85	Yes	30	95.2
F	40.5	2.531	51.26	1	51.26	4.71	No	10	30.6
AB	-43.5	-2.719	59.13	1	59.13	5.43	No	12	37.1
AC	-76.7	-4.794	183.84	1	183.84	16.88	Yes	21	66.1
AD	-87.1	-5.444	237.08	1	237.08	21.77	Yes	28	88.7
AE	22.3	1.394	15.54	1	15.54	1.43	No	4	11.3
AF	94.1	5.881	276.71	1	276.71	25.41	Yes	29	91.9
BC	65.5	4.094	134.07	1	134.07	12.31	Yes	20	62.9
BD	78.7	4.918	193.55	1	193.55	17.77	Yes	23	72.6
BE	-47.5	-2.969	70.51	1	70.51	6.47	Yes	15	46.8
BF	-61.3	-3.831	117.43	1	117.43	10.78	Yes	19	59.7
CD	-44.9	-2.806	63.00	1	63.00	5.79	Yes	13	40.3
CE	28.1	1.756	26.67	1	24.67	2.27	No	6	17.7
CF	-12.9	-0.806	5.20	1	5.20	0.48	No	2	4.8
DE	-45.9	-2.869	65.84	1	65.84	6.04	Yes	14	43.5
DF	-78.5	-4.906	192.57	1	192.57	17.68	Yes	22	69.4
EF	-35.9	-2.244	40.28	1	40.28	1.86	No	9	27.4
ABC(DEF)	-51.3	-3.206	82.24	1	82.24	7.55	Yes	16	50.0
ABD(CEF)	34.7	2.168	37.63	1	37.63	3.45	No	8	24.2
ABE(CDF)	40.5	2.532	51.26	1	51.26	4.71	No	11	33.9
ABF(CDE)	-0.5	-0.031	0.01	1	0.01	0.00	No	1	1.6
ACD(BEF)	31.1	1.944	30.62	1	30.62	2.81	No	7	21.0
ACE(BDF)	19.3	1.206	11.64	1	11.64	1.07	No	3	8.1
ACF(BDE)	-80.9	-5.056	204.53	1	204.53	18.78	Yes	26	82.3
ADE(BCF)	59.7	3.732	111.38	1	111.38	10.23	Yes	17	53.2
ADF(BCE)	-79.3	-4.956	196.52	1	196.52	18.00	Yes	25	79.0
AEF(BCD)	-82.3	-5.144	211.67	1	211.67	19.44	Yes	27	85.5
Lack of Fit			298.56	1	298.56	27.42	Yes		
Error			76.23	7	10.89				
Correction Factor			30041.36	1			F=5.59 n ₁ =1 n ₂ =7		
Total			40492.08	40					

TABLE 24. Analysis of Variance for Screening Factorial Experiment.

From Equation 24:

$$\text{Calculated Effect of } X_i = 2 \frac{\sum_{j=1}^{32} (x_{ij} (OY))^2}{\sum_{j=1}^{32} (x_{ij})^2} = \frac{2PS}{32} \quad (34)$$

For main effect A, this equals 4.944.

From Equation 25:

$$\text{Sum of Squares for } x_i = \frac{\sum_{j=1}^{32} (x_{ij} (OY))^2}{\sum_{j=1}^{32} (x_{ij})^2} = \frac{(PS)^2}{32} \quad (35)$$

Again for main effect A, it equals 195.53.

From Equation 29:

$$\text{Sum of Squares Lack of Fit} = \frac{N_c N_p}{N_c + N_p} (\overline{OY}_c - \overline{OY}_p)^2 \quad (36a)$$

$$= \frac{(8)(32)}{40} (21.94 - 28.77)^2 \quad (36b)$$

$$= 298.56 \quad (36c)$$

From Equation 28:

$$\text{Error Sum of Squares} = \sum_{k=1}^8 (OY_{jk} - \overline{OY}_j)^2 \quad (37a)$$

$$= 76.23 \quad (37b)$$

From Equation 30:

$$\text{Correction Factor} = \frac{\sum_{j=1}^{40} (OY_j)^2}{40} = 30,041.36 \quad (38)$$

From Equation 31:

$$\text{Total Sum of Squares} = \sum_{j=1}^{40} (OY_j)^2 = 40,492.08 \quad (39)$$

In the cases where $j = 1$ to 32, the eight center points have been neglected. When $j = 1$ to 40, they have been included.

The number of degrees of freedom for each effect is one, except for the error term. Eight center points were used to determine error, so there are seven degrees of freedom associated with the error term. The variance and F statistic may now be calculated as before. For $N_1=1$ and $N_2 = 7$, the F statistic at 95% confidence is 5.59. The significance of each factor or interaction may now be determined (see Table 24).

Cuthbert Daniel Half Normal Plot

A Cuthbert Daniel half normal plot may also be used to determine the significance of each variable or interaction.¹⁰⁸ Using this method, the center points are neglected and replications are not necessary. This method works best when there is a large factorial design.

A sheet of normal probability paper is divided in half at the 50% probability line. Each line above 50% is assigned the probability P' , where $P' = 2P - 100$ and P is the probability associated with that line before the paper was divided in half.

The calculated effects are then ranked, neglecting signs, in ascending order. A percent probability is assigned to each where:

$$\% \text{ Probability} = \frac{100(\text{Rank} - 0.5)}{\text{Effects Ranked}} \quad (40)$$

Thus the third effect ranked of 31 effects would have the probability $= 8.1 = \frac{100(3 - 0.5)}{31}$.

The present probability is then plotted on the y-axis and the calculated effect on the x-axis. A straight line passing through the origin is then constructed so that the best fit is obtained that passes through the points with lower probability. The points of low probabilities are assumed to be due to random errors, and would correspond to non-significant variables in the analysis of variance. The intersection of the line with the 68.3% probability gives the standard deviation as read off the calculated effect axis. Any point more than two standard deviations from this line is then considered to be significant.

When the results of the $1/2$ fractional factorial are plotted in this manner, the results are in opposition to the analysis of variance done previously. Only one

variable, instead of many, is significant. The plot is shown in Figure 18. The reason for this surprising result is not clear. The points to the left of the line suggest that experimental error becomes less as the calculated effect increases. This does not seem to be reasonable, and no explanation for these conclusions are offered.

This method is efficient because it uses non-significant effects to estimate the random error. Thus replication of the experimental design is not necessary. Also, because it is a graphical method, it lends itself to ease of interpretation and an intrinsic belief that it is an easier method to follow. Its disadvantages are the need for a large factorial experiment and the lack of a quantitative judgement in the evaluation of the data.

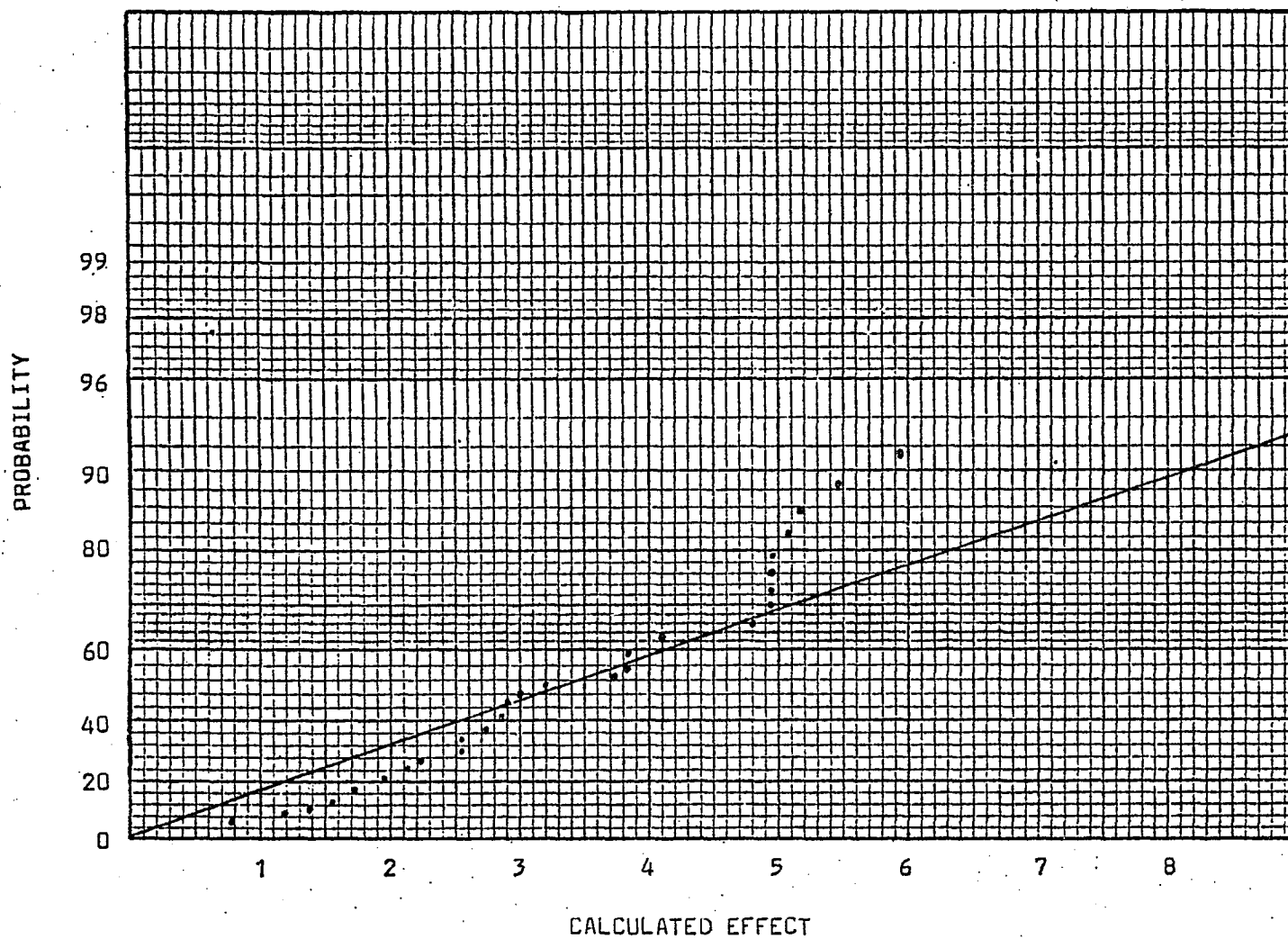


Figure 18. Cuthbert Daniel Half-Normal Plot of Screening Factorial.

RESULTS AND DISCUSSION

Ligand Synthesis

By following the method of Schrauzer et al.¹⁰⁹, we obtained the HBDM1,3pn ligand as a brownish oil that separates from the benzene reaction solvent. The oil solidified as benzene evaporated from it, but it remained colored. CHN analysis of this crude solid would sometimes agree with the calculated values. Conversion of the crude HBDM1,3pn to Co^{III} (BDM1,3pn) Br_2 results in about a 50% yield based on the crude solid. This indicated that perhaps the sample was impure and that acceptable analyses were an accident. Several purification schemes were investigated to purify the ligand. The results are shown in Table 25.

A white crystalline substance would sometimes form in the benzene solution after the oil had separated. These crystals melted from 142-144°C and gave acceptable CHN analyses. The crude solid obtained by vacuum drying the oil melted at 120-126°C, indicating impurities.

A soxhlet extraction of the crude solid with methanol probably resulted in solvolysis of the ligand. All solids quickly dissolved, but evaporation of the solvent resulted in a low melting product. Its identification was not undertaken.

Next, CH_2Cl_2 was used in a soxhlet extraction. This solvent quickly removed the color from the crude solid, but

TABLE 25
Analyses of HBDM1,3pn Ligand

	<u>C</u>	<u>H</u>	<u>N</u>
Calculated	54.98	8.39	23.31
Crude Solid	54.26	7.99	23.24
Crystalline Solid	55.30	8.28	23.10
CH ₂ Cl ₂ Extracted Solid	56.07	9.43	23.48
Acetone Crystallized	55.18	8.44	23.04

did not dissolve it. Analysis of the dried product that remained, showed it to be high in carbon and hydrogen.

The final purification method tried was crystallization of the ligand oil from acetone. As the oil separated from the benzene reaction solvent, it was dissolved in cold dry acetone. After standing for one to two hours, a white precipitate formed. This precipitate was filtered and washed with a small quantity of cold acetone. CHN analysis of this powder was acceptable, and the melting point increased to 137-140°C.

Catalyst Synthesis

$\text{Co}(\text{DMG})_2 \cdot 2\text{H}_2\text{O}$ was synthesized by the method of Schrauzer¹¹⁰, and used as needed. The dry solid remained active for several months if stored over N_2 , but lost its activity over a period of several weeks if exposed to oxygen in the air. The catalyst was also prepared in situ by addition of $\text{CoCl}_2 \cdot 6\text{H}_2\text{O}$, dimethylglyoxime and disodiumdimethylglyoximate to the reaction mixture. No great differences in the activity of the two methods have been noted. The use of isolated catalyst had the advantages of fewer weighings and an analyzed product.

$\text{Co}^{\text{II}}(\text{BDM1,3pn})^+$ was prepared in situ for each reduction because the cationic complex is difficult to isolate as the Co^{II} complex. $\text{CoCl}_2 \cdot 6\text{H}_2\text{O}$ was combined with (previously prepared) HBDM1,3pn in the reaction solvent.

Methanol (10%) in benzene is necessary to dissolve the $\text{CoCl}_2 \cdot 6\text{H}_2\text{O}$ and evaporation of the methanol once the catalyst has formed causes the cobalt complex to precipitate.

Both catalysts formed deep red-orange solutions in 9:1 (v/v) benzene-methanol solutions, which is characteristic of Co^{II} complexes of this type. During reduction of an organic substrate, the solution remained this color, and visible spectra of the solution were identical to spectra taken after initial formation of the catalyst.

$\text{Co}(\text{DMG})_2$ Reductions

$\text{Co}(\text{DMG})_2$ reductions were run with previously prepared catalyst that was stored under N_2 to prevent oxidation to Co^{III} . A variety of substrates were reduced in an attempt to find a substrate that (1) was reduced in 24 hrs or less, (2) was reduced in high yield, (3) was easily analyzed for both chemical and optical yields, and (4) was stable towards the isolation conditions employed. Once this "perfect" substrate was found, studies of the mechanism and the experimental conditions favorable to high optical yields could begin.

2,3-Butanedione, $\text{CH}_3\text{C}(\text{O})\text{C}(\text{O})\text{CH}_3$, was the first substrate to be tested, but it failed in that it was unstable during and after work-up. The $\text{CH}_3\text{C}(\text{O})\text{CH}(\text{OH})\text{CH}_3$ produced, spontaneously racemizes¹¹¹ to an inactive dimeric solid. A steady loss of rotation was observed in the isolated product.

1-Phenyl-1,2-propanedione, $\text{CH}_3\text{C}(\text{O})\text{C}(\text{O})\text{Ph}$, was chosen next for further experimentation. The substrate was smoothly and quickly reduced by the catalyst. The reaction mixture was fractionally distilled under vacuum, and at 59°C the reduction products $\text{CH}_3\text{COCH}(\text{OH})\text{Ph}$ (I) and $\text{CH}_3\text{CH}(\text{OH})\text{C}(\text{O})\text{Ph}$ (II) were obtained. These two compounds are in equilibrium at high temperatures¹¹² and have similar boiling points. The equilibrium between I and II has been studied and found to be 56% I vs. 44% II at 80°C . An nmr of the distilled reduction products show a 60% I and 40% II, agreeing with the earlier studies. Clearly a more stable product was needed.

Benzil, $\text{PhC}(\text{O})\text{C}(\text{O})\text{Ph}$, was then reduced to benzoin, $\text{PhCH}(\text{OH})\text{C}(\text{O})\text{Ph}$, in apparent 100% yield. IR analysis showed no detectable starting material, but gc analysis showed no product. The benzoin decomposed to benzil on the glpc column. UV and visible spectra of starting material and product were similar, so the reaction yield could not be determined by this method. A substitute that was more easily analyzed was sought.

Methyl benzoylformate, $\text{PhC}(\text{O})\text{COOCH}_3$, was then reduced to methyl mandelate, $\text{PhCH}(\text{OH})\text{COOCH}_3$, in high yield. This appeared to be the perfect system. Starting material and product remained in the organic layer while all other components of the reaction mixture were extracted into aqueous solutions. Evaporation of the dried organic layer yielded a moist solid that separated into methyl benzoylformate and

methyl mandelate on a 10% QF-1 glpc column. This appeared to have all the attributes desirable for further experimentation.

About this time it became evident that Y. Ohgo and coworkers⁷⁵⁻⁸¹ had performed much of the experimental work planned. Because cobalt-alkyl group studies were already underway with a similar system, $\text{Co}^{\text{II}}(\text{BDML},3\text{pn})^+$, and because a cobalt-carbon bond was postulated for an intermediate in the reduction, $\text{Co}^{\text{II}}(\text{BDML},3\text{pn})^+$ was chosen for further work.

$\text{Co}^{\text{II}}(\text{BDML},3\text{pn})^+$ Reductions

Preliminary work was done using $\text{Co}^{\text{III}}(\text{BDML},3\text{pn})\text{Br}_2$ as the starting material. Because the $\text{Co}^{\text{III}}(\text{BDML},3\text{pn})\text{Br}_2$ was not active as a catalyst, it was reduced to $\text{Co}^{\text{II}}(\text{BDML},3\text{pn})^+$ in aqueous methanol by CO. Reductions with H_2 using this catalyst either did not start, or ran very slowly. At atmospheric pressure, 14 days were required for the reaction to go to completion, while at 60 psig of H_2 pressure, 40 hours were required for a complete reaction. It was decided to prepare the $\text{Co}^{\text{II}}(\text{BDML},3\text{pn})^+$ in situ because of the low activity of the CO reduced catalyst.

When the catalyst was prepared from $\text{Co}(\text{OAc})_2 \cdot 4\text{H}_2\text{O}$ and $\text{HBDML},3\text{pn}$, its activity improves 100 fold over the CO reduced catalyst. Reactions were complete in 3 hrs at atmospheric pressure of H_2 . This increased rate of reaction may be due to a vacant site on the cobalt complex. When CO was used to reduce the $\text{Co}^{\text{III}}(\text{BDML},3\text{pn})$ to $\text{Co}^{\text{II}}(\text{BDML},3\text{pn})$,

the CO may occupy an axial site needed for coordination of H_2 or the substrate.

Because methyl benzoylformate was easily reduced by the $Co^{II}(DMG)_2$ system, it was chosen for preliminary work leading to the elucidation of the mechanism of reduction of the $Co(BDM1,3pn)^+$ system. Preliminary studies also showed that a larger number of substrates were reduced by $Co^{II}(BDM1,3pn)^+$ than by $Co(DMG)_2$. Tables 12 and 13 show the substrates reduced by the DMG and BDM1,3pn catalysts.

After running a number of reductions with methyl benzoylformate, an unknown solid precipitated from CS_2 during optical rotation measurements. Several grams of the reduction product, methyl mandelate, were combined, dissolved in CS_2 and allowed to stand. A solid precipitated from the mixture after several days. Despite the use of ir, nmr and CHN analyses, we were unable to identify the solid. It is most likely a dimer or trimer of the methyl mandelate, but its exact structure remains unknown. Ohgo⁷⁹ has reported the formation of optically active dimers under similar reaction conditions with $Co(DMG)_2$ as the catalyst. However, this unknown solid is not optically active.

GLPC analysis on a 10% QF-1 6' x 1/8" column resulted in two peaks that correspond to a 2:1 ratio of methylbenzoylformate to methyl mandelate. This suggests a trimer breaking down on the column. No other peaks were observed. IR was used originally to identify the products, and glpc was used

to monitor the reaction yield. The ir of the reduction products was almost identical to published spectra, and glpc analysis of the mixture showed only two peaks. These two peaks had retention times identical to authentic samples of methyl benzoylformate and methyl mandelate, and therefore invalidated earlier analyses.

Because of uncertainties in reaction yield caused by this unknown solid, a new substrate was sought. Except for analysis of the reaction yield, benzil appeared to be the best substrate. The acylation analysis⁸⁶ of the percent OH in a sample made the analysis of benzoin short and concise.

In many ways benzil was the perfect substrate for the major portion of the work. Both benzil and benzoin are insoluble in the aqueous solutions used to remove the other components from the reaction mixture. Both are solids with melting points above 90°C. Benzil is yellow and benzoin is white, so after workup the chemical yield can be roughly determined. A white product indicates better than 95% yield. The drawbacks are that benzoin can not be analyzed by glpc, and that a one gram sample is required for the %OH titration.

Factorial Experiments

Because the $\text{Co}^{\text{II}}(\text{BDML}, 3\text{pn})^+$ catalytic system is complex, changing one factor (variable) at a time leads to erroneous conclusions. Because of this, a factorial approach was chosen to investigate the system. Details of the mathematical operations, definitions, and advantages of a

factorial approach are given in the Statistical Analysis of Data section.

A large number of factors were deemed important, but experimental considerations forced only six to be chosen for a screening experiment, Table 19. Often a possible variable would be hard to quantify, an example is the use of several alcohols other than methanol. Other variables, such as pH, would be impossible to measure accurately in the benzene-methanol (9:1 v/v) solvent. The six variables chosen appeared to affect the optical yield of the reduction in previous experiments.

Four factorial experiments were run. A large six factor screening experiment to try to eliminate some variables was the first factorial experiment undertaken. This was followed by a two factor experiment to optimize two variables. A three factor experiment to study a three factor interaction from the screening factorial was run next. Finally, a two factor experiment studying the effect of ligand/cobalt ratio and percent methanol in benzene was run.

Six Factor Screening Experiment. A total of 2^6 runs would be required to run a full factorial experiment; so to lower the time involved, a $1/2$ factorial experiment was performed. Instead of 64 runs, only 32 are required, but much the same information may be obtained. Because only $1/2$ the runs are necessary, some method of choosing which to run is needed. The interaction ABCDEF was chosen as the

defining contrast, and set to +. The thirty-two runs that have an even number of high settings are run. The maximum information from the thirty-two runs may be obtained by choosing this particular interaction as the defining contrast.

Table 24 shows the results of this screening experiment. The Source of Variation is that independent factor (variable) that causes a variation in the optical yield response (dependent) variable. For example, AB refers to the variation caused by the effect of A on B, and of B on A. Inspection of the sign associated with the Product Summation (or Calculated Effect) tells which settings improve the optical yield. A positive value indicates that a positive setting in the Design Matrix (Table 20) results in higher optical yields (on the average) than negative settings. A negative value for the Product Summation indicates that negative settings cause the greatest improvement in the optical yield.

Inspection of the Calculated F Statistic shows which factors are most important, and which are significant at the 95% confidence limit. The quinine/cobalt ratio, B, is clearly the most important factor, followed by temperature, E. Each factor or interaction may be ranked in order of importance.

That the quinine/cobalt ratio is most important is not surprising. The step that determines the chirality of the product involves protonation by quinine. If an achiral proton donor is available, such as methanol in the solvent,

then a racemic product is more probable if protonated quinine is not available. Increasing the concentration of quinine (by increasing the quinine/cobalt ratio) results in a greater probability of protonated quinine in the area of the substrate when proton donation is required.

It is not surprising that lower temperatures favor increased optical yield. As the temperature is lowered, the number of molecules having sufficient energy to react is also lowered. This may be seen in Figure 19. As the temperature is lowered, the number of molecules with sufficient energy to form the R-isomer is reduced faster than those molecules that are able to form the S-isomer. Thus, as the temperature is lowered, the ratio of S-isomer to R-isomer increases. At a low enough temperature, only S-isomers will be produced, leading to 100% optical yield.

Beyond these two single factors, the chemical implications are confusing. The next important Source of Variation is the interaction between catalyst concentration (A) and time (F). The positive sign of the AF interaction indicates that both A and F should be set high, or both low. One would intuitively expect that a low concentration would require a long time, or a high concentration a short time. The AD interaction between catalyst concentration (A) and substrate/cobalt ratio (D) is ranked next in importance. The negative sign of the Product Summation means that high concentration and low substrate/cobalt ratio, or low concentration and high

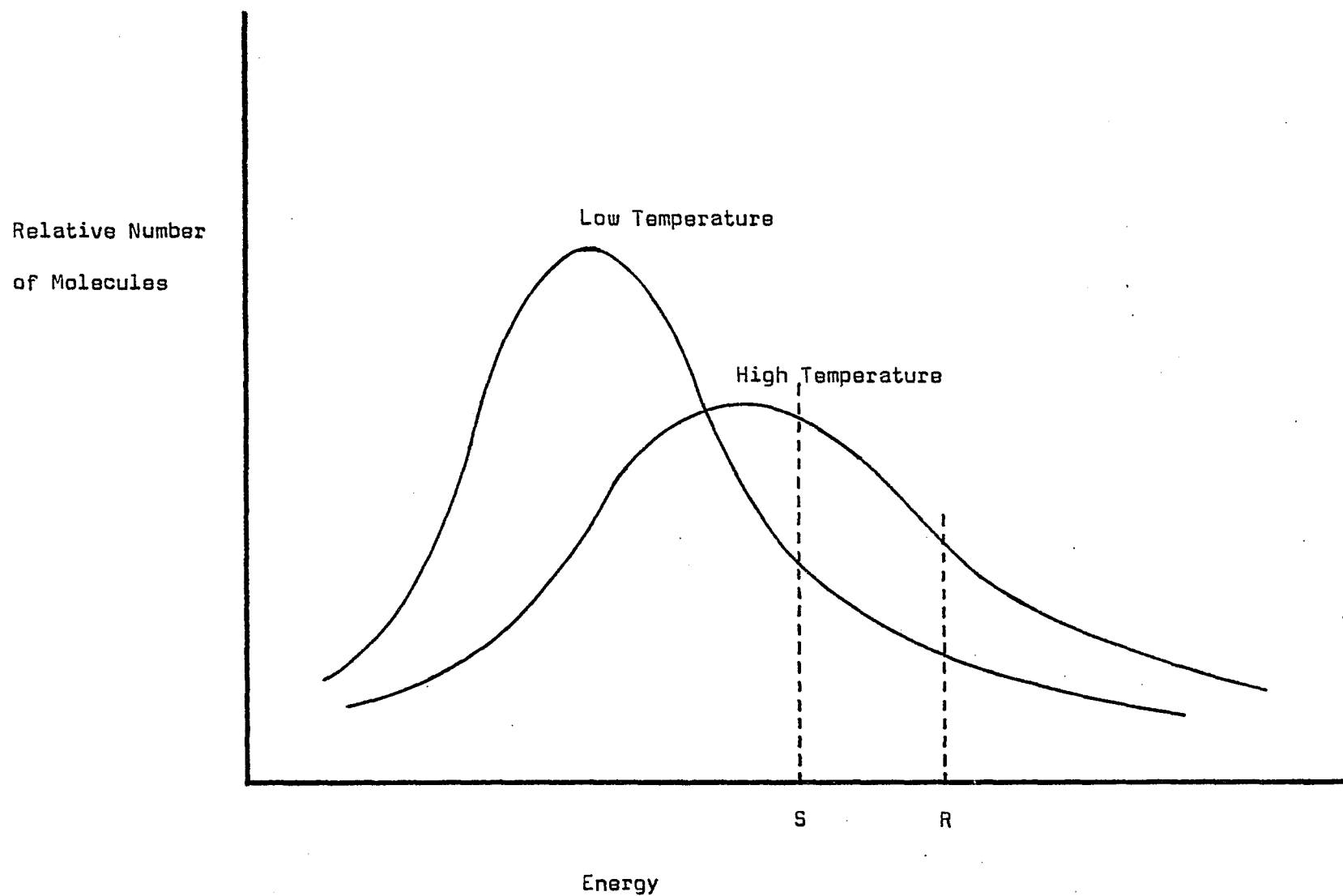


Figure 19. Relationship Between Energy Required for Formation of R and S Isomers, and the Number of Molecules Possessing that Energy.

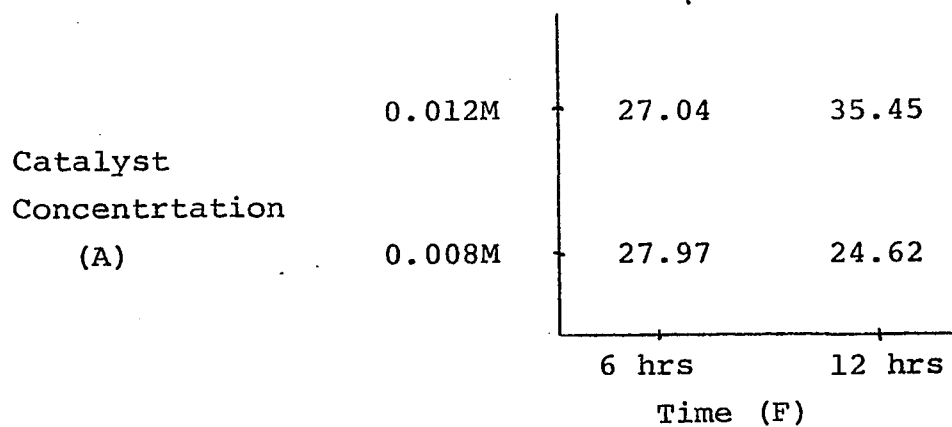
substrate/cobalt ratio, are best. The chemical significance of this is not clear. One would expect that the concentration should match the substrate/cobalt ratio, not oppose it so completely.

Three factor and higher interactions are normally assumed to reflect experimental error, and thus should not be significant. However, five of the ten possible three factor interactions are significant. Because each three factor interaction is confounded with another three factor interaction, the effects due to each are inseparable. For example, the interaction ACF is confounded with the interaction BDE. Together they have a Product Summation of -80.9, rank 26th (with 31 the most important), and are significant at the 95% confidence limit. If each three factor interaction contributed equally, each would have a Product Summation of -40.5, rank about 10th and not be significant at the 95% Confidence limit. Because the two three factor interactions are not separable, a chemical interpretation is not possible. Therefore, two methods were investigated to resolve conflicts between the differing interactions. The first method reduces the six factor screening experiment to a series of two factor experiments. The second looks at contributions due to each effect and interaction as applied to the average optical yield.

In the first method, for example, the interaction between catalyst concentration (A) and reaction time (F) is

broken down into a factorial design similar to Figure 17. This is illustrated in Figure 20. The 32 sets of experimental conditions of Table 20 are divided into four groups depending on the settings of the A and F variables. The four groups correspond to high A, high F; high A, low F; low A, high F; and low A, low F; and have eight runs in each group. Note that there are an equal number of high and low settings for each of the other four variables in each set of eight. The optical yields of the eight runs in each group are totaled and divided by eight to find the average optical yield for that set of conditions of A and F. These averages are shown plotted on the graph in Figure 20. Note that high catalyst concentration and 12 hrs reaction time produce the highest average optical yield.

If one changes one variable at a time, it is likely that the best conditions would not be found. If each number on the graph in Figure 20 represented one run, the following situation might occur. The first experiment was run with 0.008M concentration for 6 hrs, and the second with 0.008M concentration for 12 hrs. The logical conclusion would be that an increase in time adversely affects the optical yield. If the experimenter then performed an experiment at 0.012M concentration for 6 hrs, he should conclude that catalyst concentration had little or no effect on optical yield. Thus he would probably not perform an experiment at 0.012M concentration in 12 hrs time.



AF SETTINGS

	(++)	(+-)	(-+)	(--)
Run #	1, 4	18, 19	2, 3	17, 20
	6, 7	21, 24	5, 8	22, 23
	10, 11	25, 28	9, 12	26, 27
	13, 16	30, 31	14, 15	29, 32
Average Optical Yield	35.45	27.04	24.62	27.97

Figure 20. Small Factorial Using Data from Screening Factorial.

However, when interactions are studied by the first method, chemical intuition may be necessary to form correct conclusions. Some interactions, for example AF, will have the highest optical yield with a certain variable, in this case F, on the high setting. A study by this method of the BF interaction shows that the highest optical yield results with variable F at the low setting. Thus the problem of where to set F remains.

One way to overcome this problem would be to weigh each two factor interaction relative to the others. However, the assignment of each weighing factor would be arbitrary, and for this reason the method would be inaccurate. For this reason, the following method was utilized to find the best conditions for the highest optical yield.

The second and better method would be to find the average effect of each variable and each interaction over all experimental runs. The average effect for each Source of Variation can be obtained by dividing the Calculated Effect associated with that Source of Variation by two. The average effect due to each Source of Variation is then added to the average optical yield for all 32 reactions. This gives a prediction for that set of conditions. If this method is used for a full factorial experiment, the predicted optical yields and the ones obtained experimentally are identical.

For example, catalyst concentration (A) has a Calculated Effect of 4.944 as shown in Table 24. The average effect due to A is 2.472, so each time A is coded + in the Design Matrix, +2.472 is added to the average optical yield for all 32 reactions. If A is coded -, then -2.472 is added. Once the average effect is calculated for all Sources of Variation (A,B...AB,AC...etc.), the Design Matrix is used to calculate the predicted optical yield by taking the average optical yield and summing the positive or negative average effects with it. From Table 20 average for all reactions is 28.77, so the beginning of the calculation for run #5 would be $28.77 - 2.472 + 14.439 + 1.543 - 0.778 - 3.553 + 1.266 + \dots$

This calculation was made for the 64 runs that would result from the full factorial. Only main effects and two factor interactions were used in the calculation. The confounded three factor interactions were ignored, and thus predicted optical yields did not always agree with actual experimentally determined optical yields. Table 26 shows the predicted and optical yields obtained from the 32 reactions run.

The highest predicted optical yield which is not one of the reactions run, employs conditions different than those that would be predicted by looking at the main effects alone. Table 27 shows the reaction conditions predicted by looking only at the signs of the Product Summation, and by the second method. Unfortunately, neither set of reaction

TABLE 26

Optical Yields Predicted and Obtained
for the Screening Factorial Experiment

See Table 19 for explanation of symbols.

			+A				-A			
			+B		-B		+B		-B	
			+C	-C	+C	-C	+C	-C	+C	-C
D +	E +	L +	38.6 (35.0)	32.2	10.2	17.0 (10.8)	39.2	28.4 (26.6)	5.4 (10.2)	2.6
		L -	41.8	39.0 (45.7)	6.0 (16.0)	11.2	54.2 (42.5)	41.8	12.8	8.4 (9.7)
	E -	L +	44.6	47.0 (54.5)	10.4 (14.0)	20.8	59.8 (59.7)	52.6	20.0	20.8 (16.1)
		L -	49.4 (48.5)	50.2	7.6	16.4 (9.9)	64.6	55.8 (59.1)	17.2 (14.7)	16.4
D -	E +	L +	47.8	41.0 (43.8)	29.6 (26.0)	30.8	37.8 (44.1)	21.4	14.0	5.6 (6.4)
		L -	41.2 (40.5)	32.8	15.4	15.0 (9.3)	42.8	24.8 (27.2)	11.4 (9.7)	1.4
	E -	L +	48.4 (53.1)	45.2	24.2	29.0 (46.4)	52.8	40.0 (23.7)	23.0 (10.2)	18.2
		L -	43.2	38.4 (33.5)	11.4 (12.9)	14.6	47.6 (53.9)	33.2	10.2	3.8 (7.2)

38.4 = Optical yield calculated by second method.

(35.0) = Optical yield from screening factorial.

TABLE 27

Predicted Optical Yields as a Function
of Reaction Conditions

	Conditions Predicted by	
	Method 1; Main Effects Only	Method 2; Average Effects
Catalyst Concentration	0.012M	0.008M
Quinine/Cobalt Ratio	2	2
Benzylamine/Cobalt Ratio	1	1
Substrate/Cobalt Ratio	20	20
Temperature	+8°C	+8°C
Time	12 hrs	6 hrs
Calculated Optical Yield By Method 2	44.6	64.6

conditions was run during the screening factorial.

The reason for performing the screening experiment was to eliminate any factors that have no significant effect on the optical yield of the reaction. A factor must not be significant alone, or in all its interactions with other factors, in order to be eliminated. Only two factors, substrate/cobalt ratio (D) and time (F) are not significant as main effects, but both are significant in interactions with catalyst concentration (A). Because all six factors are important, all six must be considered in planning further experiments.

First Two Factor Experiment. The results of the screening factorial indicated that catalyst concentration (A) and quinine/cobalt ratio (B) were both significant as main effects and that they did not interact. The quinine/cobalt ratio was the most important variable in the screening experiment, so it was chosen in an attempt to maximize the optical yield. The catalyst concentration was chosen because of uncertainty in the use of a high or a low setting. Of the two methods discussed above, the first suggests a high catalyst concentration and the second, a low catalyst concentration. Thus these two variables were chosen for the second factorial experiment.

The factorial experiment used higher settings than the screening factorial experiment, as shown in Figure 21, with some interesting results. At 0.010M and 0.02M catalyst concen-

Source of Variation	Product Summation	Calculated Effect	Sum of Sources	Degrees of Freedom	Variance	F	95% Significant
A	10.8	2.7	14.58	1	14.58	0.54	no
B	44.8	11.2	250.88	1	250.88	9.20	yes
AB	-43.0	-10.75	231.13	1	231.13	8.48	yes
Lack of Fit			.85	1	.85	0.01	no
Error			136.23	5	27.25		
Correction Factor			<u>12089.52</u>	1			
TOTAL			12722.70				

$n_1 = 1; n_2 = 5; F = 6.61$

^aSee Figure 14 for Experimental Design

Figure 21. Results of First Two Factor Experiment^a

trations, the catalyst concentration is no longer statistically significant because the effects due to concentration at a quinine/cobalt ratio of 2 are opposite those when the quinine/cobalt ratio is 4. The net result is that the effect at one setting cancels out the effect at the other.

Again the effects of the quinine/cobalt ratio are significant and cannot be ignored. This indicates that a setting higher than 4 in further experiments may increase the optical yield obtained. Also, the interaction between the two variables, AB, is now significant. The negative sign of the AB Product Summation signifies that the two variables should have opposite settings. Inspection of the graph in Figure 21 shows that low catalyst concentration (A) and high quinine/cobalt ratio (B) results in the highest optical yield. This result is opposite that in the screening factorial for the AB interaction, if the signs of the Product Summations from the screening experiment for A and B are used, or if the 32 experiments are reduced to four groups of eight in a calculation similar to Figure 20. It is interesting to note that the results of this two factor experiment are in agreement with the best conditions predicted by the second method of analyzing the screening experiment.

A three factor factorial was run next, taking into account the conclusions drawn from the two previous factorial experiments.

Three Factor Experiment. The three factor interaction of catalyst concentration (A), substrate/cobalt ratio (D), and reaction time (F) was significant in the screening factorial. Also, each of the three two factor interactions (AD, AF, DF) was significant in the six factor screening experiment, but the settings of the variables in the two factor interactions was not clear. For these reasons a three factor experiment was undertaken to investigate the relationship among these variables.

Variable settings are shown in Figure 22, and were chosen based on the previous factorial experiments. Experiments were run at 30°C for ease in running the experiments, and because temperature is largely independent of the other variables.

The results of the factorial experiment show that the three factor interaction is not significant under these conditions. In fact, only the reaction time (F) and the interaction between catalyst concentration and substrate/cobalt ratio (AD) are significant. When one inspects the signs of the Product Summation for this factorial, there is complete agreement with the second method of examining the screening factorial. Catalyst concentration (A) wants to be low, substrate/cobalt ratio (B) wants to be high, and reaction time (F) wants to be short.

Reaction time was not significant as a main effect in the screening factorial and this may have been due to the

Run	A	D	F	AD	AF	DF	ADF	Optical Yield
1	+	+	+	+	+	+	+	17.1
2	-	+	+	-	-	+	-	28.1
3	+	-	+	-	+	-	-	19.8
4	-	-	+	+	-	-	+	21.6
5	+	+	-	+	-	-	-	29.3
6	-	+	-	-	+	-	+	42.1
7	+	-	-	-	-	+	+	33.9
8	-	-	-	+	+	+	-	19.4
9-12	0	0	0	0	0	0	0	27.0, 26.4 30.6, 34.8

VariablesSettings

	<u>High</u>	<u>Center</u>	<u>Low</u>
Catalyst Concentration (A)	0.016	0.013	0.010
Substrate/Cobalt Ratio (D)	25	20	15
Reaction Time (F)	24	18	12

Constant Settings

Quinine/Cobalt Ratio = 3
 Benzylamine/Cobalt Ratio = 1
 Temperature = 30°C

(continued on next page)

Figure 22. Design and Results of Three Factor Experiment

Figure 22. (continued)

Source of Variation	Product Summation	Calculated Effect	Sum of Squares	Degrees of Freedom	Variance	F	95% Significant
A	-11.0	-2.775	15.40	1	15.40	1.03	no
D	21.9	5.475	59.95	1	59.95	4.00	no
F	-38.1	-9.525	181.45	1	181.45	12.10	yes
AD	-36.5	-9.125	166.53	1	166.53	11.10	yes
AF	-14.5	-3.625	26.28	1	26.28	1.75	no
DF	-14.3	-3.575	25.56	1	25.56	1.70	no
ADF	18.1	4.525	40.45	1	40.45	2.73	no
Lack of Fit			28.82	1	28.82	1.92	no
Error			45.00	3	15.00		
Correction of Error			<u>9080.50</u>	<u>1</u>			
TOTAL			9670.45	12			

$n_1 = 1; n_2 = 3; F = 10.13$

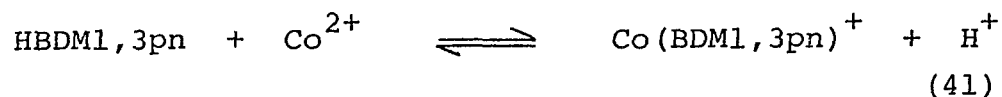
short times involved. Clearly, optical yields are reduced in a 24 hr reaction time, as shown in the three factor experiment. Benzoin might racemize when allowed to stand over the catalyst for a period of time after the reduction was complete. Also, the catalyst may hydrogenate the BDM1,3pn ligand and change the nature of the catalyst, or result in free cobalt ions.

No main effects caused by catalyst concentration alone are significant. This may be due to the small range studied, or it may be due to the settings of the constant variables. Although catalyst concentration is not significant, the sign associated with the Product Summation indicates that low concentration is best.

Second Two Factor Experiment. Two new variables were next studied using the factorial approach, percent methanol in benzene, and ligand cobalt ratio, shown in Figure 16. The racemization of benzoin during long reaction times suggested that possibly free Co^{II} ions might be responsible. For this reason 20% excess ligand was one variable, x_2 . Also, polarity of the solvent would affect acid dissociation equilibria, so this was chosen as a second variable, x_1 .

The results, Figure 17, show that both variables, and the interaction between them are statistically significant at the 95% confidence limit. The highest optical yields are obtained with 20% excess ligand and 10% methanol in benzene. It is not surprising that excess ligand enhances the optical yield if free cobalt ions cause racemization of the product.

Addition of more ligand would push the equilibrium shown in Equation 41 further to the right, with a decrease in cobalt ion concentration.



The effects due to % methanol may be caused by two properties of methanol; its polarity and/or its acidity. By increasing the polarity of the reaction medium, the ease of addition of a proton to the substrate would be increased. This would be due to solvation effects that would allow the protonated quinine to ionize easily. If the acidity of the methanol were important, increasing the percentage of methanol would make more protons available. One or both of these effects may be the cause of the decrease in optical yield with the increase in % methanol.

Factorial Conclusions. The four factorial experiments indicate that the conditions shown in Table 28 should result in high optical yields. The optimum settings of all variables have not been determined exactly, but the direction in which to change them is indicated. The factorial experiments not only direct the researcher towards the specific goal of increasing the optical yield, but also give insights to the reaction mechanism. If the reaction mechanism is not understood, the factorial method will show what variables are important, and how the variables interact with one another. The significant variables and interactions may

TABLE 28
Best Reaction Conditions

Cobalt Concentration	0.01M or lower
Ligand/Cobalt Ratio	1,2
Quinine/Cobalt Ratio	4 or higher
Benzylamine/Cobalt Ratio	1
Substrate/Cobalt Ratio	20 or better
Temperature	as low as possible
Time	as short as possible
Alcohol	2-propanol

then give clues about the mechanism that might be missed if only one variable at a time were changed.

Mechanism of the Reduction

The $\text{Co}^{\text{II}}(\text{BDM}1,3\text{pn})^+$ reduction mechanism is different than the asymmetric catalytic hydrogenation by rhodium complexes. The rhodium catalysts typically have chiral ligands that make the catalytic site on the metal asymmetric³⁶, Figure 3. This differs from the mechanism of the $\text{Co}^{\text{II}}(\text{BDM}1,3\text{pn})^+$, which appears to be one of an achiral catalytic site separate from the chirality determining substance. The suggested mechanism is similar to the one proposed by Ohgo and coworkers⁸⁰ for the $\text{Co}(\text{DMG})_2$ system. The mechanism will first be presented, then evidence in support of the mechanism will be discussed.

The proposed mechanism consists of six steps as shown in Figure 23. The first step is homolytic cleavage of H_2 by the cobalt(II) catalyst to produce the cobalt(III) hydride. This hydride then ionizes to form a proton and the cobalt(I) complex. The proton reacts with the strongly basic nitrogen on the quinuclidine ring of the quinine. The fourth step, which determines the stereochemistry of the product, consists of activation of the substrate by protonated quinine as the cobalt(I) complex forms a bond to the carbonyl carbon. As the cobalt-carbon bond forms, the proton is transferred from the quinine to the carbonyl oxygen. Protonated quinine then attacks as an electrophile in step 5 to displace the cobalt-

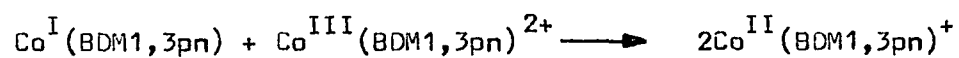
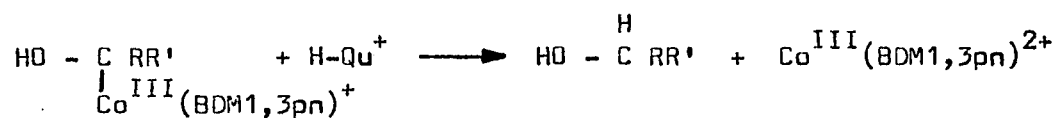
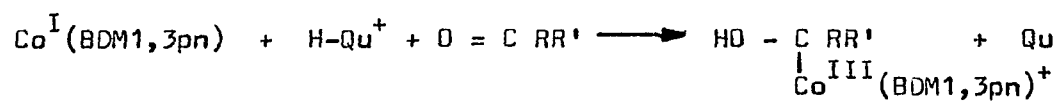
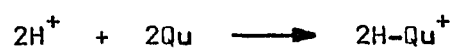
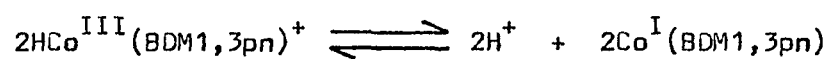
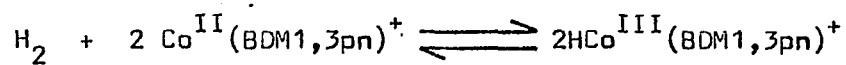


Figure 23. Co(BDM1,3pn) Reduction Mechanism.

(III) complex by backside attack. Finally, the second cobalt(I) complex produced in step 2 combines with this cobalt(III) complex to regenerate the two cobalt(II) complexes. Evidence in support of this mechanism is as follows.

Evidence for the first two steps is provided by close inspection of the reaction mixture as the reduction begins. The reaction mixture must be heated to 38°C in order to initiate the reduction. This suggests thermal dissociation of an axial ligand²⁹, most likely a water molecule from the original $\text{CoCl}_2 \cdot 6\text{H}_2\text{O}$ source of cobalt. As the reaction starts, the orange-red color of the mixture becomes visibly deeper, although this is not reflected in visible spectra of aliquots removed from the reaction flask. The deeper color is probably due to a small amount of the Co(I) complex formed in step 2. Simandi and coworkers⁷³ investigated the activation of H_2 by cobaloxime(II) and proposed a homolytic cleavage of the hydrogen molecule. Heterolytic cleavage by Co(II) is not reasonable because the unstable complexes $\text{HCo}^{\text{IV}}(\text{BDM1},3\text{pn})^{2+}$ and $\text{HCo}^{\text{II}}(\text{BDM1},3\text{pn})$ would be formed. $\text{Co}^{\text{III}}(\text{BDM1},3\text{pn})^{2+}$ does not react under these reaction conditions, and $\text{Co}^{\text{I}}(\text{BDM1},3\text{pn})$ would form a hydride in the presence of H^+ which would revert to H_2 if it heterolytically cleaved H_2 .

The cobalt(III) hydride is not the active catalyst. This was shown by preparing the hydride by careful acidification of the cobalt(I) complex in the presence of benzylamine. The hydride has a pK_a of about 3, as addition of acids with

pK_a 's higher than 3 do not form the hydride (see Experimental). The hydride does not react with benzil, 2,3-butanedione, methyl iodide, or acrylonitrile. However, when these substrates are added to the cobalt(I) complex, all but the acrylonitrile react to form a cobalt(II) complex in solution.

Further evidence for the cobalt(I) complex as the active species is provided by the addition of methyl iodide¹¹⁸ to the reaction mixture. When methyl iodide is added to the reaction mixture while benzil is being reduced, the reaction quickly stops and $\text{MeCo}(\text{BDML}, 3\text{pn})^+$ is formed quantitatively within 45 min. However, if methyl iodide is added to the reaction mixture with no H_2 present, only 1/2 the concentration of $\text{MeCo}(\text{BDML}, 3\text{pn})^+$ is obtained, with the reaction taking place slowly over a period of 6 hrs. The amount of $\text{CH}_3\text{Co}(\text{BDML}, 3\text{pn})^+$ in the two reactions may be measured spectrophotometrically ($\lambda = 460 \text{ nm}$, $\epsilon = 2120 \text{ m}^{-1} \text{ cm}^{-1}$).¹¹³ When the methyl-cobalt complex is exposed to light, the carbon-cobalt bond is homolytically cleaved to form the red $\text{Co}^{\text{II}}(\text{BDML}, 3\text{pn})^+$.¹¹³

In the second reaction without H_2 , there are two possible mechanisms. The $\text{Co}^{\text{II}}(\text{BDML}, 3\text{pn})^+$ may disproportionate to form 50% each of the cobalt(I) and cobalt(III) complexes. The cobalt(I) complex is free to react with the methyl iodide, and does so as fast as it is formed.^{67,68} The second possibility is a free radical reaction between the methyl iodide and the cobalt(II) complex to produce equal amounts of $\text{MeCo}^{\text{III}}(\text{BDML}, 3\text{pn})^+$ and $\text{ICo}^{\text{III}}(\text{BDML}, 3\text{pn})^+$. Irrespective of the

mechanism, the reaction is slow and not the same mechanism as takes place when H_2 is present.

Evidence of a different mechanism is as follows. When H_2 is present, the $Co^{II}(BDMl,3pn)^+$ reacts as shown in Figure 23 to form the $Co^I(BDMl,3pn)$. This then reacts immediately with the methyl iodide to form the $MeCo(BDMl,3pn)^+$ quantitatively. The speed of reaction when H_2 is present proves that the two possible mechanisms when H_2 is absent are not taking place.

The $Co^I(BDMl,3pn)$ must be reactive to act as a catalyst. If the complex is stable and unreactive, it will not form a carbon-cobalt bond with the substrate. If a phosphine is added to the reaction mixture, it stabilizes the cobalt(I) oxidation state⁶⁸, the reaction mixture turns blue-green and the reduction stops or slows considerably. Pyridine also acts to stabilize the $Co^I(BDMl,3pn)$, but not to the extent of a phosphine. The reaction mixture is blue, but reduction takes place at a slow rate. By performing these reactions in a relatively non-polar reaction medium (9:1 v/v benzene-methanol), the uncharged $Co^I(BDMl,3pn)$ is favored over the charged $RCo^{III}(BDMl,3pn)^+$. If an axial base such as Bu_3P is added to the mixture, it is able to stabilize the uncharged cobalt(I) complex to the point where it will not react with the substrate to be reduced.

Another piece of evidence that indicates the $Co^I(BDMl,3pn)$ is the active species is the color of the reaction

mixture when all the substrate has been reduced. The reaction mixture turns the blue color of the cobalt(I) complex for 5-30 min when H_2 uptake stops, and then turns orange-brown. The orange-brown color is probably due to catalyst partially decomposed by hydrogenation of the ligand system.

The nucleophilic⁶⁹ $Co^I(BDM1,3pn)$ attacks the relatively positive carbonyl carbon of the substrate in step 4. Two electrons in the axial d_{z^2} orbital form a bond between the cobalt atom and the carbonyl carbon as the proton bonds to the carbonyl oxygen. These two electrons are only available in the cobalt(I) oxidation state. The addition of axial nitrogen bases other than the ever present quinine increases the rate of reduction, but does not change the visible spectra. The increased rate of reduction may be attributed to the increased nucleophilicity of the cobalt(I) complex.⁶⁹ The axial base increases the electron density in the d_{z^2} orbital and thus increases its nucleophilicity.

Both benzylamine ($pK_a = 9.33$)¹¹⁵ and triethylamine ($pK_a = 11.01$)¹¹⁵ increase the rate of reduction, but triethylamine lowers the optical yield of the reduction. Its basicity is great enough to increase the nucleophilicity of the attacking cobalt(I) complex to the point where it will react with any carbonyl carbon, not solely ones activated by protonated quinine. If there is nothing to direct the attack to a particular face of the molecule, then a racemic product will result. Triethylamine may also protonate in-

stead of quinine and act as an achiral proton donor.

The addition of the proton to the carbonyl oxygen in step 4 occurs at the same time the cobalt-carbon bond forms. The source of the proton is of great importance. If the proton comes from an achiral molecule, such as the methanol in the solvent, both enantiomers may be formed in equal amounts. If the proton comes from the chiral quinine, then one enantiomer is preferred over the other. Figure 24 shows how quinine blocks one face of a benzil molecule to produce only the desired enantiomer. Space filling models must be constructed to show why one face is preferred to the other. Thus one face of the substrate molecule will have the correct geometry for addition of the proton to the carbonyl oxygen.^{80,81} If quinidine, which is the mirror image of quinine, is used in place of quinine, the opposite enantiomer is produced in approximately the same optical yields. This is because the opposite face of the substrate molecule becomes the correct one for addition of the proton. If concurrent addition of a proton to the carbonyl oxygen was not a condition for reduction, then there would be no reason for high optical yield. The excess substrate would have a greater probability of being attacked with the result being a racemic product. Thus there must be a concerted reaction where a proton is donated as the carbon-cobalt bond forms.

If achiral components of the reaction mixture are able to donate a proton as the cobalt-carbon bond forms,

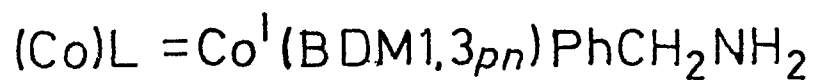
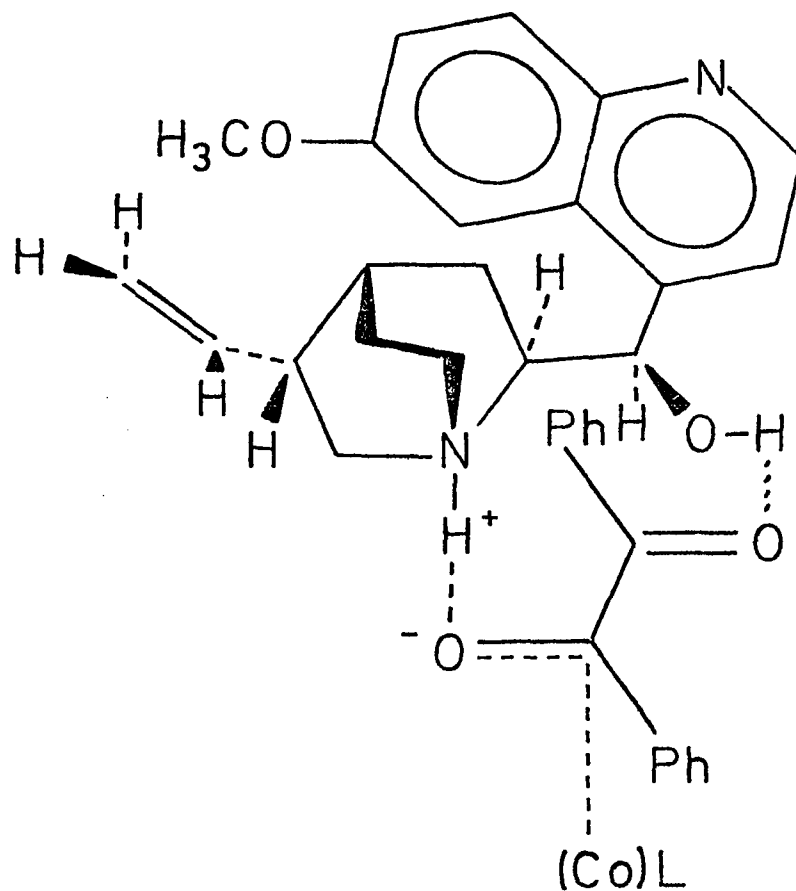


Figure 24. Relationship Between Quinine and Benzoin at the Point that the Stereochemistry of the Product is Determined.

there will be nothing to direct the formation of one enantiomer over the other, and a racemic product would form. Methanol has an acidic hydrogen from its hydroxyl group which may be abstracted by the carbonyl oxygen as the carbon-cobalt bond forms. To investigate this possibility several experiments were run with 2-propanol and 2-methyl-2-propanol to determine if the pK_a of the hydrogen on the alcohol had an effect on the optical yield obtained. Methanol has an approximate pK_a (relative to water) of 16 for the $CH_3OH \rightleftharpoons CH_3O^- + H^+$ dissociation. Both the 2-propanol and the 2-methyl-2-propanol have approximate pK_a 's (relative to water) of 18.¹¹⁴ Under conditions that produce an optical yield of 64% with methanol, the use of 2-propanol resulted in 79% optical yield. The alcohol must be present in the reaction solvent, or the catalyst will not dissolve. A racemic product results when the proton comes from the achiral alcohol instead of the chiral protonated quinine.

Step 5 in the reduction mechanism is the cleavage of the ³ carbon-cobalt bond to form the reduced substrate. For $Co(DMG)_2$ there are two methods of cleavage cited in the literature. Ohgo and coworkers⁸⁰ report backside attack by H^+ from protonated quinine, and Ricroch and Gaudemer⁸² show heterolytic cleavage to form a carbanion. The formation of a carbanion may be ruled out because stereochemistry would not be maintained once the carbon-cobalt bond was

broken, and a racemic product would result. Ohgo and co-workers have shown that backside attack by H^+ results in the correct enantiomer.⁸⁰

Deuteration experiments were run to determine the source of the bond breaking proton on the hydroxyl carbon. When MeOD is used in place of MeOH, and H_2 is used as usual, the protons formed from the homolytic cleavage of H_2 will exchange with the deuterium atoms on the methanol. The quinine is then free to pick up D^+ for cleavage of the carbon-cobalt bond with the resulting product containing deuterium in place of hydrogen on the hydroxyl carbon. For the reduction of benzil the predicted product is $PhC(O)CD(OH)Ph$. After extraction in the usual manner for a benzil reduction, nmr analysis showed 55% $PhC(O)CD(OH)Ph$ and 45% $PhC(O)CH(OH)Ph$. Next, two experiments using D_2 and MeOD were run. The first had benzylamine present to increase the speed of the reduction, and the product contained 60% hydrogen; the second had no benzylamine and the product contained 50% hydrogen. The final deuterium experiment was run with D_2 and MeOH in the presence of benzylamine, and the product contained 95% hydrogen. Table 29 shows reaction conditions and results.

The incorporation of hydrogen in experiments 2 and 3 may be explained by exchange of deuterium for hydrogen in the ligand¹¹⁶ and in the CH_3 group of the methanol. This exchange dilutes the acidic deuterium atoms with hydrogen.

TABLE 29
Deuterium Experiments and Results

Experiment Number	Conditions ^a	Hydroxyl Carbon in %H in Product ^b
1	MeOD, H ₂ , BA ^c	45%
2	MeOD, D ₂ , BA	60%
3	MeOD, D ₂	50%
4	MeOH, D ₂ , BA	95%

^a0.010M catalyst concentration
 3:1 quinine/cobalt ratio
 1:1 benzylamine/cobalt ratio (if present)
 20:1 substrate/cobalt ratio
 30°C reaction temperature
 6 hrs reaction time
 9:1 (v/v) benzene-methanol solvent

^bProduct in PhC(O)CH(OH)Ph

^cBA = benzylamine

This hydrogen may then be incorporated into the product, which lowers the percentage of deuterium in the product. The higher percentage of hydrogen in the second, as opposed to the third deuterium experiment, may be explained by the presence of the benzylamine. The benzylamine increases the nucleophilicity of the cobalt(I) complex, and consequently more deuterium-hydrogen exchange takes place.

In the first experiment, this process continues to take place and produces a product with 45% hydrogen incorporated. In the final deuterium experiment, the only source of deuterium in the homolytic cleavage of D_2 by the catalyst. With exchange again taking place as before, the available hydrogen is increased and 95% of the product contains hydrogen.

These results suggest that the proton of deuterion (D^+) determines what type of atom will be on the hydroxyl carbon. There is rapid exchange between the H^+ or D^+ on the quinine and the H^+ or D^+ on the oxygen of the methanol in each case. Alkyl-cobalt complexes are dealkylated by electrophiles to give a cobalt(III) complex, with the electrophile bonded to the alkyl group.¹¹³ The H^+ or D^+ on the quinine acts as an electrophile, displaces the cobalt(III) complex and forms the reduced benzoin. Exchange of deuterium on the hydroxyl carbon for hydrogen in the aqueous extractions may be ruled out because this type of exchange would require the benzoin to be quite acidic, which it is not.

The final step in the reduction is reaction between $\text{Co}^{\text{III}}(\text{BDML},3\text{pn})^{2+}$ and $\text{Co}^{\text{I}}(\text{BDML},3\text{pn})$ to form two moles of the starting material $\text{Co}^{\text{II}}(\text{BDML},3\text{pn})^+$. If equal amounts of the cobalt(I) and cobalt(III) complexes are combined in methanol, the red cobalt(II) complex is the product. This is a fast reaction, for if it was a slow reaction, all the cobalt could be tied up as either an alkyl complex, or as the inactive cobalt(III) complex.

This proposed mechanism accounts for all aspects of the reduction, from the initial cleavage of H_2 to the regeneration of the starting cobalt(II) complex. The mechanism is unusual because the chirality determining site is not on the metal catalyst but separate from it. This is similar to many reactions that take place in biological systems where the site that determines the stereochemistry of the reaction is separated from the active catalytic site.

BIBLIOGRAPHY

1. Oxford Universal Dictionary, 3rd ed., Oxford, Clarendon Press, 1955, p 274.
2. J. J. Berzelius, Jahresber Chem., 15, 237 (1836).
3. W. Ostwald, Rev. Sci., 1, 640 (1902).
4. G. W. Castellan, "Physical Chemistry", Addison-Wesley, Reading, MA, 1964, p 623.
5. Kiss, Rec. Trav. Chim., 43, 68 (1923).
6. C. K. Brown and G. Wilkinson, J. Chem. Soc., A, 2753 (1970).
7. M. Calvin, Trans. Faraday Soc., 34, 1181 (1938).
8. I. Wender and H. Sternberg, Adv. Catalysis, 9, 594 (1957).
9. G. H. Flynn and H. M. Hulbuet, J. Amer. Chem. Soc., 76, 3393 (1954).
10. M. E. Volpin and I. S. Kolomnikov, Russian Chem. Rev., 38, 273 (1969).
11. G. Dolcetti and N. W. Hoffman, Inorganica Chim. Acta, 9, 269 (1974) and references cited therein.
12. L. Marko and B. Heil, Catal. Rev., 8, 269 (1973).
13. J. D. Morrison, W. F. Masler and K. M. Neuberg, "Advances in Catalyses and Related Subjects", Vol. 25, Academic Press, New York, 1976, p 81.
14. R. E. Harmon, S. K. Gupta and D. J. Brown, Chem. Rev., 73, 21 (1973).
15. B. J. Luberoft, "Homogeneous Catalysis", Advances in Chemistry Series No. 70, American Chemical Society, Washington, D. C., 1968.
16. D. Forster and J. F. Roth, "Homogeneous Catalysis II", Advances in Chemistry Series No. 132, American Chemical Society, Washington, D. C., 1974.

17. C. A. Tolman, Chem. Soc. Rev., 1, 337 (1972).
18. G. N. Schrauzer, "Transition Metals in Homogeneous Catalysis", Marcel Dekker, Inc., New York, 1971.
19. G. N. Schrauzer, Acc. Chem. Res., 1, 97 (1968).
20. J. Halpern, Acc. Chem. Res., 3, 386 (1970).
21. J. P. Collman, Acc. Chem. Res., 1, 136 (1968).
22. G. H. Olive and S. Olive, Angew. Chem. Int. Ed., 10, 105 (1972).
23. L. Vaska, Inorg. Chim. Acta, 5, 295 (1971).
24. R. R. Schrock and J. A. Osborn, J. Amer. Chem. Soc., 93, 2397 (1975).
25. R. R. Schrock and J. A. Osborn, J. Amer. Chem. Soc., 93, 3089 (1971).
26. J. M. Whitesides, J. F. Gaasch and E. R. Stedronsky, J. Amer. Chem. Soc., 94, 5258 (1972).
27. J. Kwiatek in "Transition Metals in Homogeneous Catalysis", G. N. Schrauzer, Ed., Marcel Dekker, Inc., New York, 1971, p 20.
28. J. Halpern, "Homogeneous Catalysis", Advances in Chemistry Series No. 70, American Chemical Society, Washington, D. C., 1968, p 1.
29. F. A. Cotton and G. Wilkinson, "Advanced Inorganic Chemistry", 3rd ed., Interscience, New York, 1972, pp 788-789.
30. Reference 28, page 4.
31. S. Akabori, S. Sakurai, Y. Izumi and Y. Fujii, Nature, 178, 323 (1956).
32. Y. Izumi, Angew. Chem. Int. Ed., Eng., 10, 821 (1971).
33. W.S. Knowles and M. J. Sabacky, J. Chem. Soc. Chem. Commun., 1445 (1968).
34. C. Horner, H. Siegel and H. Buthe, Angew. Chem. Int. Ed. Eng., 7, 942 (1968).
35. J. D. Morrison, R. E. Burnett, A. M. Aguiar, C. J. Morrow and C. Phillips, J. Amer. Chem. Soc., 93, 1301 (1971).

36. T. P. Dang and H. B. Kagan, J. Chem. Soc., Chem. Commun., 481 (1971).
37. W. S. Knowles, M. J. Sabacky and B. D. Vineyard, J. Chem. Soc., Chem. Commun., 10 (1972).
38. W. S. Knowles, M. J. Sabacky, B. D. Vineyard and D. J. Weinkauff, J. Amer. Chem. Soc., 97, 2567 (1975).
39. P. Bonvicini, A. Levi, G. Modena and G. Scorrano, J. Chem. Soc., Chem. Commun., 1188 (1972).
40. I. Ojima, Chem. Lett., 223 (1974).
41. I. Ojima and T. Kogure, Tetrahedron Lett., 1889 (1974).
42. M. Tanaka, Y. Watanake, T. Mitsudo, Y. Yasunori and Y. Takegami, Chem. Lett., 137 (1974).
43. R. B. Merrifield, J. Amer. Chem. Soc., 85, 2149 (1963).
44. R. H. Grubbs and L. H. Kroll, J. Amer. Chem. Soc., 93, 3062 (1971).
45. C. U. Pittman, Jr. and C. R. Smith, J. Amer. Chem. Soc., 97, 1749 (1975).
46. H. Hirai and T. Futura, Polymer Lett., 9, 459 (1971).
47. W. Dumont, J. C. Poulin, T. P. Dang and H. B. Kagan, J. Amer. Chem. Soc., 95, 8295 (1973).
48. J. P. Candlin, K. A. Taylor and D. T. Thompson, "Reactions of Transition Metal Complexes", Elsevier, Amsterdam, 1968.
49. Z. Nagy-Magos, G. Boc and L. Marko, J. Organometallic Chem., 20, 205 (1969).
50. D. T. Thompson and R. Whyman, "Transition Metals in Homogeneous Catalysis", G. N. Schrauzer, ed., Marcel Dekker, Inc., New York, 1971, p 154.
51. F. Piacenti, M. Bianchi, E. Benedetti and P. Frediani, J. Organometallic Chem., 23, 257 (1970).
52. R. Lai and E. Ucciani, "Homogeneous Catalysis II", Advances in Chemistry Series No. 132, American Chemical Society, Washington, D. C., 1974, p 1.
53. C. W. Bird, Chem. Rev., 62, 283 (1962).

54. P. Pino, G. Consiglio, C. Bollighi and C. Salomon, "Homogeneous Catalysis II", Advances in Chemistry Series No. 132, American Chemical Society, Washington, D. C., 1974, p 295.
55. A. Rosenthol and I. Wender, "Organic Syntheses via Metal Carbonyls", I. Wender and P. Pino, eds., Interscience, New York, 1968, Vol. 1, p 405.
56. L. Marko, B. Heil and S. Vostag, "Homogeneous Catalysis II", Advances in Chemistry Series No. 132, American Chemical Society, Washington, D. C., 1974, p 27.
57. H. M. Feder and J. Halpern, J. Amer. Chem. Soc., 97, 7186 (1975).
58. W. P. Griffith and G. Wilkinson, J. Chem. Soc., 2757 (1959).
59. M. G. Burnett, P. J. Connolly and C. Kemball, J. Chem. Soc. (A), 991 (1968).
60. T. Funabiki and K. Tarama, Tetrahedron Lett., 1111 (1971).
61. G. M. Schwab and G. Mandre, J. Catal., 12, 193 (1968).
62. T. Suzuki and T. Kwan, Nippon Kagaku Zasshi, 88, 395 (1967); C.A. 67:28836j.
63. T. Suzuki and T. Kwan, Nippon Kagaku Zasshi, 88, 400 (1967); C.A. 67:43325k.
64. Y. Ohgo, S. Takeuchi and J. Yoshimura, Bull. Chem. Soc. Japan, 43, 505 (1970).
65. Y. Ohgo, K. Koboyashi, S. Tabeuchi and J. Yoshimura, Bull. Chem. Soc. Japan, 45, 933 (1972).
66. Y. Ohgo, S. Takeuchi and J. Yoshimura, Chem. Lett., 583 (1971).
67. G. N. Schrauzer and R. J. Windgassen, Chem. Ber., 99, 602 (1966).
68. G. N. Schrauzer and R. J. Windgassen, J. Amer. Chem. Soc., 89, 1999 (1967).
69. G. N. Schrauzer and E. Deutsch, J. Amer. Chem. Soc., 91, 3341 (1969).

70. G. N. Schrauzer and R. J. Holland, J. Amer. Chem. Soc., 93, 1505 (1971).
71. G. Costa, G. Mestroni and G. Tauzler, J. C. S. Dalton, 450 (1972).
72. T. Yamaguchi, N. Nakayawa and T. Tsumura, Chem. Lett., 1231 (1972).
73. T. Yamaguchi and T. Tsumura, Chem. Lett., 409 (1973).
74. L. I. Simandi, Z. Syeverenyi and E. Budo-Zahonyi, Inorg. Nucl. Chem. Lett., 11, 773 (1975).
75. Y. Ohgo, S. Takeuchi and S. Yoshimura, Bull. Chem. Soc. Japan, 44, 283 (1971).
76. Y. Ohashi, Y. Sasada, Y. Tashiro, Y. Ohgo, S. Takeuchi and J. Yoshimura, Bull. Chem. Soc. Japan, 46, 2589 (1973).
77. S. Takeuchi, Y. Ohgo and J. Yoshimura, Chem. Lett., 265 (1973).
78. Y. Ohgo, S. Takeuchi, Y. Natori and J. Yoshimura, Chem. Lett., 33 (1974).
79. Y. Ohgo, Y. Natori, S. Takeuchi and J. Yoshimura, Chem. Lett., 709 (1974).
80. Y. Ohgo, Y. Natori, S. Takeuchi and J. Yoshimura, Chem. Lett., 1327 (1974).
81. S. Takeuchi, Y. Ohgo and J. Yoshimura, Bull. Chem. Soc. Japan, 47, 463 (1974).
82. M. N. Ricroch and A. Gaudemer, J. Organomet. Chem., 67, 119 (1974).
83. H. Aoi, M. Ishimori, S. Yoshikawa and T. Tsuruta, J. Organometal. Chem., 85, 271 (1975).
84. Y. Tatsuno, A. Koniski, A. Nakamura and S. Otsuka, J. Chem. Soc., Chem. Commun., 588 (1974).
85. A. J. Gordon and R. A. Ford, "The Chemists Companion", John Wiley & Sons, New York, 1972, p 429.
86. S. Siggia, "Quantitative Organic Analysis", 3rd ed., John Wiley & Sons, New York, 1966, p 12.
87. Reference 85, p 221.

88. "Sadttler Standard Spectra", Sadttler Research Laboratories, Philadelphia, PA, 1965.
89. R. Jacquier, Bull. Soc. Chim. France, D83 (1950).
90. Reference 88, IR Spectrum #25017.
91. E. Browning, "Toxicity and Metabolism of Industrial Solvents", Elsevier, New York, 1965.
92. "Benzene: Uses, Toxic Effects, Substitutes", Geneva, ILO, 1968.
93. W. G. Cochran and G. M. Cox, "Experimental Designs", 2nd ed., J. Wiley & Sons, Inc., New York, 1957.
94. O. Kempthorne, "The Design and Analysis of Experiments", John Wiley & Sons, New York, 1952, Chap. 13, 20.
95. W. J. Vonden, "Statistical Methods for Chemists", John Wiley & Sons, New York, 1951.
96. E. Bauer, "A Statistical Manual for Chemists", 2nd ed., Academic Press, New York, 1971.
97. Reference 93, p 154.
98. Reference 93, pp 6-8.
99. Most statistical books use a letter code, a,b,c,ab,... to define the response variables for the various experiments. The sign of each letter is dependent upon the elements of the design matrix.
100. Reference 93, Chapter 5.
101. Reference 96, p 8.
102. Reference 93, p 342.
103. Reference 93, p 55.
104. Reference 93, p 57.
105. W. H. Beyer, "Handbook of Tables for Probability and Statistics", Chemical Rubber Co., Cleveland, OH, 1966, p 240.
106. Reference 93, Chapter 6A.
107. "Fractional Factorial Experiment Designs for Factors at Two Levels", National Bureau of Standards Applied Mathematics Series 48, 1957.

108. C. Daniel, Technometrics, 1, 311 (1959).
109. G. N. Schrauzer, J. W. Sibert and R. J. Windgassen, J. Amer. Chem. Soc., 90, 6681 (1968).
110. G. N. Schrauzer, "Inorganic Syntheses", Vol. XI, W. L. Jolly, ed., New York, McGraw Hill, 1968, p 64.
111. T. M. Lowrey and W. C. G. Baldwin, J. Chem. Soc., 704 (1935).
112. I. Elphimoff-Felkin and M. Verrier, Bull. Soc. Chim. France, 1052 (1967).
113. V. E. Magnuson, Ph.D. Thesis, University of New Hampshire, 1974.
114. W. K. McEwen, J. Amer. Chem. Soc., 58, 1124 (1936).
115. R. C. Weast, "Handbook of Chemistry and Physics", Chemical Rubber Co., Cleveland, OH, 1967, p D87.
116. R. L. Beach, Tetrahedron Lett., 1913 (1972).
117. J. March, "Advanced Organic Chemistry: Reactions, Mechanisms, and Structure", McGraw-Hill, New York, 1968, p 452.
118. R. W. Waldron and J. H. Weber, Inorganica Chim. Acta, 18, 23 (1976).